NUREG/CR-1642
R6, RA

Site-Dependent Response at El Centro, California Accelerograph Station Including Soil/Structure Interaction Effects

Manuscript Completed: May 1979
Date Published: October 1980

Shannon & Wilson, Inc.
1105 North 38th Street
Seattle, WA 98103

Agbabian Associates
250 North Nash Street
El Segundo, CA 90245

Prepared for
Division of Reactor Safety Research
Office of Nuclear Regulatory Research
U.S. Nuclear Regulatory Commission
Washington, D.C. 20555
NRC FIN No. B3015
Under Contract No. NRC-04-76-200

ABSTRACT

The El Centro Terminal Substation Building, where many strong motion records have been measured, is underlain by a massive foundation block and rests on deep deposits of soft soil materials. These conditions suggest important soil/structure interaction effects; therefore, the current study has been carried out to analytically investigate the extent to which such effects may cause motions recorded in the basement of this building to differ from the motions of the free field. The investigation was based on two-dimensional models of the building and soil medium and on two different techniques--SHAKE/FLUSH and TRI/SAC codes--for analyzing the response of the free field and the building/soil system. Both techniques showed that, at frequencies above 1.5 Hz, the horizontal and vertical motions computed at the accelerograph location in the building basement fell below the free field motions computed at the corresponding location along the ground surface, by factors ranging from 20% to 100%. At lower frequencies, the horizontal motions of the basement and free field were nearly identical, whereas the vertical motions of the basement fell below those of the free field.

SUMMARY

The accelerograph station in the basement of the El Centro Terminal Substation Building has contributed more records to the current library of strong motion data than any other station in the United States. However, this building is underlain by a massive foundation block and rests on deep deposits of soft soil materials. These factors, considered together suggest that earthquake motions measured in the basement of the Terminal Substation Building could have been influenced by soil/structure interaction, causing them to differ from the free-field motions they were intended to represent.

This study has consisted of an analytical assessment of how soil/structure interaction may affect motions recorded at the El Centro Terminal Substation Building. It is based on field measurements of the subsurface soil properties and the dimensions of the foundation block, and on the use of two state-of-the-art finite element analysis techniques to perform the calculations--SHAKE/FLUSH code and TRI/SAC code. The SHAKE/FLUSH analysis technique can consider strain-dependent soil properties but only vertically incident body waves; the TRI/SAC code, on the other hand, considers only elastic soil properties but can accommodate input motions from arbitrarily incident seismic waves.

Both the SHAKE/FLUSH and TRI/SAC analyses were based on two-dimensional planar models of the Terminal Substation Building and the surrounding soil medium. For each analysis, the free-field response of the soil medium subjected to a given set of input motions was calculated first; then an analysis of the response of the building and soil medium was carried out using an identical set of input motions and an identical soil grid. The free-field motions from the first calculation were compared with the basement motions at the accelerograph location from the second calculation. These comparisons were the basis for assessing the importance of soil/structure interaction at the El Centro Terminal Substation.

Both the SHAKE/FLUSH and TRI/SAC analyses indicated potentially important effects of soil/structure interaction at this accelerograph station. At frequencies above 1.5 Hz, the horizontal and vertical motions of the basement at the accelerograph location were shown to fall well below the free-field motions at the corresponding location along the ground surface, by factors ranging from about 20% to over 100%. These trends were attributed to the significant mass of the foundation block and the presence of the soft soil medium, which would cause a filtering of higher-frequency excitations applied to the Terminal Substation Building. At lower frequencies, the horizontal motions of the basement and free field were nearly identical, whereas the vertical motions of the basement (computed only from TRI/SAC) fell below those of the free field.

CONTENTS

CONTENTS (CONTINUED)

ILLUSTRATIONS

ILLUSTRATIONS (CONCLUDED)

TABLES

ILLUSTRATIONS (CONTINUED)

ILLUSTRATIONS (CONTINUED)

TABLES (CONCLUDED)

PREFACE

This report describes a study of soil/structure interaction effects at the El Centro Terminal Substation accelerograph site. It has been prepared by the Shannon & Wilson/Agbabian Associates joint venture under Contract NRC-04-76-200 with the United States Nuclear Regulatory Commission.

The project manager for the SW/AA joint venture is R.P. Miller of Shannon & Wilson, Inc. Project engineer for Agbabian Associates is S.D. Werner. S.A. Adham, Y.C. Lee, and H.S. Ts'ao of Agbabian Associates were principal investigators for this study. Significant contributions to the study were made by I. Arango of Woodward-Clyde Consultants (formerly with Shannon & Wilson, Inc.), W.P. Grant and J. Musser of Shannon & Wilson, Inc., and D.P. Reddy of Agbabian Associates. J. Harbour of the U.S. Nuclear Regulatory Commission has served as technical monitor for the SW/AA joint venture.

Several individuals and agencies outside of the joint venture provided valuable assistance to SW/AA during this investigation. D.A. Twogood and R. Ogilvie and their staff of the Imperial Valley Irrigation District Power Department were most helpful in providing us with information and facilities during our visits to the El Centro site. In addition, A.G. Brady of the U.S. Geological Survey furnished valuable information on recent earthquakes in the El Centro area and on the Terminal Substation Building. Finally, the Automobile Club of Southern California granted permission for us to use their maps of El Centro and the surrounding area as a means for representing locations of accelerograph stations and recent earthquake epicenters.

CHAPTER 1

INTRODUCTION AND SUMMARY OF RESULTS

1.1 BACKGROUND INFORMATION

For the past several years, the joint venture of Shannon & Wilson, Inc. and Agbabian Associates (SW/AA) has investigated and evaluated procedures and available data for developing vibratory ground motion criteria. These procedures employ site-response analysis techniques and measured records from the current library of strong-motion data. Results of various studies carried out by the joint-venture effort have been documented in numerous reports.

During fiscal years 1974 and 1975, the joint venture prepared a report that assessed the current technology for developing vibratory ground motion criteria at nuclear power plant sites (SW/AA, 1975a). Important features of this report were (1) a discussion of the lack of definitive subsurface soils data that existed at strong motion accelerograph sites at that time; and (2) a recommendation that such data be obtained in the near future to provide a necessary basis for evaluating the influence of local soil conditions on earthquake ground motions. As a result, SW/AA has, since 1975, been carrying out comprehensive geotechnical investigations at accelerograph sites throughout the western United States and, in addition, has been using soils data from these investigations to assess the potential importance of local site conditions on the ground shaking measured at these stations (SW/AA, 1976; 1977a, b, c; 1978a, b, c, d).

Of the various accelerograph stations at which the above geotechnical investigations were carried out, one of the more important is the El Centro California Terminal Substation Building. This station has contributed more records to the current library of strong motion data than any other station in the western United States; in addition, the ground shaking measured at the El Centro Terminal Substation during the May 1940 Imperial Valley earthquake was the strongest measured in the United States until the 1971 San Fernando earthquake.

In view of the importance of this accelerograph site, it is important to carefully evaluate its characteristics and how they may influence the accelerograph records measured there. With this in mind, there are two particular characteristics of the site that may be important. First, the El Centro Terminal Substation Building that houses the accelerograph is a rather unique structure, in that it is underlain by a solid concrete foundation block 20 ft deep and 24 ft wide that extends beneath a major portion of the basement of the building.* Second, the geotechnical data obtained by SW/AA during their investigation at this site shows the site to consist of very soft soil deposits that extend to substantial depths (SW/AA, 1976). These factors, considered together, suggest that the earthquake motions measured in the basement of the Terminal Substation Building could have been influenced by soil/structure interaction, causing them to differ from the free-field conditions they were intended to represent. The implications of this possibility are significant, when it is considered that several sets of strong motion records measured in this building have been used in the development of free-field seismic input criteria for nuclear power plants and other major structures.

1.2 PURPOSE

This report describes results of an analytical assessment of how earthquake records measured in the basement of the El Centro, California, Terminal Substation Building may be influenced by soil/structure interaction. This assessment is based on soils data obtained from the SW/AA (1976) geotechnical investigations of the site and on field measurements defining the dimensions of the building and of the massive foundation block that underlies the station basement.

---

*As noted in Chapter 2, the foundation block was originally used to support a large gas engine that has long since been removed from the Terminal Substation Building. The dimensions of the block and of the entire building were verified by SW/AA as part of this study.

1.3 SCOPE

To fulfill the goals of this investigation, two sets of dynamic analyses, each employing a different state-of-the-art analysis technique, have been employed. These analysis techniques--one involving the use of the SHAKE and FLUSH codes (Schnabel et al., 1972; Lysmer et al., 1975) and the other employing the TRI/SAC code (AA, 1976)--each have certain relative advantages and limitations. For example, the SHAKE and FLUSH codes provide a means for incorporating the strain-dependent soil properties at the site, as measured by SW/AA (1976b), into the dynamic analysis; however, the codes can consider only vertically propagating shear or compression waves--which represent only two of numerous wave types and directions of incidence that can comprise the ground shaking at a site. The TRI/SAC code, on the other hand, which is an extension of the SAP code originally developed by Wilson (1970), can consider nonvertically incident seismic excitation but is limited to a linear elastic representation of the subsurface soil materials. Both sets of analyses utilize a two-dimensional model of the three-dimensional soil/structure system.

Each analysis technique is employed in a similar way to assess how the Terminal Substation building characteristics influence motions measured at this site. For each technique, two sets of computations are carried out. The first set uses a model of only the soil profile to calculate free-field ground response, whereas the second set uses a model of the soil profile and structure to compute the response of the Terminal Substation Building. Comparisons between the free-field ground surface response and the response of the building at the accelerograph location are used to assess the potential importance of soil/structure interaction at this site. It is noted that, for each analysis technique, the two sets of calculations are each based on the same assumed input motions, site soil model, and assumed nature of the wave propagation. The calculations therefore provide a consistent basis for comparing the free field and building responses and for thereby assessing soil/structure interaction effects.

During this investigation, two supplementary tasks have been carried out in support of the dynamic analyses. The first has consisted of measurement and verification of the building layout and foundation-block dimensions by SW/AA personnel. The building layout, including all aboveground dimensions and equipment locations, has been verified during a visit to the Terminal Substation Building in the early stages of this investigation (Chapt. 2). The dimensions of the underlying foundation block, which has a major influence on the soil/structure interaction phenomena at this site, has been verified by a microreflection survey carried out by SW/AA personnel midway through the investigation (App. C).

A second supplementary task has consisted of an attempt to use strong motion measurements to verify the soil/structure interaction effects indicated for the Terminal Substation Building by the dynamic analysis results. Specifically, the goal of this task was to find and compare earthquake motions recorded simultaneously in the basement of the building and at nearby free-field stations during the same earthquake event. Unfortunately, however, a careful review of the current strong motion data base and discussions with personnel from the United States Geological Survey showed that no processed data suitable for this purpose is now available from the El Centro area (App. D).

1.4 SUMMARY OF RESULTS

The most significant results from the SHAKE/FLUSH and TRI/SAC analyses are briefly summarized as follows:

- Both the SHAKE/FLUSH and the TRI/SAC results indicated potentially important effects of soil/structure interaction on the horizontal motions at the El Centro Terminal Substation accelerograph site. Both sets of analyses showed that, at frequencies below 1.5 Hz, horizontal motions computed in the basement were nearly identical with those computed at the corresponding location along the ground surface in the free

field. However, at higher frequencies, the horizontal basement motions from both sets of analyses fell below those of the free field, by factors ranging from about 20% to over 100%. These trends were attributed to the significant mass of the foundation block, which would tend to filter higher frequency excitations applied to the Terminal Substation Building.

- Vertical motions of the Terminal Substation Building and the free field were computed only by TRI/SAC. Comparisons of higher-frequency components of these motions (above 1.5 Hz) showed that the basement motions fell below the free-field ground surface motions by factors even greater than those observed from the horizontal motion comparisons.

- At lower frequencies (below 1.5 Hz) the vertical basement motions also fell below the free-field ground surface motions--a trend different from that observed from the horizontal motion comparisons. This difference in the lower frequency comparisons between horizontal and vertical motions was attributed, at least in part, to differences in the attenuation with depth of the computed horizontal and vertical free-field motions. The lower frequency free-field vertical motions attenuated much more sharply with depth; therefore, reduced loads applied along the embedded foundation block by these attenuated vertical motions could have reduced the vertical response of the basement. This, in turn, could have affected the comparisons of this response with the free-field vertical motions *at the ground surface*.

- Certain aspects of the SHAKE/FLUSH analyses procedure were investigated as part of this study. One such aspect involved the deconvolution procedures inherent in the SHAKE code. When used to deconvolve the 1940 El Centro records applied at the

ground surface of the soil profile defined by SW/AA measured data at El Centro, the resulting subsurface motions were seen to be very sensitive to certain details of the site model. As a result, this deconvolution procedure was judged to be not sufficiently reliable for computing subsurface input motions to soil/structure interaction analyses at this particular site.

- Another aspect of the SHAKE/FLUSH analysis procedure that was assessed was the influence of soil/structure-interaction-induced soil nonlinearities on the computed building response. This assessment first involved defining strain-dependent soil properties from the final iteration of the free-field calculations using SHAKE code. Such properties, when used in the first iteration of the FLUSH analysis of the soil/structure system, produced soil and building responses that did not change noticeably during subsequent iterations. Therefore, the strain-dependent soil properties obtained from SHAKE were seen to provide an excellent basis for computing the soil/structure system response in FLUSH.

1.5 REPORT ORGANIZATION

The remainder of this report is organized into four chapters and four appendixes. Chapter 2 describes the structure and site characteristics at the El Centro Terminal Substation. The analysis and modeling procedures used in the calculations are described in Chapter 3. Results from the SHAKE/FLUSH analysis results and TRI/SAC analyses are provided in Chapters 4 and 5 respectively. Appendix A provides details of the Terminal Substation structure and Appendix B contains a USGS (1977) memorandum that briefly outlines the substation building and site characteristics. A microreflection survey used to verify the dimensions and properties of the foundation block is contained in Appendix C, and an assessment of the availability of measured records suitable for assessing soil/structure interaction effects at the Terminal Substation site is provided in Appendix D.

CHAPTER 2

STATION AND SITE DESCRIPTION

2.1 STATION DESCRIPTION

This section briefly summarizes the El Centro accelerograph station characteristics, including the Terminal Substation location, structural characteristics, and strong motion instrumentation.

2.1.1 LOCATION AND HOUSING STRUCTURE

The city of El Centro is located in the southern part of California, about 120 mi east of San Diego (Fig. 2-1). The city is situated on the central portion of a vast, trough-like depression (most of which is below sea level) running from the San Bernardino Mountains to the Gulf of California.

The accelerograph station being investigated is located near the intersection of Third Street and Commercial Avenue in El Centro (Fig. 2-2). The instrument is currently installed in the northeast corner of the operating building of a terminal substation at that location (Figs. 2-3, 2-4). When the accelerograph was installed in this building in July 1932, the complex was owned by the Southern Sierra Power Company. Ownership of the building has changed several times during past years. The property is currently owned by the Imperial Valley Irrigation District.

The two-story building is of heavily reinforced concrete construction. Existing information regarding the contents of the building (particularly during the 1940 earthquake) was difficult to find. Therefore SW/AA personnel spent several days at the El Centro site (in April 1977), and obtained detailed measurements of the building with the aid of a local surveying crew. Data on the layout of the building (Fig. 2-5a) and the weights, geometries, and locations of machinery within the building were also obtained from (1) discussions with personnel from the Imperial Valley Irrigation District and with experienced earthquake engineers and scientists who are familiar with the history of the

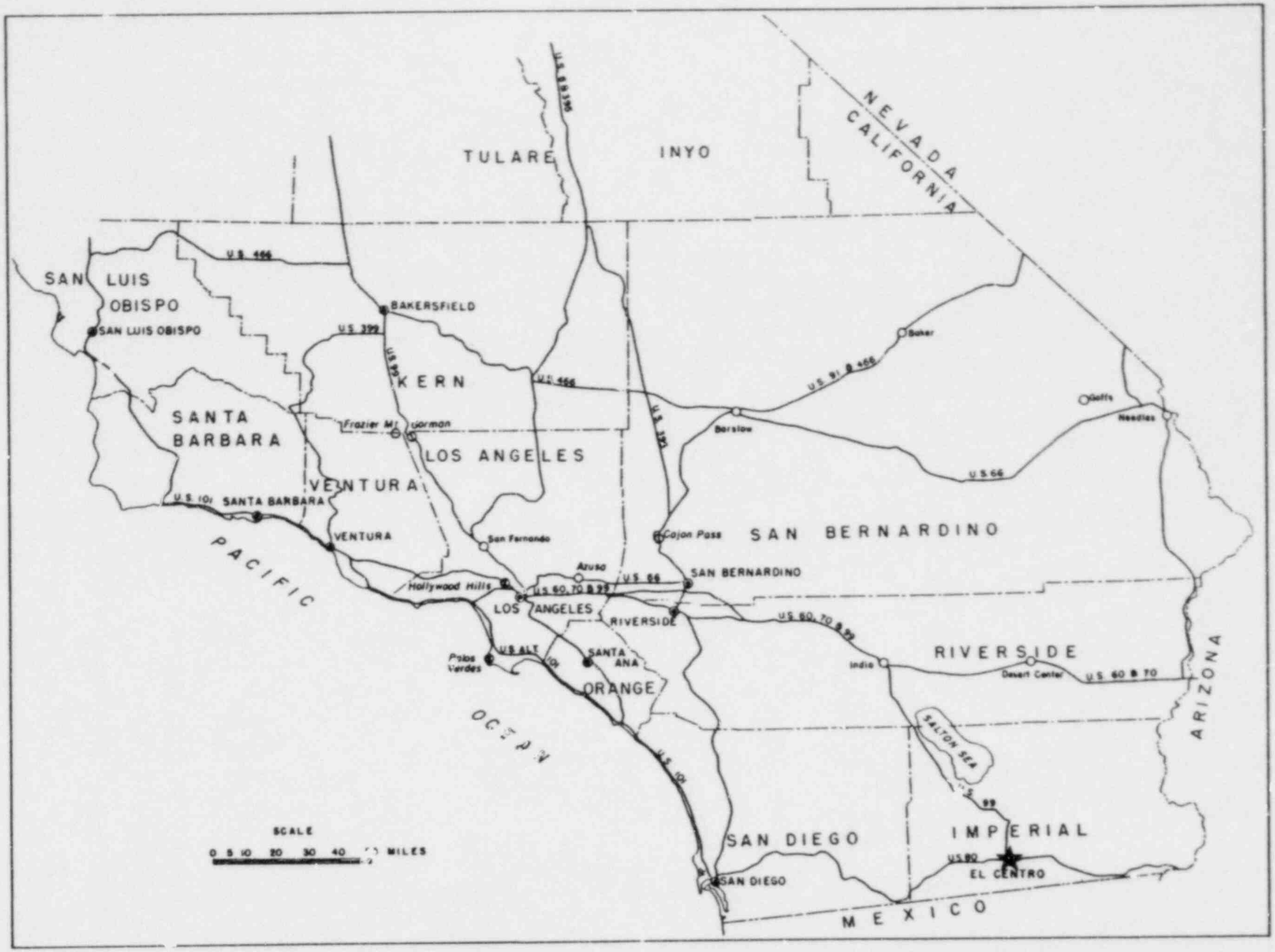

FIGURE 2-1 LOCATION OF EL CENTRO IN SOUTHERN CALIFORNIA (Modified from Division of Mines and Geology, 1954)

FIGURE 2-2. LOCATION OF EL CENTRO TERMINAL SUBSTATION

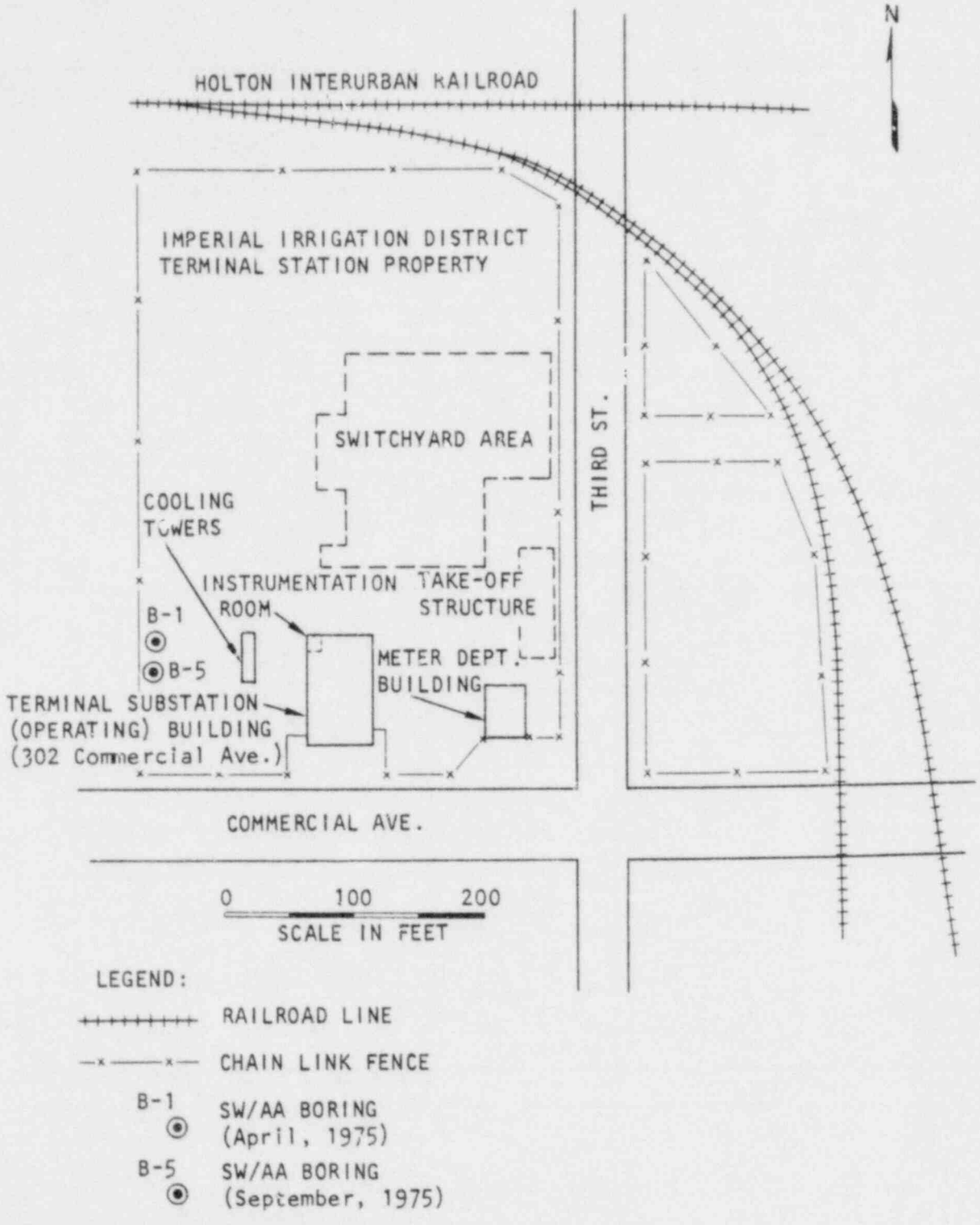

FIGURE 2-3. SITE PLAN AND SW/AA BORING LOCATIONS AT EL CENTRO TERMINAL SUBSTATION (SW/AA, 1976)

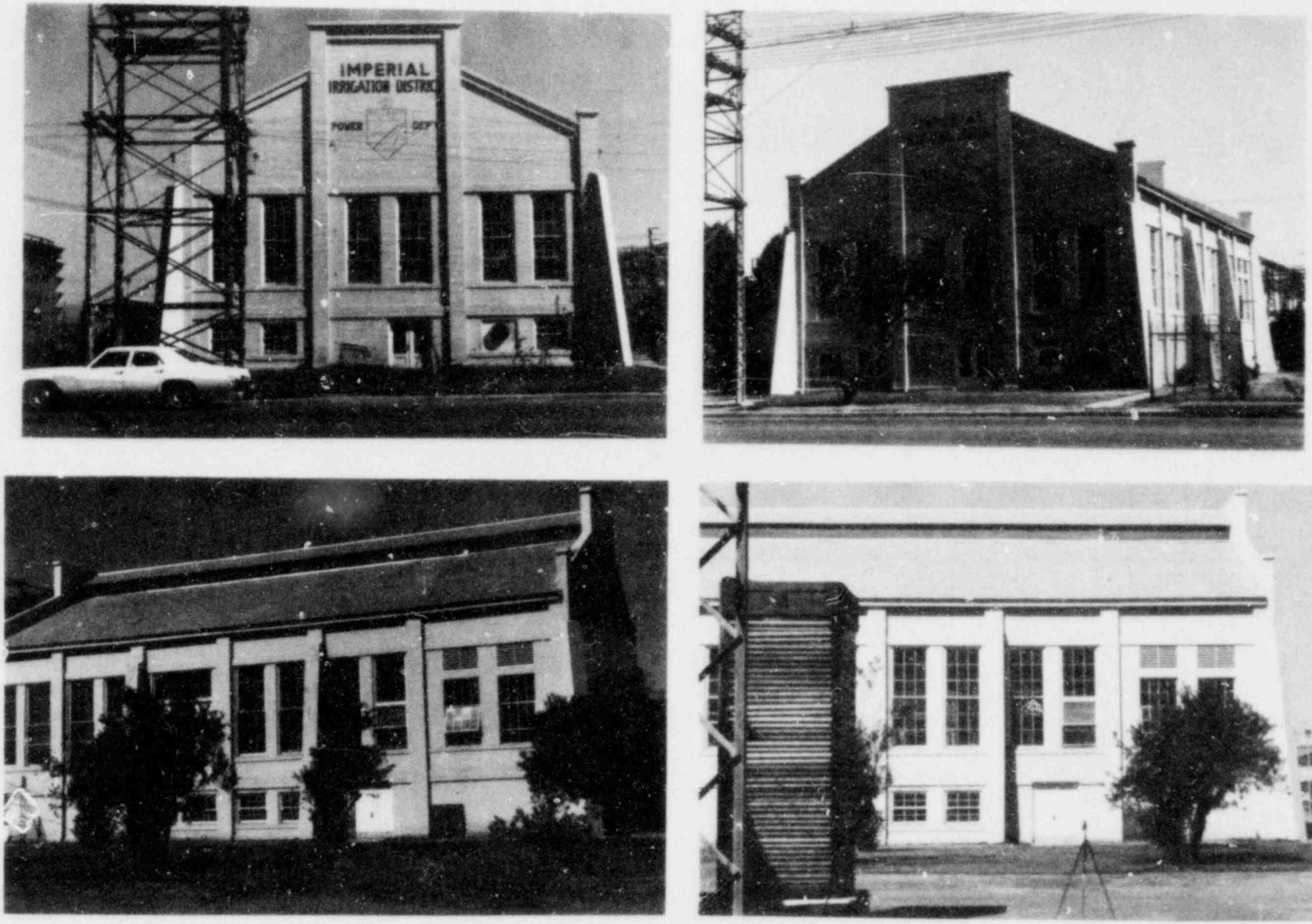

FIGURE 2-4. EL CENTRO TERMINAL SUBSTATION BUILDING

building;* (2) available engineering drawings of the building and its contents (SSPC, 1926; WE&M, 1926); and (3) a USGS memorandum that describes the building and foundation configuration (USGS, 1977), (see App. A and B).

Originally, the building was designed to house a gas engine that was, at that time, the largest on the Pacific coast. A special foundation for the engine was constructed (Fig. 2-5b) from a massive block of concrete that extends about 20 ft into the ground beneath the basement floor. The portion in the center of the block, shown in Figure 2-5b, was removed in 1914 when the old engine was broken up and removed (USGS, 1977; SSPC, 1926). Data describing the depth and other dimensions of the block was originally available only in sketches provided by USGS (1977). No engineering drawings or other data to verify the block dimensions could be found. Therefore, because of the importance of this block for this particular study, its dimensions and properties have been specially measured and verified by SW/AA, using microreflection survey techniques (see App. C).

The main floor slab is 7 in thick and is constructed of reinforced concrete, strengthened by I-beams spaced at intervals that range from 5 ft to 6 ft 3 in. The main floor supports two synchronous condensers, 6000 KVA (Unit 1) and 5000 KVA (Unit 2), as shown in Figure 2-5a (SSPC, 1926). The largest of these two units weighs 58,500 lbs (WE&M, 1926). According to all sources, both units were installed long before the 1934 Imperial Valley Earthquake. The main floor also supports the switch units. Control is provided from the operation room, which is separated from the main hall by a 9 in thick reinforced concrete wall.

The heavy walls of the building are 9 in thick aboveground and flare out to 12 in thick underground (Figs. 2-5 and 2-6). These walls are strengthened at sides and corners by massive buttresses (Figs. 2-5 and 2-7). The roof of the building is supported by a steel truss.

---

*Along these lines, valuable information was provided by P. Belsky of Westinghouse Electric Corporation, Los Angeles; A.G. Brady and G.N. Bycroft of the United States Geological Survey, Menlo Park; W.K. Cloud of the University of California, Berkeley; P.C. Jennings of the California Institute of Technology, Pasadena; J. Nielson of the United States Geological Survey, Los Angeles; R. Ogilvie of the Imperial Valley Irrigation District, El Centro; and F. Udwadia of the University of Southern California, Los Angeles.

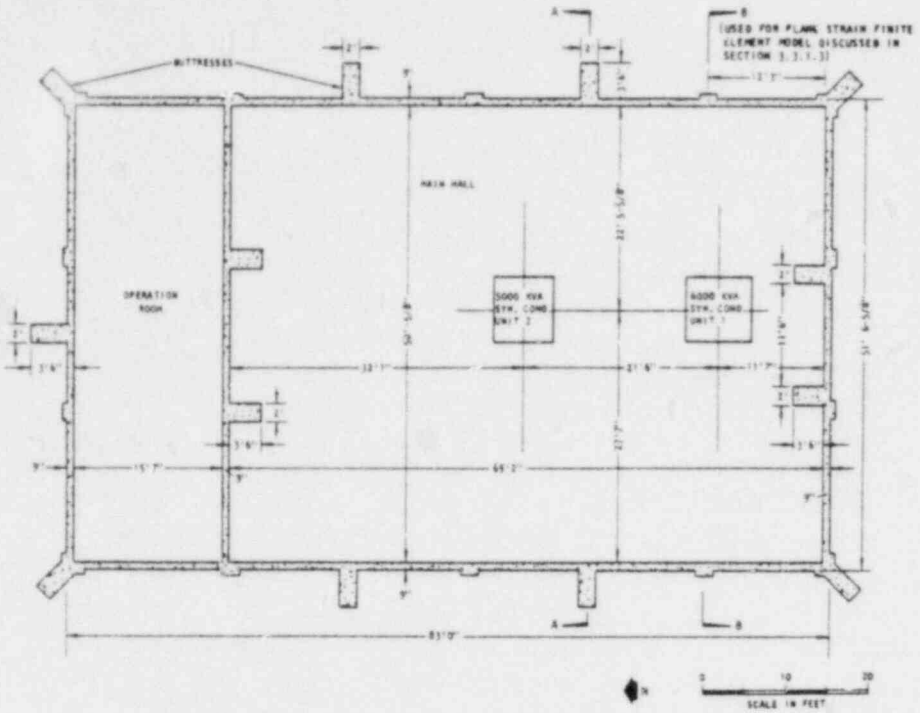

(a) Main floor plan

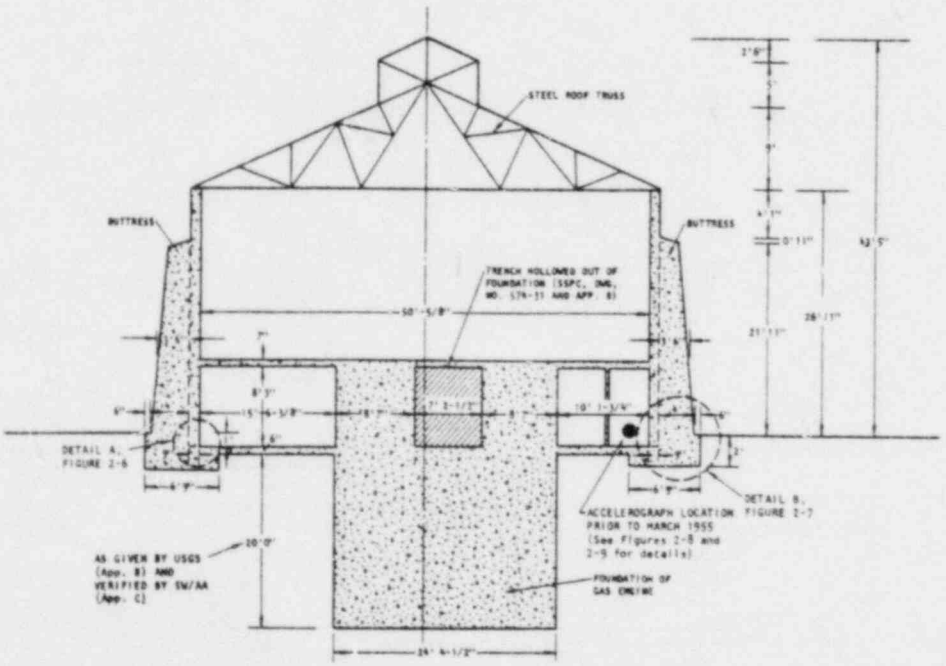

(b) Section A-A

FIGURE 2-5. PLAN VIEWS AND CROSS SECTIONS OF EL CENTRO TERMINAL SUBSTATION BUILDING (SSPC, 1926)

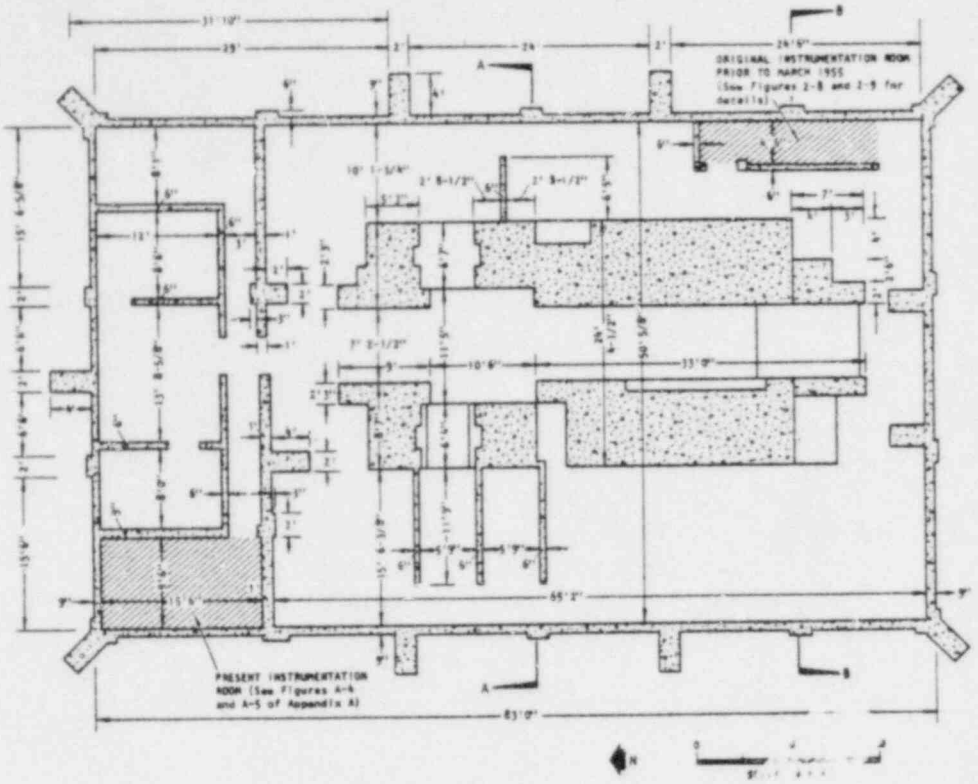

(c) Basement plan

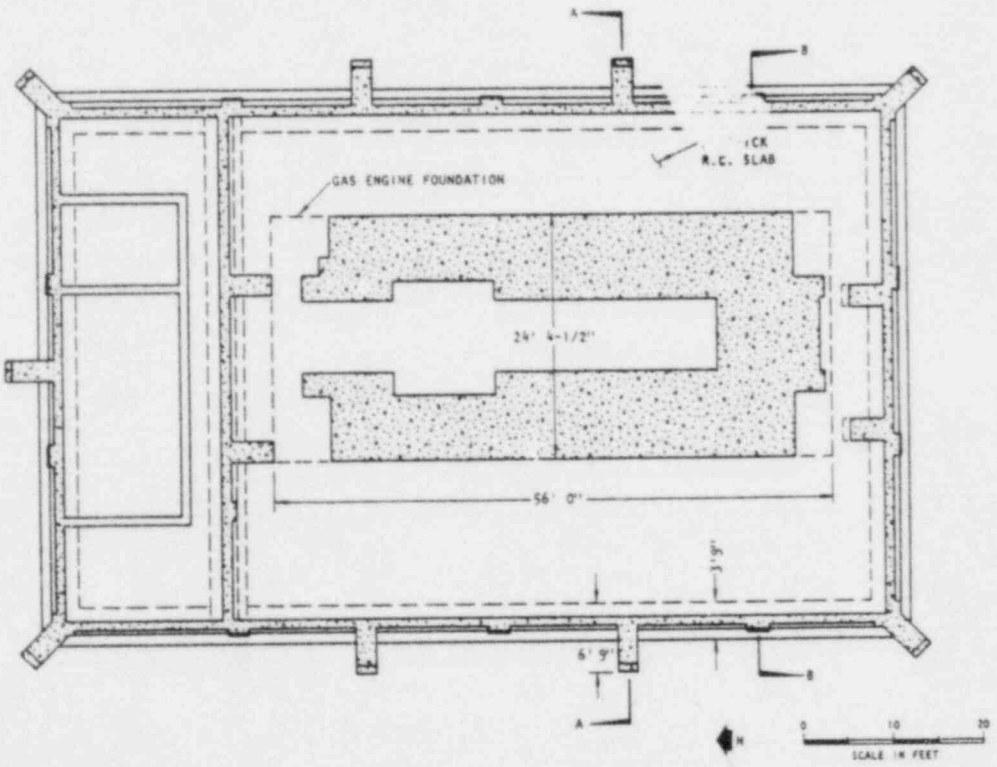

(d) Wall and gas engine foundations

FIGURE 2-5. (CONCLUDED)

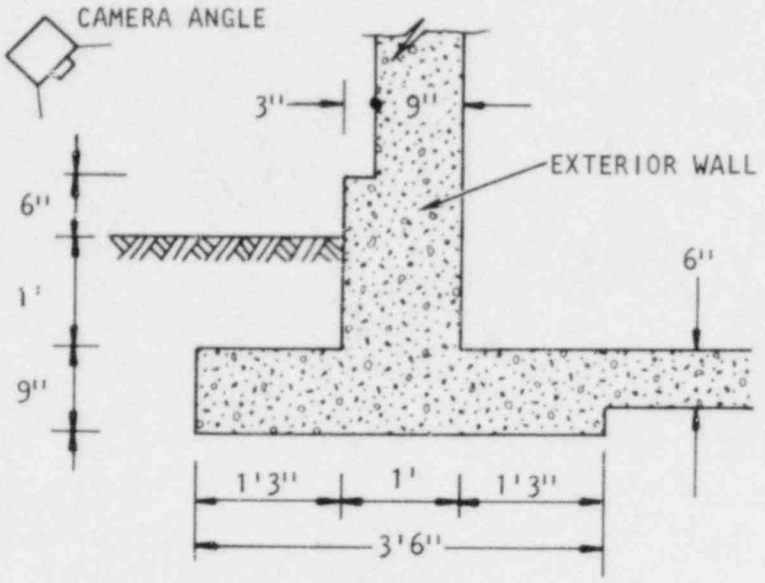

(a) Detail A of foundation for 9" exterior walls

(b) Photograph of details of foundations for exterior wall

FIGURE 2-6. DETAIL OF EXTERIOR WALL

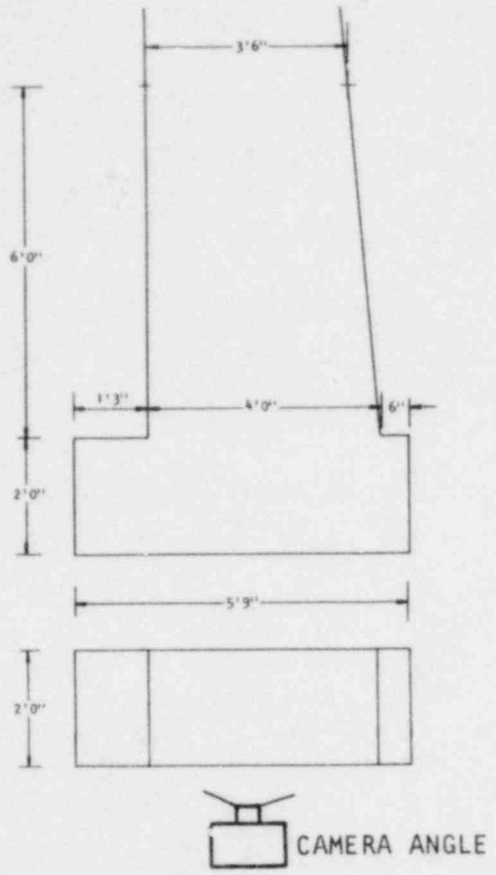

(a) Detail B of buttresses

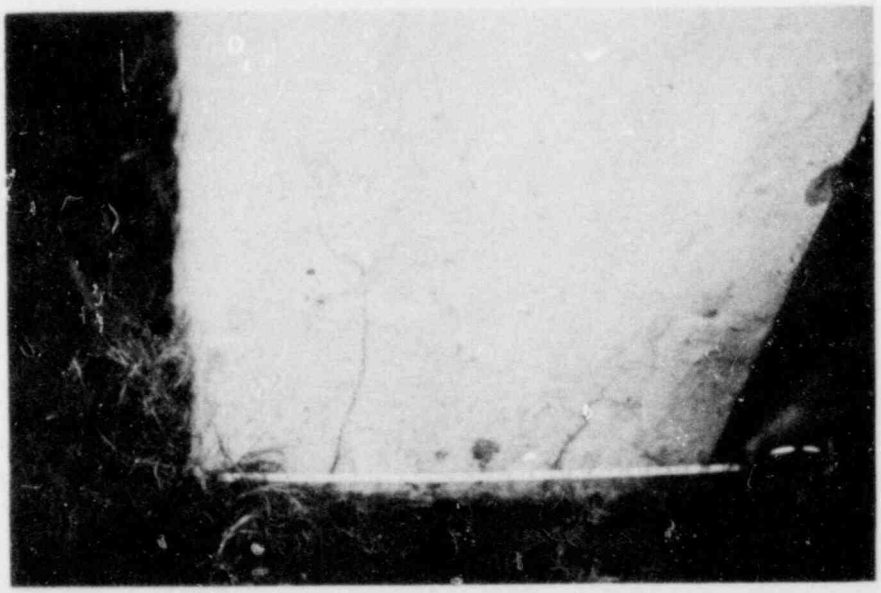

(b) Photograph of details of buttresses

FIGURE 2-7. DETAIL OF BUTTRESSES

2.1.2 INSTRUMENTATION

In July 1932 a Coast and Geodetic Survey strong motion accelerograph was installed in the operating building of the Terminal Substation. This device, mounted on a concrete pier, functioned for several years beneath the stairway that leads to the main floor in the southeastern portion of the building (Figs. 2-8 and 2-9). The strong ground motions of the 1940 El Centro earthquake were recorded while the accelerograph installation was still in this location.

On 25 November 1952, a Carder displacement meter was added to the facilities. On 17 March 1955, the accelerograph and Carder displacement meter were relocated to the northwestern section of the building and a second displacement meter was added to the instrumentation. A seismoscope was installed about 1964. Details of the current instrumentation are presented in Appendix A.

Many alterations have been made to the original instrumentation. For example, accelerographs and recorders have been replaced and upgraded. In both the prior and the present locations, the accelerographs have measured components of motion oriented in the vertical, north-south, and east-west directions (Perez and Schwartz, 1973).

2.2 SITE DESCRIPTION

This subsection contains a brief summary of the geology and faulting, seismic history, and subsurface conditions at El Centro. These items are discussed more fully in SW/AA (1976).

2.2.1 GEOLOGY AND FAULTING

El Centro lies in the central portion of the Salton Trough, an arid, low-lying depression that extends southeastward from the San Bernardino Mountains (of the Transverse Ranges) to the Gulf of California. The Salton Trough is bounded by the Peninsular Ranges in the west and the Mohave Desert

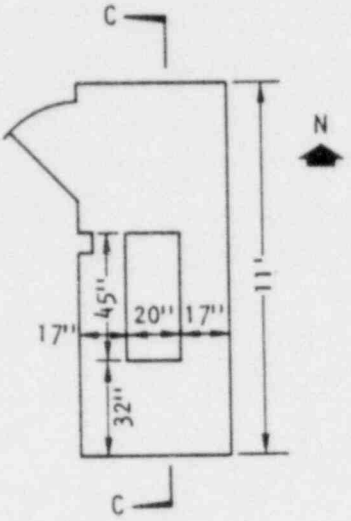

(a) Plan

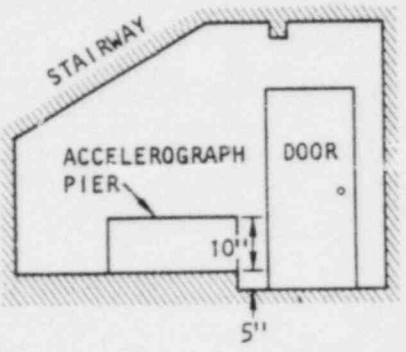

(b) Section C-C

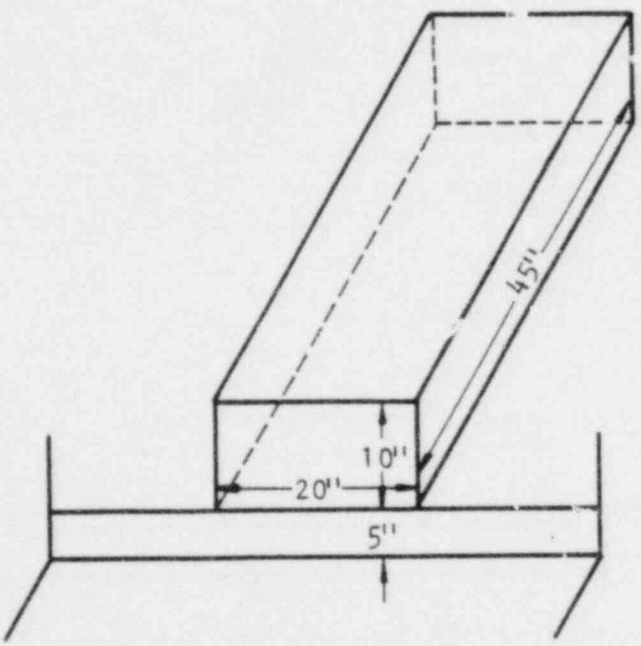

(c) Solid unreinforced concrete mounting pier

FIGURE 2-8. LAYOUT OF INSTRUMENTATION ROOM (Prior to March 1955)

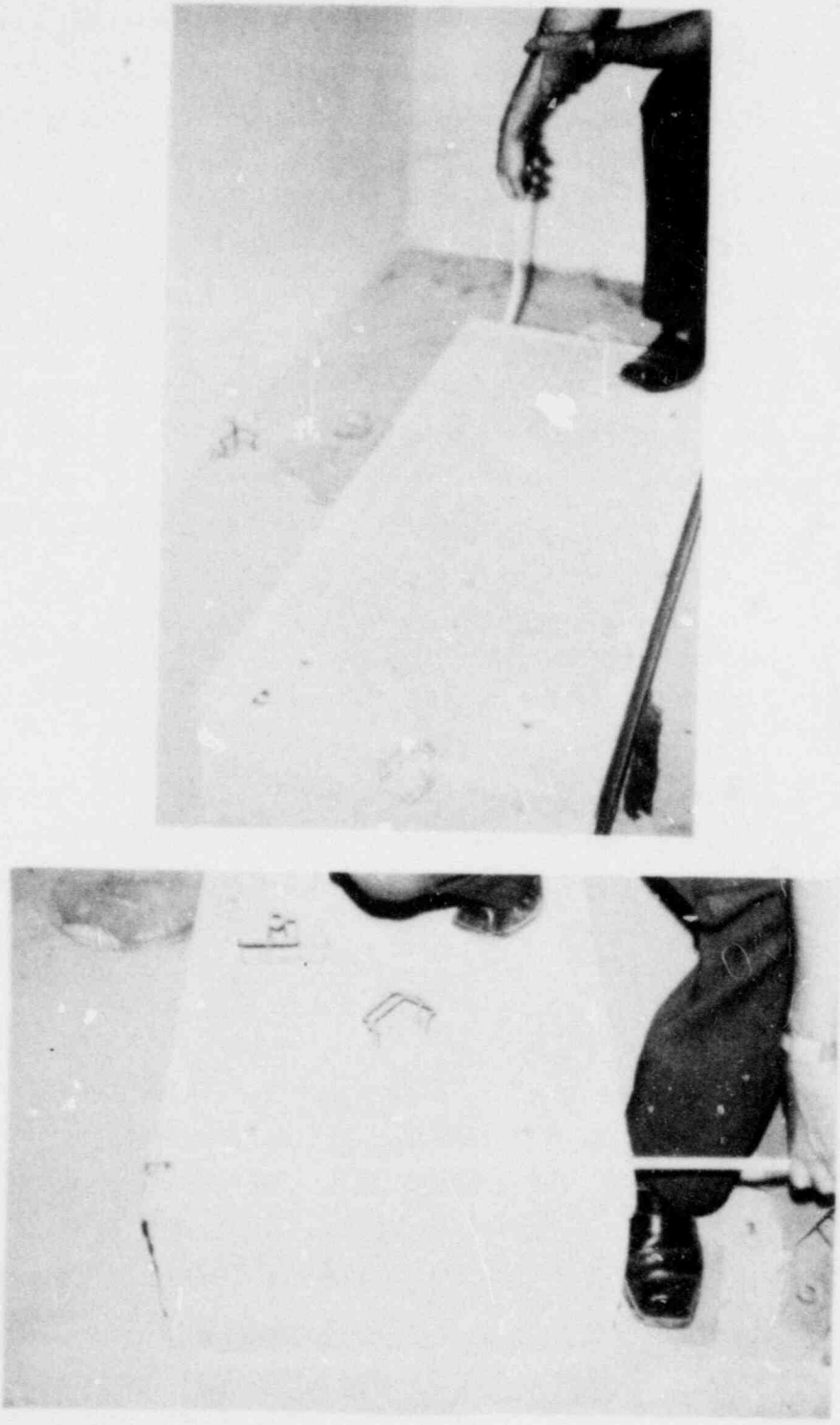

NOTE: Accelerograph was mounted on 10-in. high pier

FIGURE 2-9. INTERIOR OF INSTRUMENTATION ROOM

in the east. It consists of Tertiary-to-Quaternary sedimentary rocks and alluvial deposits that overlie a basement complex of varied pre-Cenozoic metasedimentary rocks, metamorphic rocks, and intrusive igneous rocks.

The Imperial Valley and Salton Trough region are cut by a number of recently active, high-angle, northwest-trending faults or fault zones, all of which are of the right-lateral, strike-slip variety (Fig. 2-10). Faults with a historic record of surface displacement include the San Jacinto fault, Imperial fault, Superstition Hills fault, and Coyote Creek fault, all of which are regarded by some as belonging to the San Jacinto fault system. Magnitude 6.5 earthquakes were triggered along the Imperial fault near El Centro (in 1940), along the Coyote Creek fault in the Borrego Mountains (in 1968), and along the San Jacinto fault in Mexico (in 1934).

Other faults are shown in Figure 2-9 that exhibit evidence of displacements during Quaternary time but have no historic record of movement; these include the Superstition Mountain fault, Brawley fault, Calipatria fault, and the faults comprising the Elsinore fault system. Except for the slippage triggered by the 1968 Borrego Mountain earthquake, the San Andreas fault has no detectable record of Quaternary displacements south of the Salton Sea.

2.2.2 SEISMIC HISTORY

Because it has operated in a seismically active zone over a period of 45 years (since 1932), the Terminal Substation accelerograph in El Centro has measured several significant records of strong ground shaking. Earthquakes with magnitudes as high as 6.5 have been recorded, many of which were centered near El Centro. The proximity of the major faults to the recorded El Centro earthquake epicenters is shown in Figure 2-10).

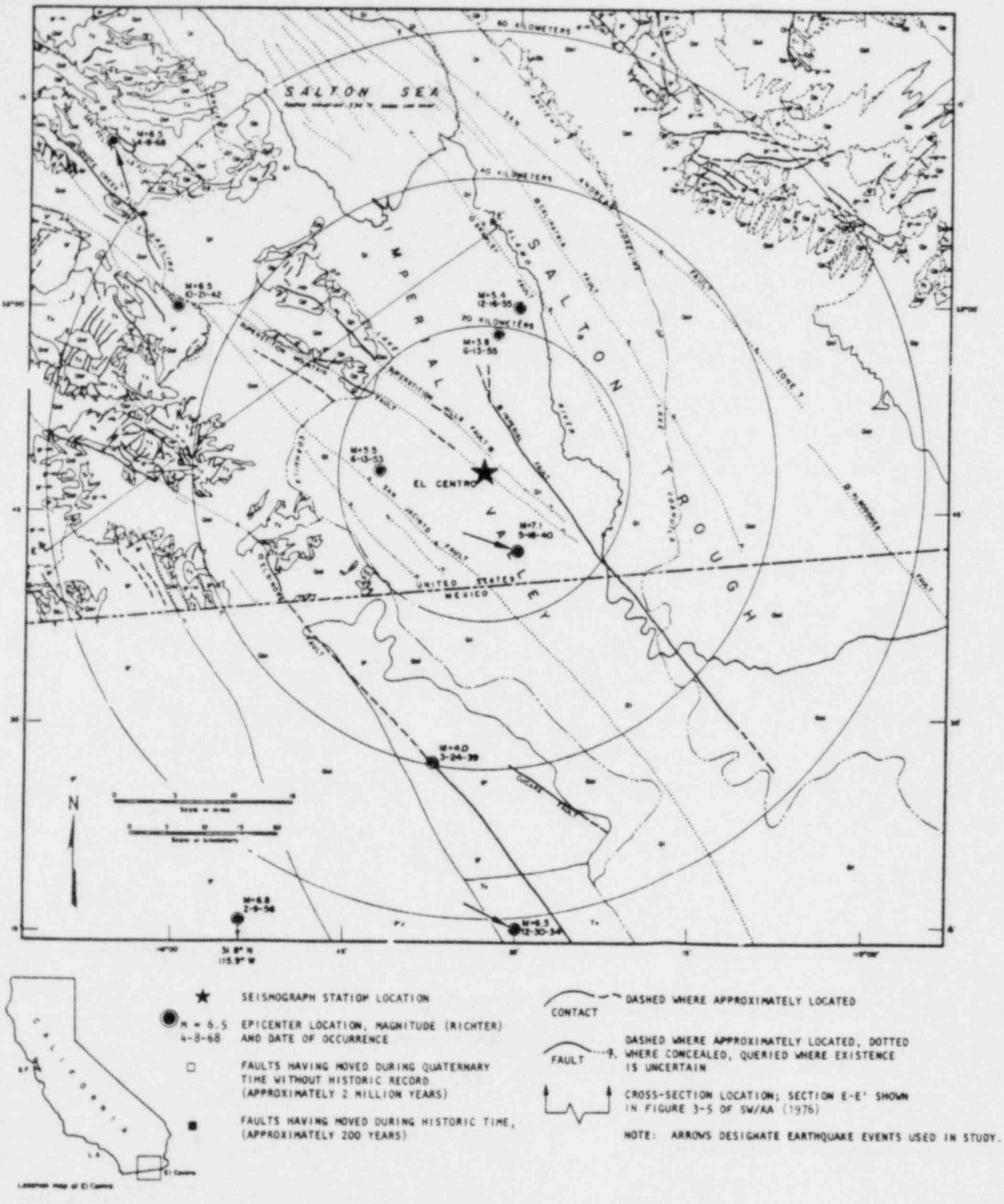

FIGURE 2-10. EL CENTRO ACCELEROGRAPH LOCATION, PROXIMITY OF MAJOR FAULTS AND HISTORICAL EARTHQUAKES (SW/AA, 1976)

2.2.3 SUBSURFACE CONDITIONS

The subsurface conditions at the site of the El Centro Terminal Substation have been defined from the SW/AA (1976) geotechnical investigations. The investigation included boring and sampling of the subsurface soil materials to a depth of 400 ft; locations of the SW/AA borings within the Terminal Substation site are shown in Figure 2-3. Field and laboratory tests of these materials were conducted to define index properties, shear strengths, dry densities, standard-penetration resistances, and shear-wave velocities. The in-situ impulse test (see SW/AA, 1975b; Werner and Van Dillen, 1977; Troncoso et al., 1977) was also carried out in the field, to a depth of 140 ft. In the laboratory, resonant-column tests were conducted for soil materials to a depth of 180 ft; cyclic triaxial tests were carried out for samples taken at depths of 40 ft, 115 ft, and 175 ft.

The boring log and the results of the field and laboratory tests are summarized in Figures 2-11 and 2-12. These data indicate that within the 400 ft depth of the boring, the El Centro site profile consists primarily of silty clays with some layers of fine sand. Small-strain shear-wave velocities for these materials increase from about 400 fps at the ground surface to 1400 fps at a depth of 400 ft. SW/AA (1976 and 1977c) provides further discussion of the dynamic characteristics of these materials.

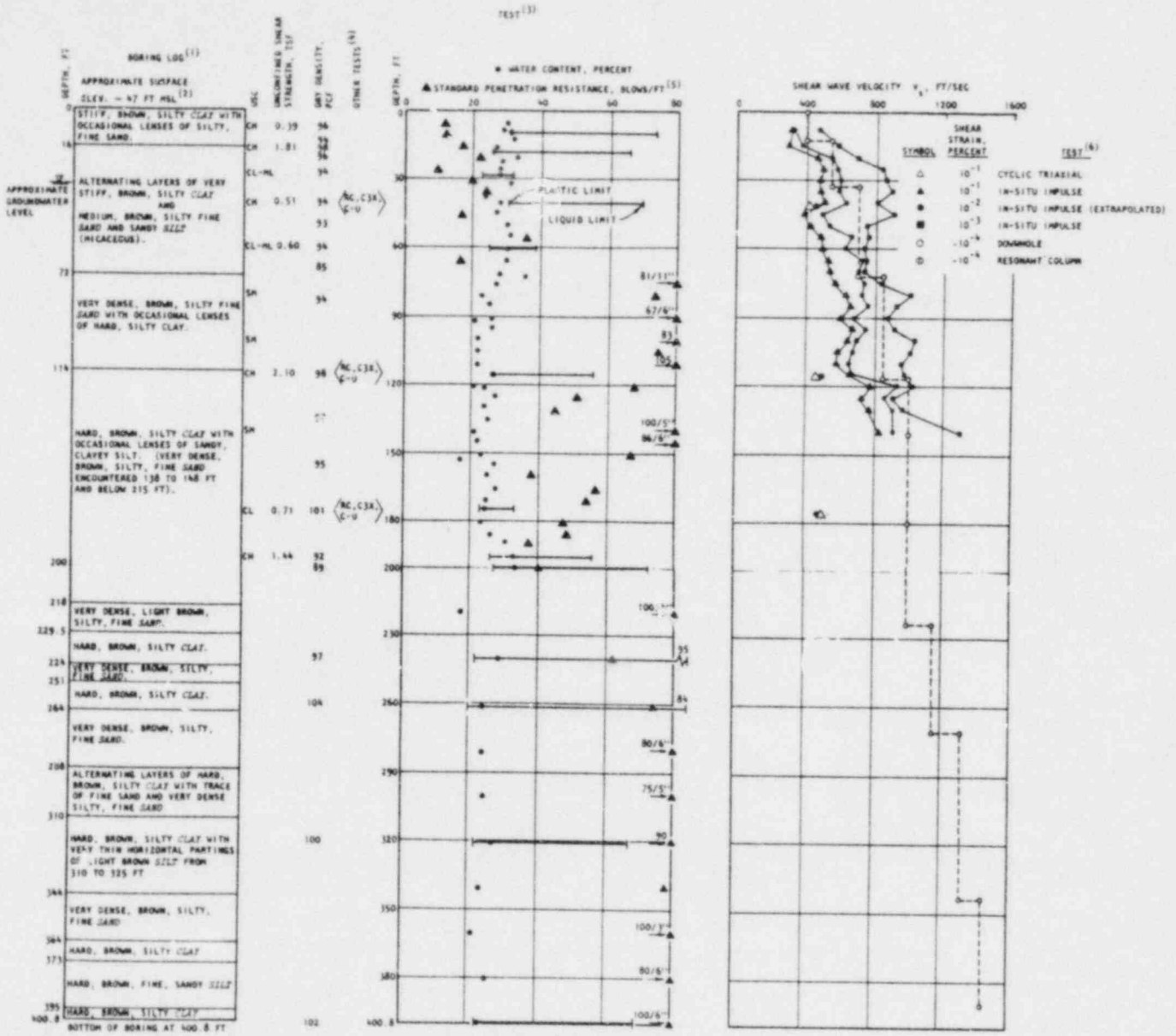

NOTES:

(1) THE STRATIFICATION LINES IN THE BORING LOG REPRESENT THE APPROXIMATE BOUNDARIES BETWEEN SOIL TYPES, AND THE TRANSITION MAY BE GRADUAL.

(2) ELEVATION OBTAINED BY HAND LEVELING FROM USGS B.M. (ELEV. 953.72) AT RAILWAY STATION (SEE SW/AA [1976], FIG. 3-1).

(3) LABORATORY TESTS PERFORMED ON SAMPLES FROM INDICATED DEPTH (SEE SW/AA [1976], APP. 3C).

(4) OTHER TESTS (SEE SW/AA [1976], APP. 3C):
RC RESONANT COLUMN
C3X CYCLIC TRIAXIAL
C-U CONSOLIDATED-UNDRAINED TRIAXIAL

(5) BLOW COUNT BASED ON 140 LB HAMMER FALLING 30 IN.

(6) FIELD V_s VALUES CONTAINED IN SW/AA (1976), APPENDIX 3B. V_s DETERMINED FROM LABORATORY TESTS BY THE FOLLOWING:

$$V_s = \sqrt{G/\rho} = \sqrt{E/2(1+\mu)\rho}$$

FIGURE 2-11. BORING LOG AND PROFILE OF SOIL TEST RESULTS--EL CENTRO ACCELEROGRAPH STATION SITE (SW/AA, 1976)

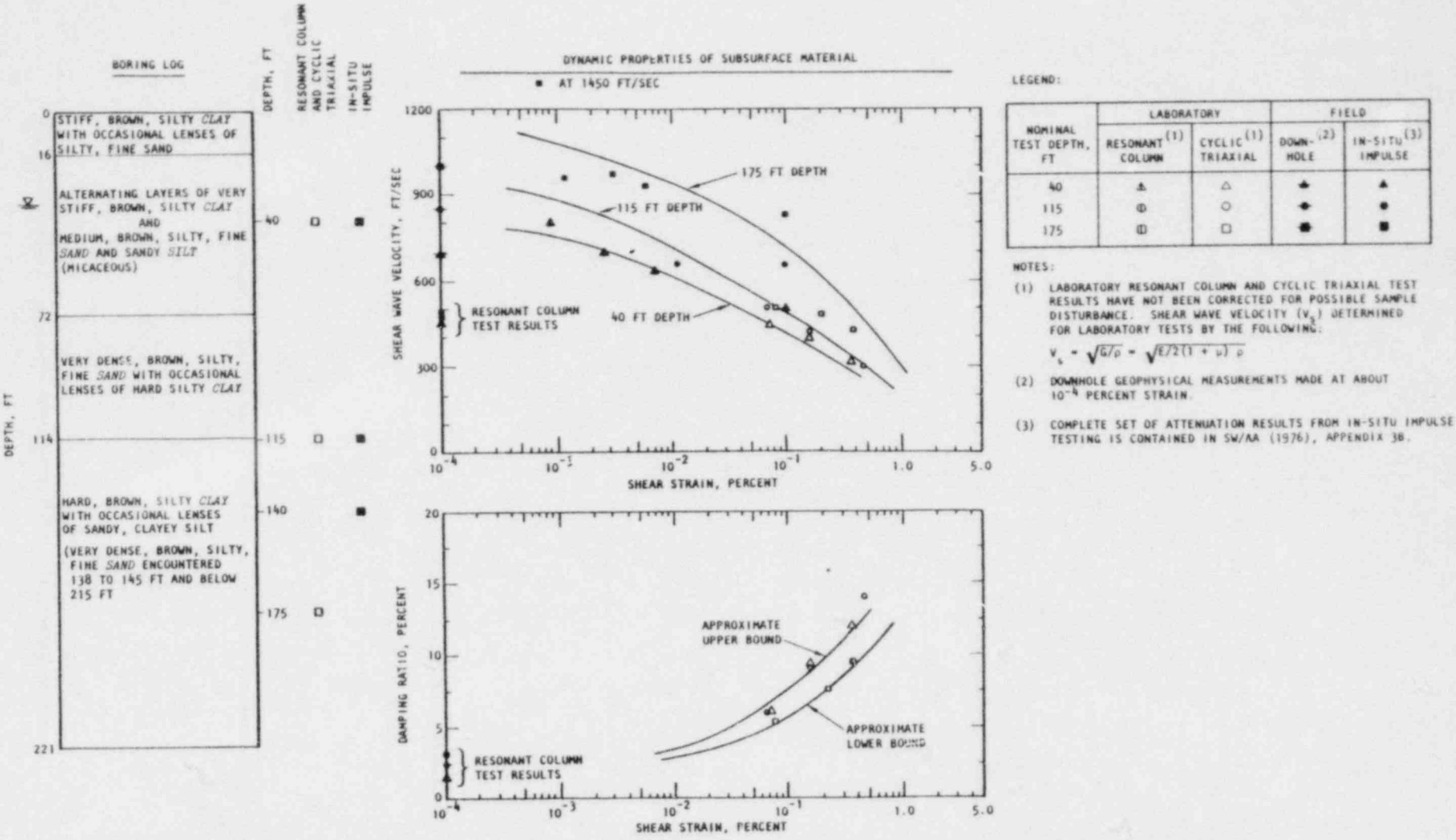

LEGEND:

NOMINAL TEST DEPTH, FT	LABORATORY		FIELD	
	RESONANT COLUMN (1)	CYCLIC TRIAXIAL (1)	DOWN-HOLE (2)	IN-SITU IMPULSE (3)
40	▲	△	▲	▲
115	◐	○	●	●
175	◨	□	■	■

NOTES:

(1) LABORATORY RESONANT COLUMN AND CYCLIC TRIAXIAL TEST RESULTS HAVE NOT BEEN CORRECTED FOR POSSIBLE SAMPLE DISTURBANCE. SHEAR WAVE VELOCITY (V_s) DETERMINED FOR LABORATORY TESTS BY THE FOLLOWING:

$$V_s = \sqrt{G/\rho} = \sqrt{E/2(1+\mu)\rho}$$

(2) DOWNHOLE GEOPHYSICAL MEASUREMENTS MADE AT ABOUT 10^{-4} PERCENT STRAIN.

(3) COMPLETE SET OF ATTENUATION RESULTS FROM IN-SITU IMPULSE TESTING IS CONTAINED IN SW/AA (1976), APPENDIX 3B.

FIGURE 2-12. STRAIN-DEPENDENT DYNAMIC PROPERTIES AND BORING LOG FOR UPPER 221 FT AT EL CENTRO ACCELEROGRAPH SITE (SW/AA, 1976)

CHAPTER 3

ANALYSIS AND MODELING PROCEDURES

3.1 SCOPE OF ANALYSES

As noted in Chapter 1 two sets of calculations were carried out to assess soil/structure interaction effects at the El Centro Terminal Substation. The first involves a free-field analysis and the second involves a soil/structure system analysis using the same input motions, site soil model, and assumptions regarding the nature of the seismic wave propagation in the vicinity of the structure. The procedures and site models used to carry out these two sets of calculations using the SHAKE and FLUSH codes and the TRI/SAC code are described in this chapter.

3.2 ANALYSIS TECHNIQUES

3.2.1 *SHAKE* AND *FLUSH* CODES

3.2.1.1 General Description

The first procedure used to assess soil/structure interaction effects at the El Centro Terminal Substation site involved the use of the SHAKE and FLUSH codes to analyze the free-field response and the soil/structure system response respectively. These codes consider the soil medium to be comprised of a system of horizontal viscoelastic layers of infinite horizontal extent that are subjected to input motions from vertically incident shear waves or compression waves. An iterative solution technique is employed in both codes in conjunction with an equivalent linear model to represent the strain dependence of the material properties of each soil layer. In this iterative approach, the solution is carried out in the frequency domain and is then transformed back into the time domain through the use of Fast Fourier Transform techniques (Cooley and Tukey, 1965).

The following subsections further describe the equivalent linear model and corresponding iterative solution technique common to both codes, together with summaries of the features of each code.

3.2.1.2 Equivalent Linear Model and Solution Technique

The equivalent linear model was developed by Seed and Idriss (1969) as an approximate means for representing the strain dependence of the dynamic properties of each soil layer or element. This model uses an iterative solution technique in conjunction with two equivalent linear parameters--the shear modulus and damping ratio. These parameters are defined for each soil layer or element from the nonlinear cyclic behavior of the material in that layer or element, as shown in Figure 3-1. They are assumed to be independent of frequency and dependent only on strain level.

The iterative approach used in conjunction with the equivalent linear model involves initially assuming the shear modulus and damping ratio for each layer or element. Then the system is analyzed using these properties, and acceleration and strain time histories are computed throughout the soil deposit. From these time histories, effective soil-strain amplitudes are estimated in each soil element, and curves similar to Figure 3-1b are consulted to see if the moduli and damping values used in the response evaluation are compatible with the strains developed. If the soil properties are not compatible, these curves are used to provide improved values of moduli and damping for the next iteration and the process is repeated until convergence has occurred, usually within three to five iterations. The response from the last iteration is considered to correspond to the nonlinear response.

An important feature of this iterative approach is the manner in which the system response is analyzed for a given set of assumed soil properties. In both FLUSH and SHAKE codes, this analysis is carried out in the frequency domain, i.e., utilizing the Fourier Transform of the input motions to represent these motions as the superposition of harmonic signals of different frequencies. The frequency-dependent transfer function of the system is obtained by computing the response of the system to unit harmonic input

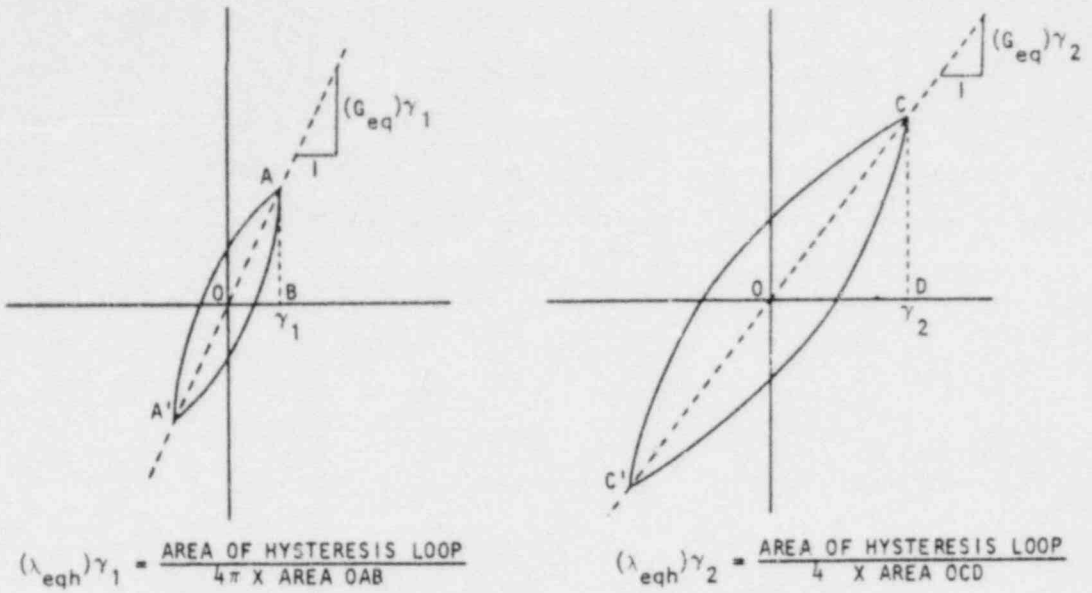

(a) Determination of equivalent shear modulus, G_{eq}, and damping ratio, λ_{eqh}

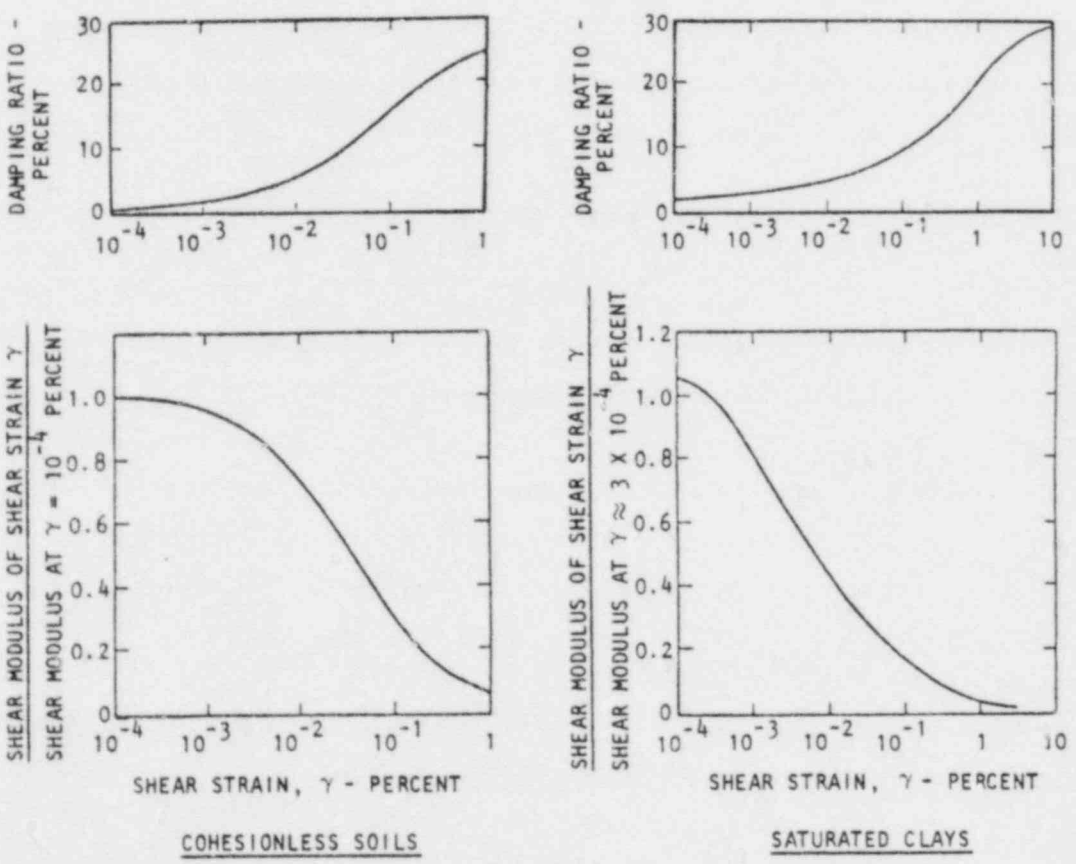

(b) Typical curves used to define strain-dependent properties

FIGURE 3-1. EQUIVALENT LINEAR METHOD (Seed and Idriss, 1969)

motions. The time-dependent system response to the actual input motions is then obtained as the inverse Fourier Transform of the product of the system transfer function and the various harmonic signals that comprise the input motion. As noted previously, Fast Fourier Transform procedures are used to carry out the required transformations between the time and frequency domains.

3.2.1.3 SHAKE Code

To analyze the free-field response of a horizontally layered site subjected to vertically incident shear waves or compression waves, SHAKE employs a continuum solution to the one-dimensional wave equation (Kanai, 1950). This solution is used to compute the frequency-dependent transfer function of the soil deposit which, as described above, is used with Fast Fourier Transform techniques to compute the response of the soil deposit to transient input motion.

Input motions for the SHAKE code can be specified at any location within the site profile in one of the following ways:

a. By directly specifying input motions at a rock-like medium at the base of the soil layers.

b. By first defining motions along the surface of rock outcropping and then computing corresponding subsurface motions in an identical rock medium a given distance below the surface. This computation is based on the difference in boundary conditions between the free rock surface and the subsurface rock medium that is constrained by the overlying soil layers.

c. By a deconvolution procedure which consists of defining input motions at the surface soil layer and then using the wave equation to compute corresponding subsurface motions. However Schnabel et al. (1972) indicate that results from this procedure can be quite sensitive to small differences in surface input motions or in subsurface soil properties.

The corresponding response of the site can be obtained at any location in terms of strain levels of the soil medium as well as time histories and spectra of the response motions. Since the solution technique employed in SHAKE is one dimensional, only a single component of motion can be computed at any location (horizontal, for vertically incident shear waves, or vertical, for vertically incident compression waves).

3.2.1.4 FLUSH Code

The FLUSH code computes the two-dimensional response of a soil/structure system in which, as previously noted, the soil medium is comprised of a system of homogeneous viscoelastic soil layers of infinite horizontal extent. The system is subjected to only vertically incident shear waves or compression waves.

A two-dimensional finite element model is used to represent the soil/structure system. This system can be modeled using either a conventional plane strain model or a modified two-dimensional model which attempts to simulate three-dimensional wave propagation effects through the use of in-plane viscous dampers attached to each node point of the soil medium (Sec. 3.3.1.3). For either of these modeling procedures, the structure is represented as a combination of two-dimensional elastic planar elements and elastic beam elements, while the soil medium is represented using plane strain finite elements bounded by a rigid base and by transmitting boundaries along the sides of the soil grid.

The above finite element grid is used in the FLUSH code to define the frequency-dependent transfer function of the soil/structure system which, in turn, is used in the computation of the system response (Sec. 3.2.1.2). Input motions are applied at the rigid base of the grid as horizontal motions (from vertically incident shear waves) or as vertical motions (from vertically incident compression waves) but not both simultaneously. The system response is defined in terms of time histories and spectra of motions at any location, as well as stress and strain levels.

3.2.2 TRI/SAC CODE

3.2.2.1 General Description

The TRI/SAC code is a general purpose technique for two-dimensional or three-dimensional analyses of structural systems using the finite element approach. The code incorporates a variety of different element types and analysis capabilities as described in AA (1976) and summarized below.

The element types included in TRI/SAC are trusses, beams, membranes, axisymmetric solids, three-dimensional solids, plates, shells, and nonlinear springs and dashpots. More general types of elements may be obtained by combinations of these elements. The structural elements in TRI/SAC were taken from the SAP code, which was first developed under the direction of Professor E.L. Wilson at the University of California, Berkeley (Wilson, 1970).

TRI/SAC can carry out several different types of analyses including static response, dynamic response by the normal mode method, dynamic response by the direct integration method, response spectral analyses, and determination of mode shapes and frequencies. The program includes a capability for the solution of certain nonlinear dynamic problems by the direct integration method.

3.2.2.2 Application in Present Study

In this study, TRI/SAC is used to assess soil/structure interaction effects at the El Centro Terminal Substation accelerograph site through the use of two-dimensional dynamic analyses of the soil profile itself (to compute free-field motions) and soil/structure system (to compute the structure response). The direct integration approach is used for these analyses. This approach involves integrating the equations of motion directly with respect to time.

In using TRI/SAC to carry out such two-dimensional analyses, the soil medium can be simulated as an assemblage of membrane elements and the structure can be represented as any combination of planar, beam, or truss elements. The side and bottom boundaries of the soil grid can be either free, fixed, or attached to a special energy-absorbing damper to prevent unwanted reflections from these artificial boundaries. Input motions in the form of horizontal and vertical acceleration, velocity, or displacement time histories can be specified independently at any location(s) in the grid.

The direct integration approach incorporated in TRI/SAC is a modified form of the linear acceleration method, with a parameter selected by the user to control higher mode damping introduced by the integration process. In this, an integration time step is selected based on consideration of costs, the highest frequency of interest in the analysis, and the principal characteristics of the input motion time variation. The TRI/SAC direct integration approach is unconditionally stable with regard to time step.

3.2.3 COMPARISONS OF ANALYSIS TECHNIQUES

The capabilities of SHAKE and FLUSH codes and of TRI/SAC code, with regard to their performing two-dimensional analyses of soil/structure systems, are compared in Table 3-1. This table shows that the most important advantages of the SHAKE and FLUSH codes is their ability to incorporate effects of the strain-dependent nature of the shear moduli and damping ratios, by means of the equivalent linear model. Also, the costs required to compute free field and structure motions as required for this study are much lower for SHAKE and FLUSH than for TRI/SAC. However, an important limitation of the SHAKE-FLUSH methodology is that they can consider only horizontally layered sites and horizontal or vertical motions solely from vertically incident shear waves or compression waves respectively. Also, in the FLUSH code, the input motions can be applied only along a rigid base of the soil grid.

TABLE 3-1. COMPARISONS OF *SHAKE/FLUSH* AND *TRI/SAC* CODES FOR CARRYING OUT TWO-DIMENSIONAL SOIL/STRUCTURE INTERACTION ANALYSES

Feature	SHAKE and FLUSH Codes	TRI/SAC Code
Analysis Procedure	One-dimensional continuum (SHAKE code) and two-dimensional finite element (FLUSH code).	Two-dimensional finite element. (Three-dimensional capability also available.)
Site Configuration	Horizontal layers of infinite extent. In FLUSH code, base of site profile must be rigid.	Arbitrary.
Soil Property Representation	Equivalent linear model to represent strain-dependent shear moduli and damping ratios.	Linear elastic. Soil material damping represented only from overall system Rayleigh damping matrix.
Solution Technique	In frequency domain (using Fast Fourier Transform technique). Iterative method assures soil element shear moduli and damping ratios compatible with computed soil strains.	In time domain (using direct integration of coupled equations of motion).
Input Motions	Horizontal *or* vertical motions from vertically incident shear waves or compression waves respectively.	Horizontal *and* vertical motions from any arbitrary combinations of waves.
Application of Input Motions	SHAKE: At any location along depth of soil profile. FLUSH: Along rigid base of soil grid only.	Can be applied independently at any location within grid.
Costs	Lower.	Higher.

The most important advantage of the TRI/SAC code is its generality in accommodating different types of input motions. Both horizontal and vertical motions that represent any types of seismic waves and directions of incidence can be defined at any location(s) in the grid. Also, the TRI/SAC code is not limited to considering only horizontal soil layers although, for the present investigation, this application is satisfactory. The primary limitation of TRI/SAC is its representation of the soil strata as linear elastic materials. Because of this, strain-dependent results from the SHAKE and FLUSH code have been used to guide the definition of linear elastic soil properties for the TRI/SAC calculations in this investigation.

3.3 MODELS

3.3.1 *SHAKE* AND *FLUSH* CODES

3.3.1.1 Soil Properties

The soil properties that form the basis for both the SHAKE and FLUSH models are depicted in Table 3-2 and in Figures 3-2 and 3-3. Table 3-2 shows that properties at the El Centro Terminal Substation Building site have been defined to a depth of 900 ft. Only the soil properties to a depth of 400 ft were actually measured for SW/AA; the properties of the lower strata were estimated as depicted in Table 3-2.

The strain-dependent shear moduli and damping ratios used to represent the clay and sand layers in the SHAKE and FLUSH models are shown in Figures 3-2 and 3-3. The shear modulus curves for the clay layers are based on average values from SW/AA in-situ impulse tests at three different depths; however since no in-situ impulse tests were conducted at depths corresponding to the sand layers, strain-dependent shear moduli for the sand layers were based on state-of-the-art curves (SW/AA, 1972) normalized to be consistent with small strain shear wave velocities measured at the site by

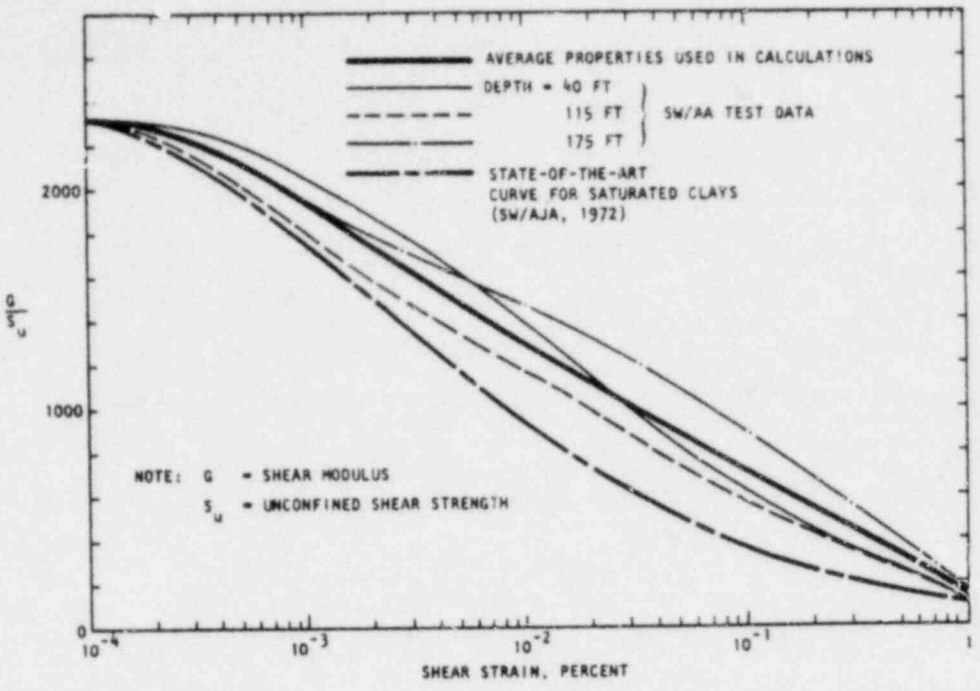

(a) Shear modulus

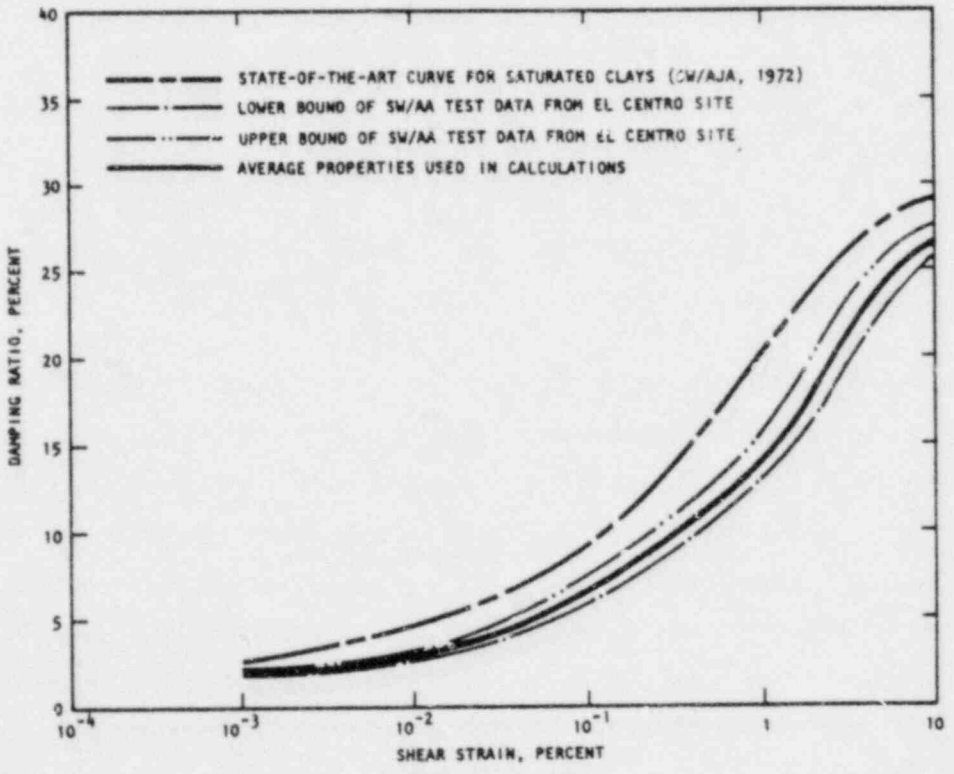

(b) Damping ratios

FIGURE 3-2. DYNAMIC SOIL PROPERTIES FOR CLAY MATERIALS IN UPPER 175 FT OF EL CENTRO SITE (SW/AA, 1976)

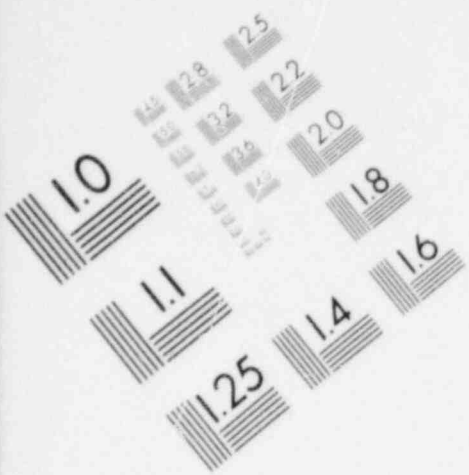

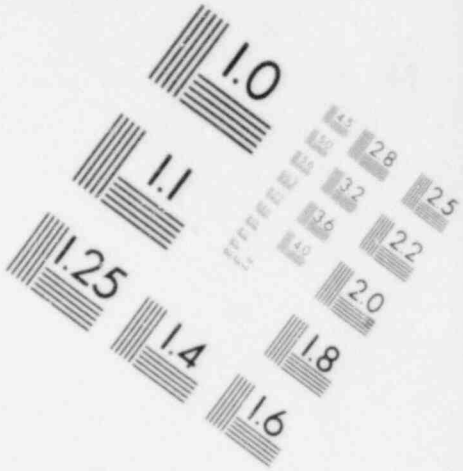

IMAGE EVALUATION
TEST TARGET (MT-3)

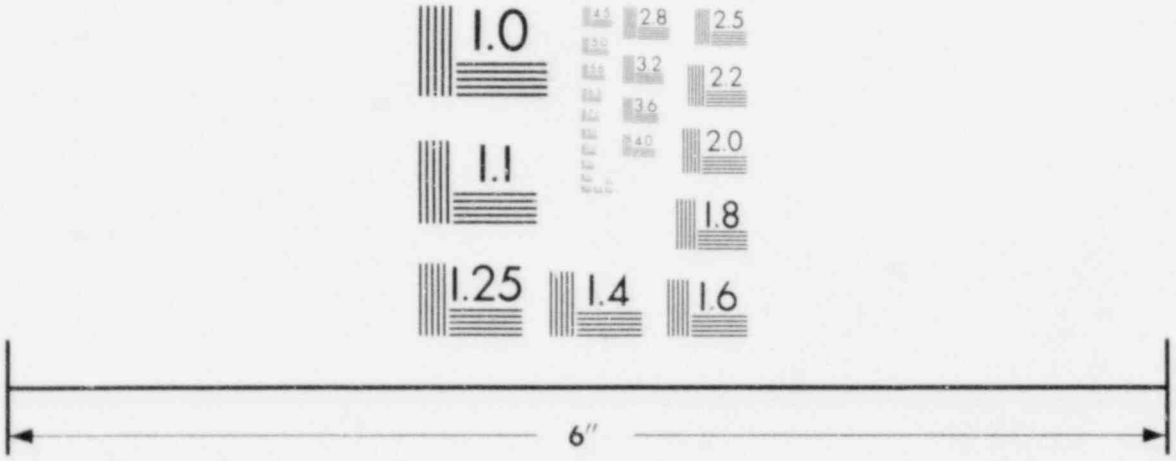

MICROCOPY RESOLUTION TEST CHART

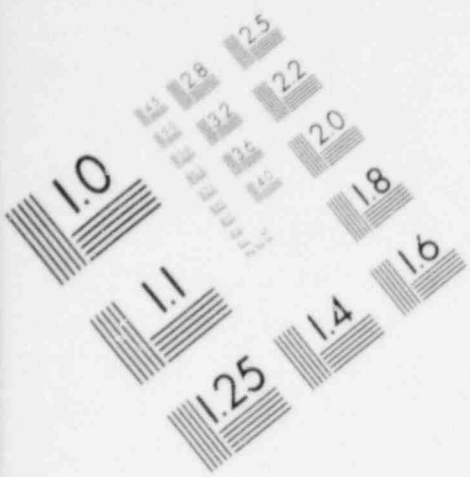

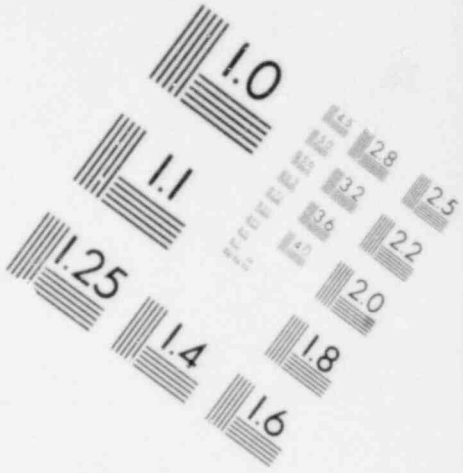

IMAGE EVALUATION
TEST TARGET (MT-3)

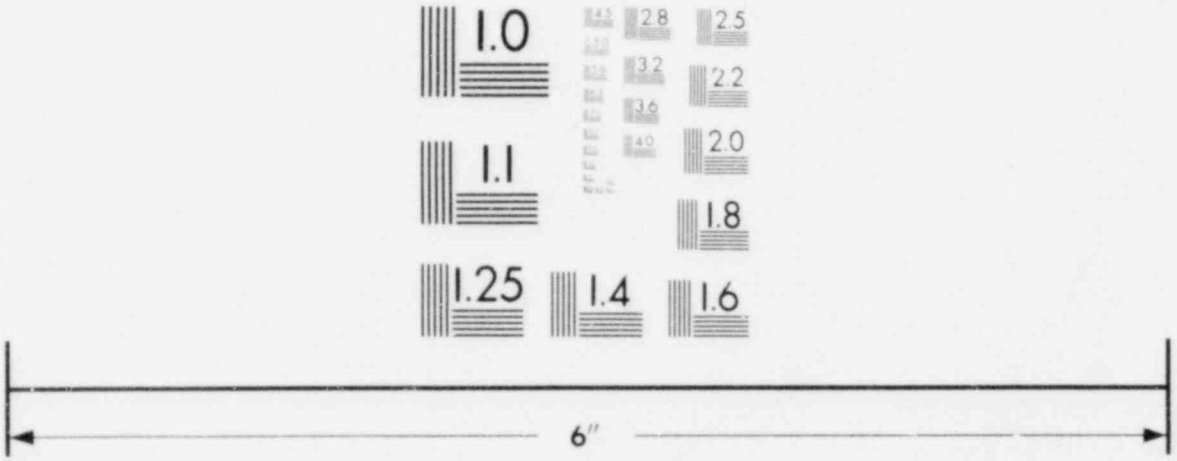

MICROCOPY RESOLUTION TEST CHART

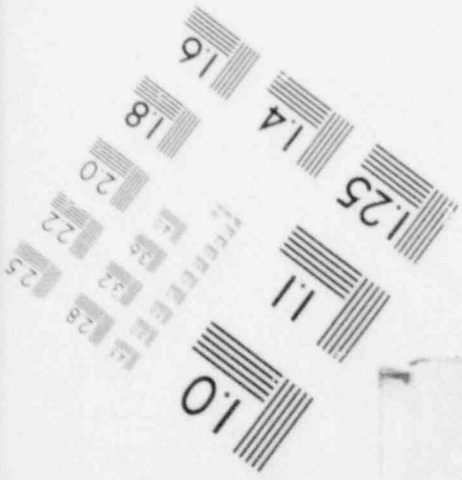

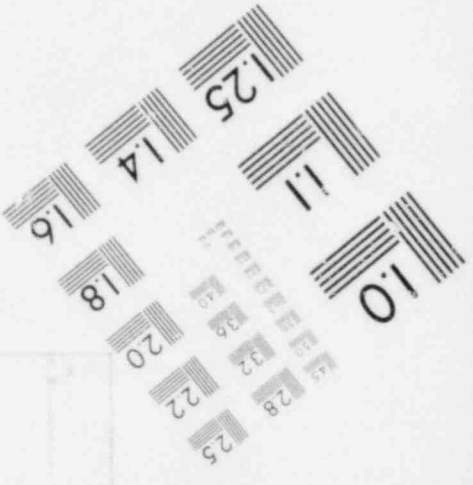

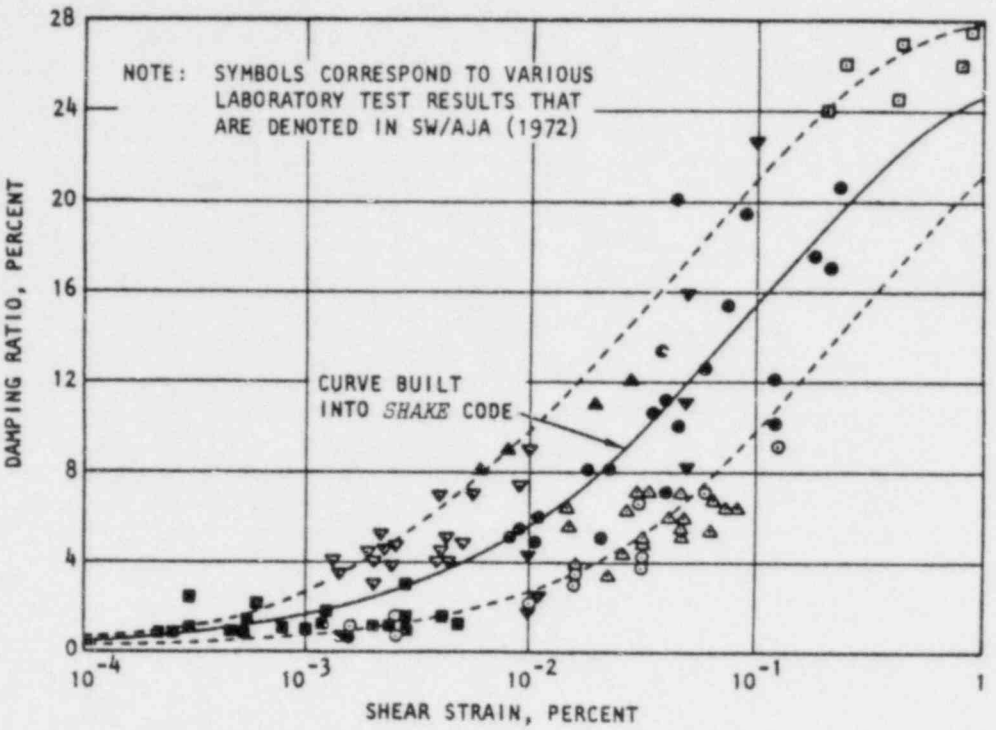

(a) Damping ratios for sands

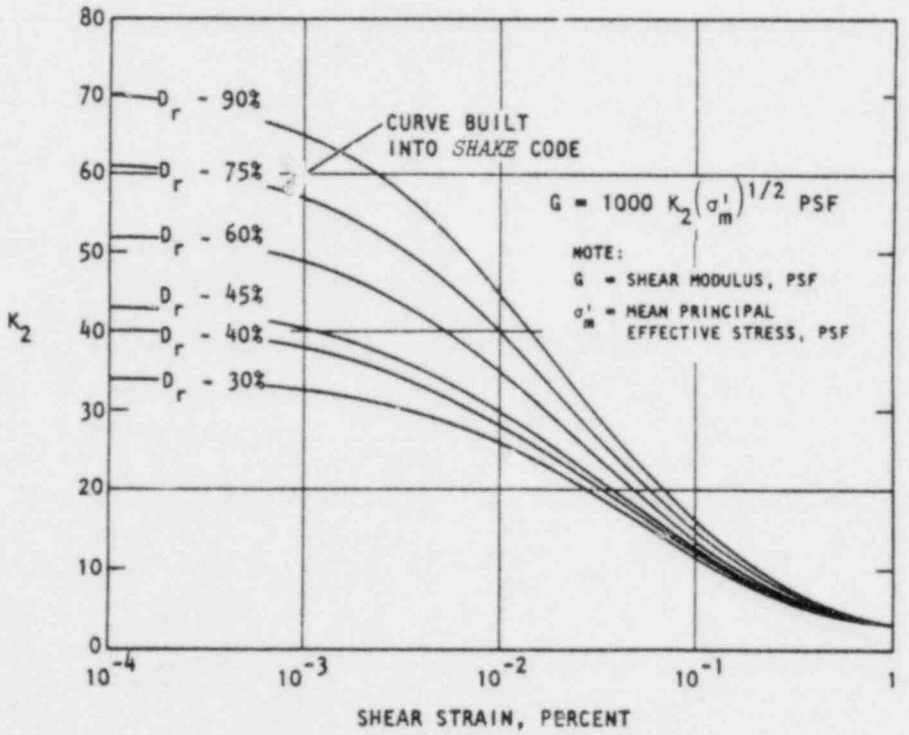

(b) Shear moduli of sands at different relative densities

FIGURE 3-3. STRAIN-DEPENDENT DAMPING RATIOS AND SHEAR MODULI FOR SANDS (SW/AJA, 1972)

TABLE 3-2. *SHAKE* MODELS FOR EL CENTRO ACCELEROGRAPH STATION SITE (SW/AA, 1976 and 1977c)

Elevation, ft	Layer Thickness, ft	Material Description	Layer No.	Material Type*	Number of Divisions in Sublayer	Unit Weight, pcf	Shear-Wave Velocity, fps
0							
	6	Stiff, brown silty clay with occasional lenses of silty, fine sand	1	1	1	120	350
-16	10		2		1		430
GWT	16	Alternating layers of very stiff, brown silty clay and medium brown, silty, fine sand and sandy silt	3	1	1	120	550
-60	28		4		1		800
	54	Very dense, brown, silty, fine sand with occasional lenses of hard, silty clay	5	2	1	122	850
-114							
	52	Hard, brown silty clay with occasional lenses of sandy, clayey silt	6	1	1	143	1000
	52	(Very dense, brown, silty fine sand encountered at depth of 138 ft to 148 ft)	7	1	1	143	1180
-218							
	70	Alternating layers of silty fine sand and hard brown silty clay	8	2	1	130	1250
	112	Alternating layers of hard brown silty clay and silty fine sand	9	1	1	127	1400
Base of 400 ft SHAKE Models		Bottom of Boring					
-400							
	500	Clay	10	1	1	130	1900
Base of 900 ft SHAKE Model							
-900							
Rock half-space for † V_s = 2500 fps							

NOTE:

* Material Type 1 corresponds to clay material and uses strain-dependent properties based on SW/AA (1976) test results (Fig. 3-2).

Material Type 2 corresponds to sand material and uses strain-dependent properties based on SW/AJA (1972) state-of-the-art curves to represent strain-dependent properties (Fig. 3-3)

† Model presumes soil materials extend to depth of 900 ft in which lowar 500 ft consists of clay materials with shear-wave velocity of 1900 fps. Underlying rock half-space is assumed to have shear-wave velocity of 2500 fps.

SW/AA using downhole tests. Similarly, strain-dependent damping ratios for the clay materials were based on SW/AA laboratory test results whereas, for sands, they were based on state-of-the-art curves.

3.3.1.2 SHAKE Code Model

The SHAKE code model for computing free-field motions consists of a one-dimensional continuum representation of the El Centro Terminal Substation site profile, to depths of 400 ft and 900 ft (see Table 3-2 and Chapt. 4). Each soil layer is divided into sublayers to provide an improved definition of the site response, particularly near the ground surface. Different sets of input motions were used in computing the site response, as discussed in Chapter 4.

3.3.1.3 FLUSH Code Model

Two different two-dimensional finite element models of the soil/structure system at the El Centro Terminal Substation site have been developed for use with the FLUSH code to compute the system response. The first corresponds to a plane strain model of the system, and the second is a modified two-dimensional (2-D) model which, as noted previously, uses in-plane viscous dampers at the soil node points to simulate three-dimensional wave propagation effects. The grid configuration is the same for each model; only the element properties vary to reflect the two different modeling procedures.

The paragraphs that follow describe first the FLUSH code grid and then the plane strain and modified 2-D modeling procedures.

a. Finite Element Grid

The finite element grid configuration for both FLUSH code models of the soil/structure system is shown in Figures 3-4 and 3-5. Figure 3-4 shows the overall grid and the particular node points at which responses were monitored during the

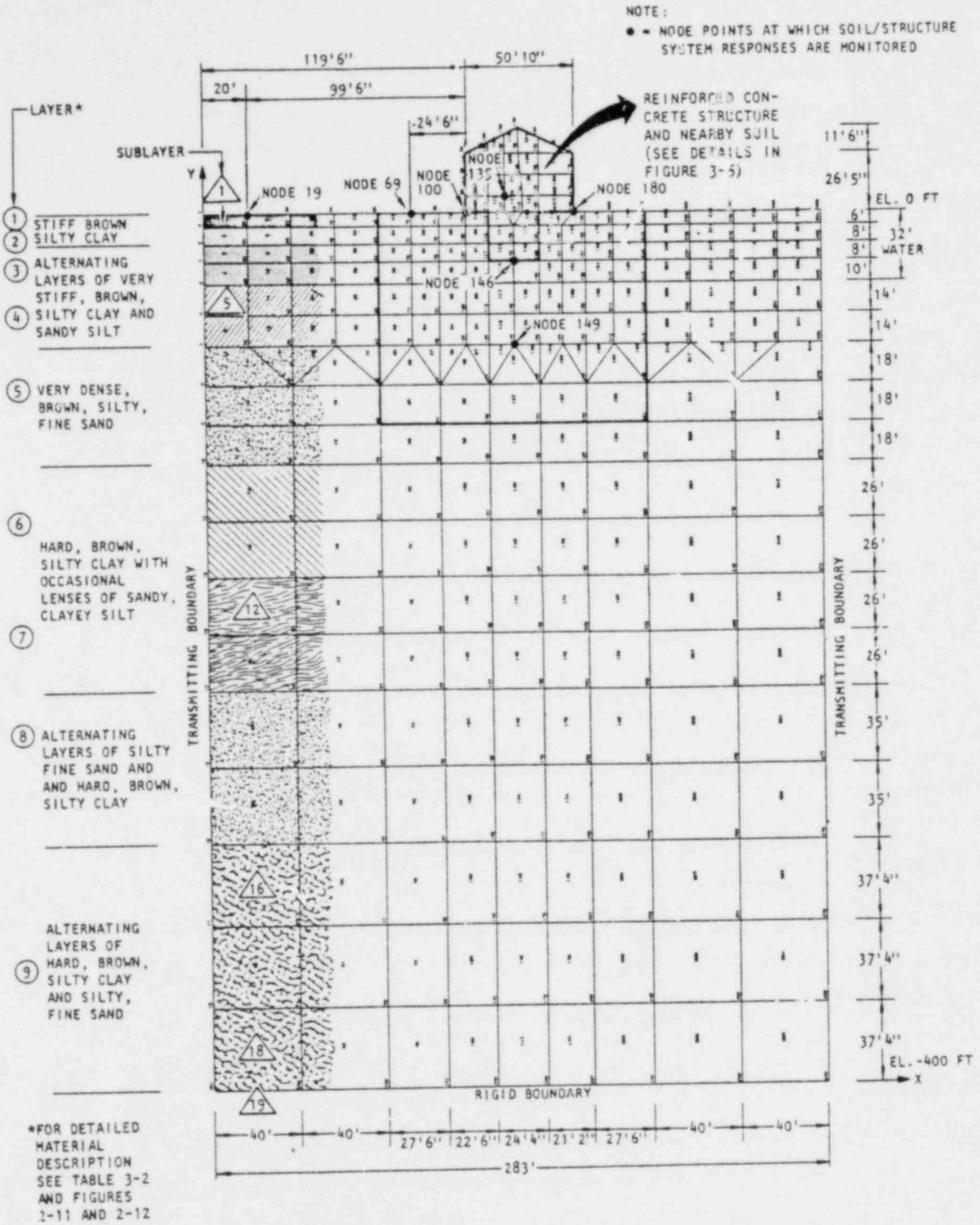

FIGURE 3-4. FINITE ELEMENT MODEL OF SOIL/STRUCTURE SYSTEM USED IN *FLUSH* CODE ANALYSIS

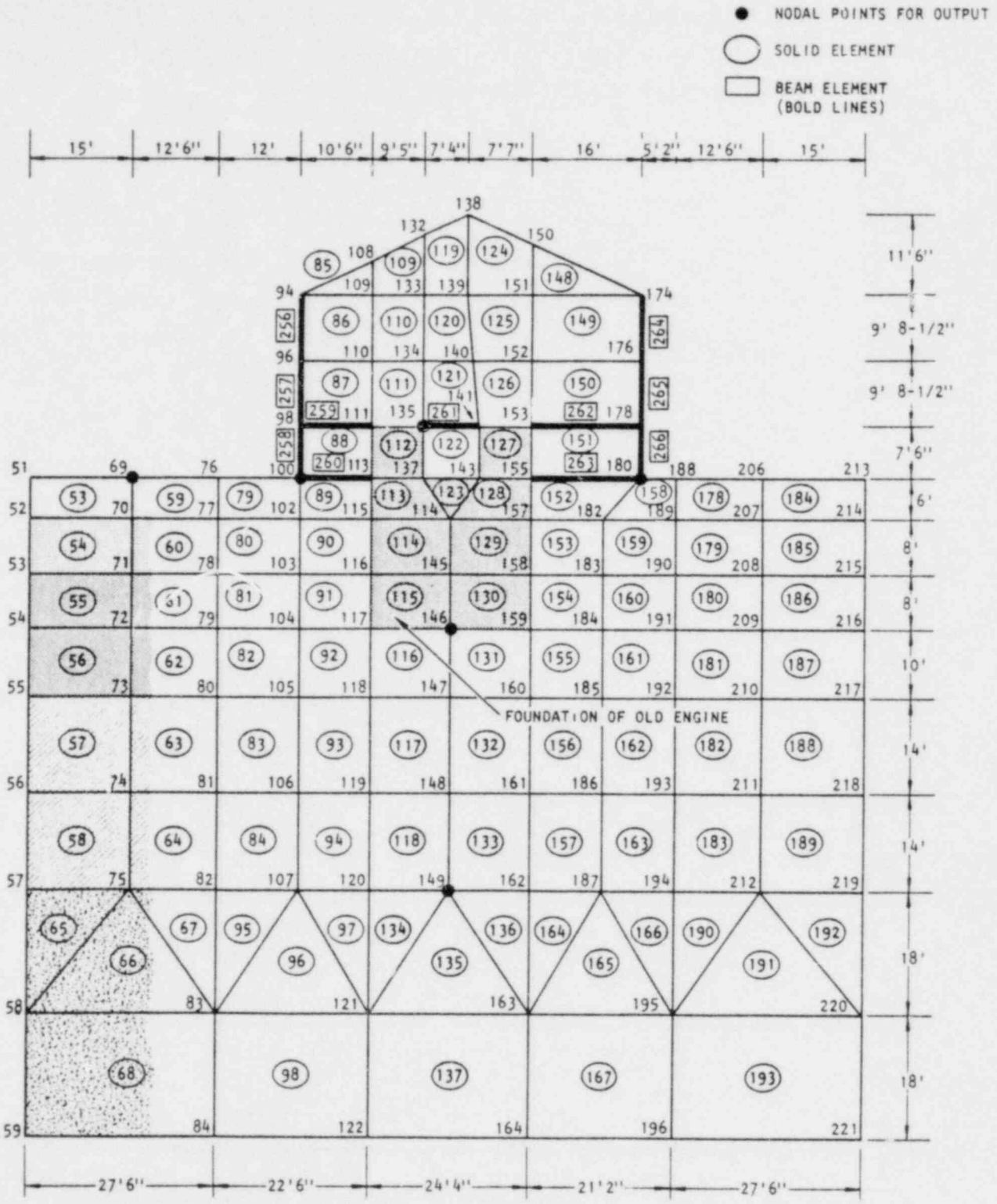

FIGURE 3-5. NEAR-STRUCTURE REGION OF FINITE ELEMENT MODEL FOR *FLUSH* CODE ANALYSIS

calculations; Figure 3-5 contains details of the near-structure region of the grid. These figures indicate the grid to have the following features:

- The grid extends over a region of the soil medium that measures 283 ft in width and 400 ft in depth.

- The side boundaries are represented using transmitting boundary conditions and are located nearly 120 ft from the sides of the structure. As shown in Chapter 4, this distance is sufficient to avoid structure response distortions due to signals reflected from the boundaries.

- The rigid base of the grid has been located so that (1) its depth is sufficient to avoid distortions of the near-surface response that are caused by signals reflected from the base; and (2) its depth is not unduly excessive to result in an unnecessarily expensive and time-consuming calculation. With these considerations, a series of SHAKE code calculations has been used to locate the base at a depth of 400 ft below the ground surface (see Chapt. 4).

- The grid represents a view looking south toward the El Centro Terminal Substation. In this view, the present location of the accelerograph corresponds approximately to Node Point 180 in the lower right corner of the structure model; the location of the accelerograph prior to 1955 is denoted approximately by Node Point 100 in the lower left corner (Fig. 2-5c).

- The structure is represented using a combination of two-dimensional quadrilateral elements and one-dimensional beam elements. The quadrilateral elements represent the effective in-plane stiffness and mass of the shear walls

and foundation block, while the beam elements represent the wall slabs and floor slabs that extend normal to the plane of the model. The heavy synchronous condenser units within the structure are modeled as discrete lumped masses at appropriate node point locations. The values of the element stiffnesses and masses that are used in the plane strain and modified two-dimensional models are obtained using procedures described below.

- The soil medium is represented using 18 rows of elements. The spacing of the soil node points is finest in the vicinity of the structure, which is the region of primary interest in the analysis.

b. Plane-Strain Model

The plane-strain modeling approach represents the in-plane response of a unit slice through the soil/structure system; i.e., it assumes that the response of this slice is representative of the in-plane response of any parallel section within the entire structure (Fig. 3-6). This modeling approach implies the existence of the following two sets of conditions. First, the system should not exhibit significant out-of-plane responses when it is subjected to in-plane forces or motions. Second, the properties of the system should be such that, in the direction normal to the plane of the slice (1) the building is sufficiently long and uniform so that the in-plane response of any two interior cross sections are reasonably similar; (2) the soil medium is reasonably homogeneous; and (3) the input motions are nearly uniform. Because these conditions are seldom met by actual soil/structure systems, the plane-strain modeling approach involves certain approximations to the actual system response.

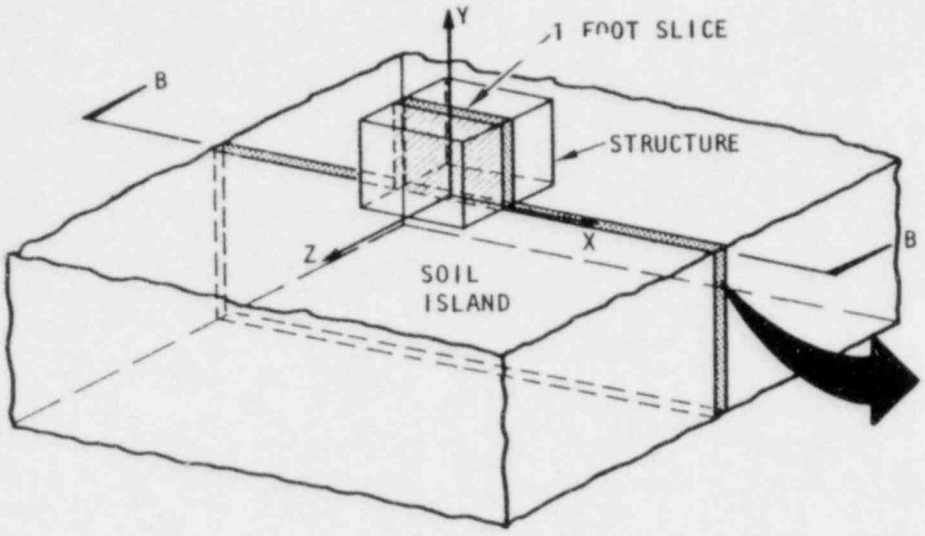

(a) Soil/structure system

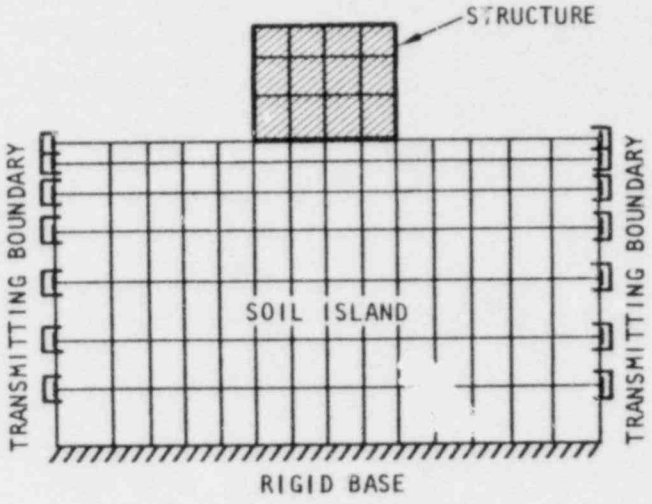

(b) Finite element model, view B-B

FIGURE 3-6. DEVELOPMENT OF PLANE STRAIN FINITE ELEMENT MODEL

The development of the plane strain model is based on a simulation of the stiffness and inertial characteristics of Section B-B in Figure 2-5c, which corresponds to the present location of the accelerograph in the El Centro Terminal Substation. The manner in which the contributions of the various structure elements are simulated in this model is briefly summarized in the paragraphs that follow.

i) Shear Walls (Quadrilateral Elements)

Only the shear wall at the south end of the Substation Building is considered to contribute to the in-plane stiffness and mass of the quadrilateral elements. This contribution is based on a reduced stiffness and mass of the shear wall in order to account for (1) its distance from Section B-B; and (2) the presence of the other structural elements (besides those in Sec. B-B) that resist the load transmitted to the interior of the building by the shear wall.

ii) Out-of-Plane Walls and Floor Slabs (Beam Elements)

The mass* and the axial, transverse shear, and bending stiffness* of the out-of-plane walls and floor slabs is represented using beam elements. The contribution of the buttresses is also included by averaging their area over the total length of the wall.

iii) Synchronous Condensers (Discrete Masses)

Of the two synchronous condensers presently on the Terminal Substation main floor, only Unit 1 (located at Sec. B-B) is included in the plane-strain model (Fig. 2-5a). This

*Per unit length normal to the plane of the model.

unit is represented as discrete masses concentrated at two node points that correspond to the two edges of the unit. The distributed mass per unit width at each node point is reduced to account for the support of the condenser by the floor slab adjacent to Section B-B.

iv) Foundation Block (Quadrilateral Elements)

The massive foundation block located beneath the center of the basement floor slab is modeled using quadrilateral elements with the full effective properties of concrete.

v) Roof Truss (Discrete Masses)

The contribution of the roof truss to the in-plane stiffness at Section B-B is assumed negligible when compared to the stiffness contributions of the south-end shear wall and the out-of-plane walls and floor slabs. Only the weight of the roof truss is represented, using discrete masses concentrated at the appropriate node point locations.

c. Modified Two-Dimensional Model

The modified two-dimensional (2-D) model differs from the plane-strain model in two respects. First, it does not consider a unit slice through the soil/structure system; rather it corresponds to an analysis of a slice whose width is equal to the out-of-plane width of the structure. Second, and most important, it uses viscous dashpots attached to the soil node points in order to simulate the propagation of scattered shear waves in a direction normal to the plane of this slice (Fig. 3-7). This assumption is based on prior work by Lysmer and Richart (1966) and by Lysmer and Kuhlemeyer (1969), who used viscous dashpots to simulate an infinite soil medium. It

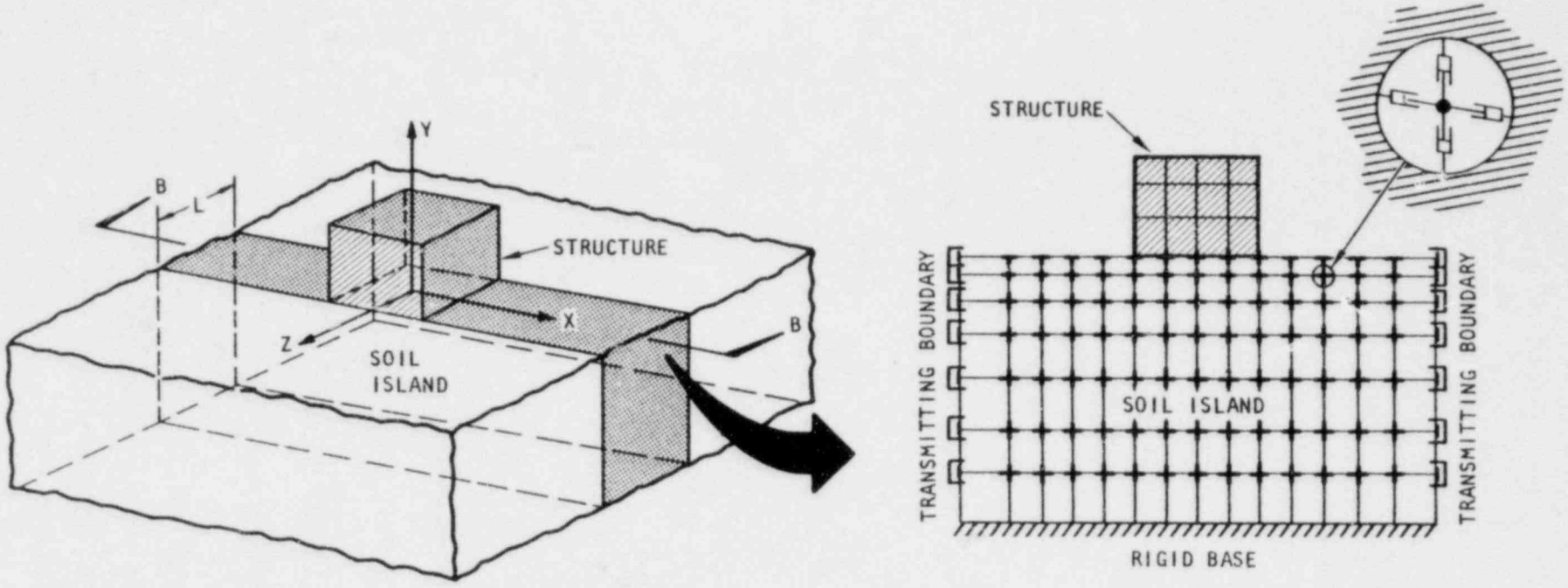

(a) Soil/structure system

(b) Finite element model, view B-B (Lysmer, et al., 1975)

FIGURE 3-7. DEVELOPMENT OF MODIFIED TWO-DIMENSIONAL FINITE ELEMENT MODEL

essentially corresponds to replacing the soil mass outside of the slice by viscous dashpots on both sides of the slice. Therefore, the modified 2-D model attempts to represent, in a simplified manner, some three-dimensional wave scattering effects. However, it is misleading to denote this model as "simplified three-dimensional," as termed by Lysmer et al. (1975), since only in-plane, two-dimensional responses of the soil and structure can be computed.

Because the modified 2-D model considers the entire width of the structure, rather than a unit slice through a single cross section, the procedures for constructing the model differ from those summarized previously for the plane-strain case. The manner in which the contributions of the various structure elements are represented in the modified 2-D model is described in the following paragraphs.

i) Shear Walls (Quadrilateral Elements)

To simulate the mass and in-plane stiffness of the quadrilateral elements the contributions of three shear walls will be considered. These correspond to the exterior walls at the north and south ends of the building and the interior wall about 16 ft from the north end. The mass and stiffness of each shear wall is averaged over the out-of-plane length of the building in order to obtain the quadrilateral element properties.

ii) Out-of-Plane Walls and Floor Slabs (Beam Elements)

The out-of-plane walls and floor slabs are represented by using beam elements in a manner identical to that described for the plane strain model except that, for the modified 2-D case, the total stiffness and mass of the walls and floor slabs, rather than the unit properties, are considered.

iii) Synchronous Condensers (Discrete Masses)

In the modified 2-D model, both synchronous condenser units are included by averaging their total weight over the out-of-plane length of the building. The resulting average weight is then represented as discrete masses concentrated at two node points that represent the two edges of the units.

iv) Foundation Block (Quadrilateral Elements)

The properties of the quadrilateral elements that represent the foundation block in the modified 2-D model are obtained by averaging the total mass and stiffness of the block over the out-of-plane length of the building.

v) Roof Truss (Discrete Masses)

The weight of the roof truss is represented by lumping discrete mass elements at appropriate node points in the structure model (as described previously for the plane-strain model).

3.3.2 TRI/SAC MODELS

The TRI/SAC code has been used to carry out two-dimensional analyses of both the free-field response and the soil/structure system response. The same soil grid, soil properties, and input motions were used for both sets of analyses.

The two grids used for the free field and the soil/structure system analyses are shown in Figures 3-8a and 3-8b, respectively. Features of these two grids are as follows.

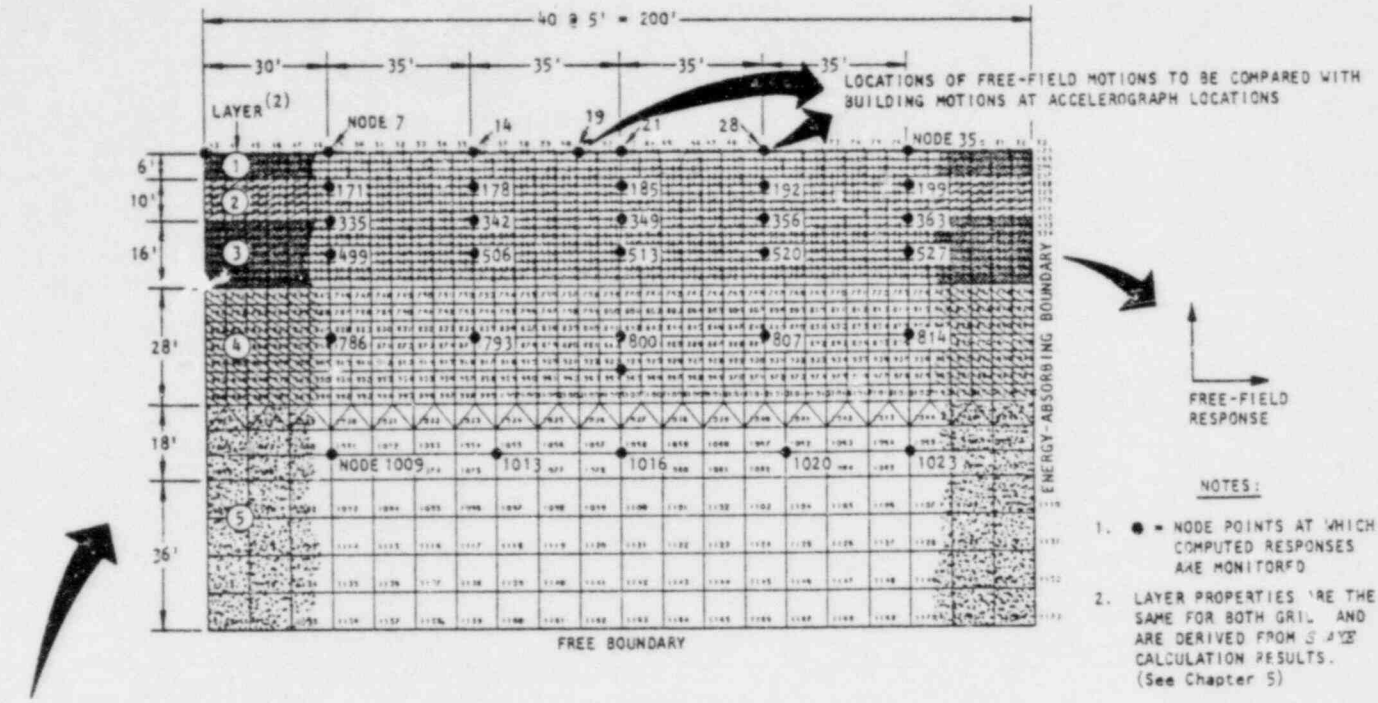

(a) Free-field grid

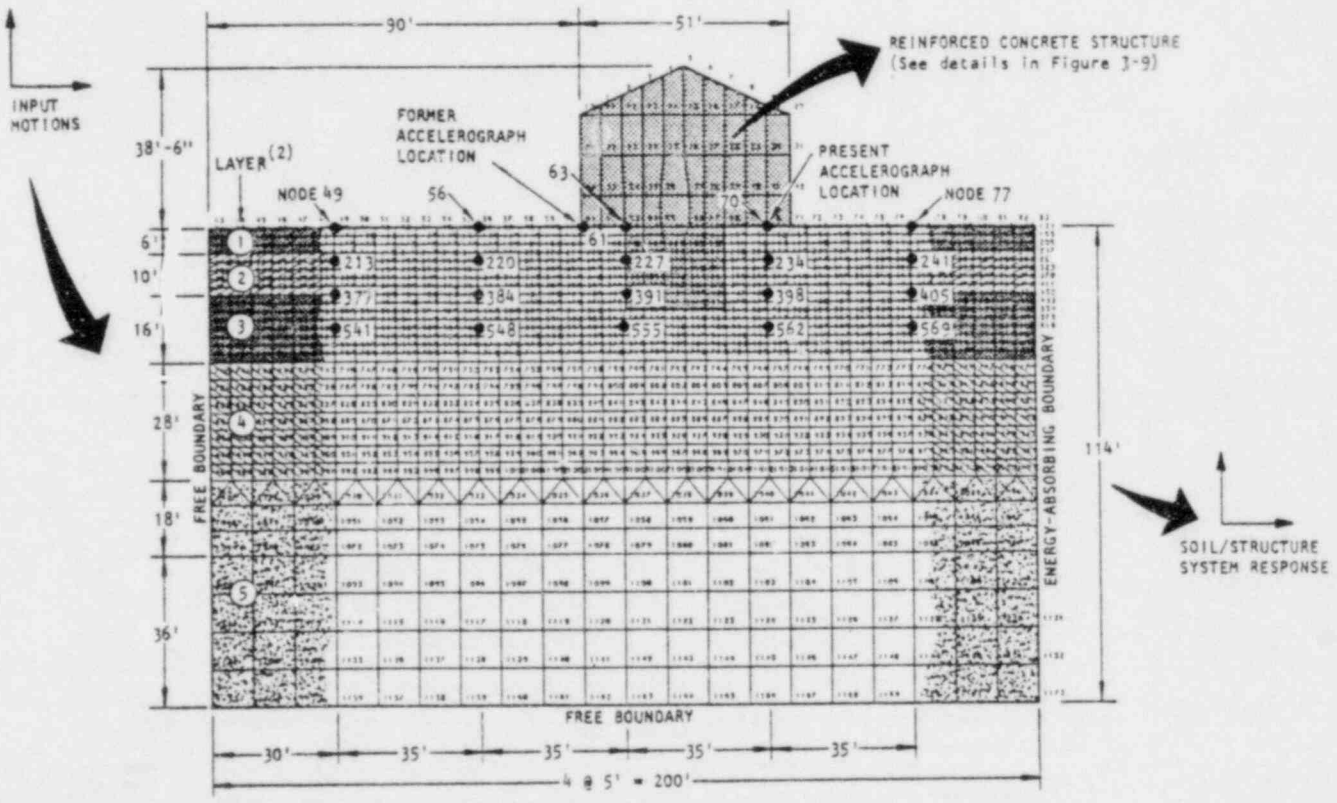

(b) Soil/structure grid

FIGURE 3-8. FINITE ELEMENT MODELS USED IN *TRI/SAC* ANALYSIS

- Both grids are of the same overall size, extending over a region of the soil medium that measures 200 ft in width and 114 ft in depth.

- Both grids employ identical representation of the soil medium, in terms of the node point spacing and the soil material properties. Each grid contains a total of five different soil layers with depths shown in Figures 3-8a and 3-8b. The elastic properties of these layers are based on iterated properties from the FLUSH calculations and are provided in Chapter 5. The spacing of the soil node points in both grids is finest near the ground surface, which is the region of primary interest in these calculations

- The boundary conditions at the edges of the soil grid are identical for the two grids. As shown in Figures 3-8a and 3-8b, the left and bottom boundaries of each grid are free, whereas, the right boundary has energy-absorbing viscous dampers of the type derived by Lysmer and Kuhlemayer (1969).

- Input motions are applied uniformly along the left boundary of each grid. The input motions are identical for both grids and, for reasons discussed in Chapter 5, correspond to the first 3 sec of the S45E and vertical components of motion recorded during the 30 June 1941 earthquake at Santa Barbara, California.

- As in the FLUSH calculations, the soil/structure grid (Fig. 3-8b) represents a view looking south toward the El Centro Terminal Substation. The location of the accelerograph (since 1955) is represented as Node 70 in Figure 3-8b; the computed structure response at this location will be compared to the motion computed at the corresponding location in the free-field grid (Node 28 of Figure 3-8a). In addition, motions at several other corresponding locations in the free-field and soil/structure grids will be compared (as shown in Figs. 3-8a and 3-8b).

- The modeling of the structure for the TRI/SAC analysis is shown in Figure 3-9. This figure shows the structure to be represented using a combination of two-dimensional quadrilateral elements (to represent the mass and in-plane stiffness of the shear walls and foundation block), beam elements (to represent the wall slabs and floor slabs that extend normal to the plane of the model), and lumped mass elements (to represent the synchronous condenser units), Comparison of Figures 3-9 and 3-5 shows that the element types used to model the structure for the TRI/SAC calculation are identical to those used for the FLUSH calculations; only the node point spacings differ slightly for the two structure models. Furthermore, the development of the properties of the structure elements in the TRI/SAC grid corresponds identically to the plane-strain approach described for the FLUSH code in Section 3.3.1.3.*

*The only difference between the TRI/SAC and FLUSH plane strain models of the structure is the equivalent modulus of the foundation block, which was reduced in the TRI/SAC calculations to be consistent with SW/AA microseismic tests of the block (App. C) that were carried out after the FLUSH calculations were completed.

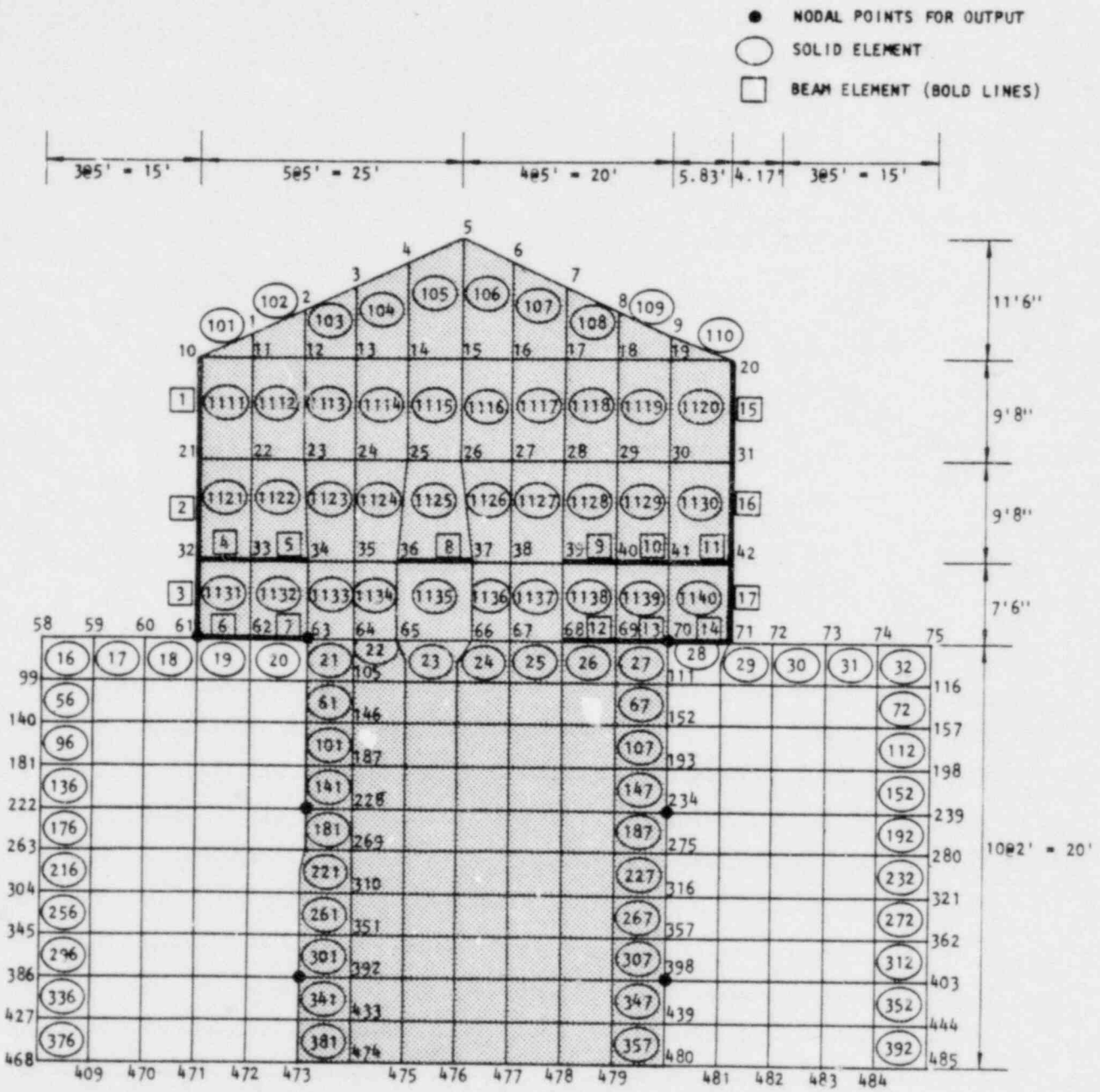

FIGURE 3-9. NEAR-STRUCTURE REGION OF FINITE ELEMENT MODEL FOR *TRI/SAC* ANALYSIS

CHAPTER 4

ANALYSIS RESULTS USING *SHAKE* AND *FLUSH* CODES

4.1 FREE-FIELD RESPONSE

The two different approaches used in conjunction with the SHAKE code to compute free-field ground surface motions and input base motions for the soil/structure interaction analyses are depicted in Figure 4-1. One approach uses scaled rock outcrop motions as a basis for computing corresponding subsurface rock motions and ground motions at the surface of the El Centro site profile. The other consists of the deconvolution of a strong motion record measured at El Centro. In this section, results from both approaches are presented and assessed; one of these sets of results is then selected for use in conjunction with the soil/structure interaction analysis, whose results are presented in Section 4.2 and 4.3. Both sets of results are developed to represent shaking from a moderate-sized earthquake (Magnitude 6.5) centered near the site (epicentral distance = 5 mi). These conditions are similar to those under which accelerograms were measured at El Centro during the 18 May 1940 Imperial Valley earthquake.

4.1.1 USE OF SCALED ROCK OUTCROP MOTIONS

The use of rock outcrop motions as a basis for computing free-field motions at El Centro involves the following steps (Fig. 4-1a):

- Step 1--Select a suitable accelerogram that was measured on rock outcropping or on very firm soil.
- Step 2--Scale this record to correspond to a Magnitude 6.5 earthquake centered 5 mi from the site.
- Step 3--Use SHAKE code to compute subsurface rock motions as well as motions within the soil profile.

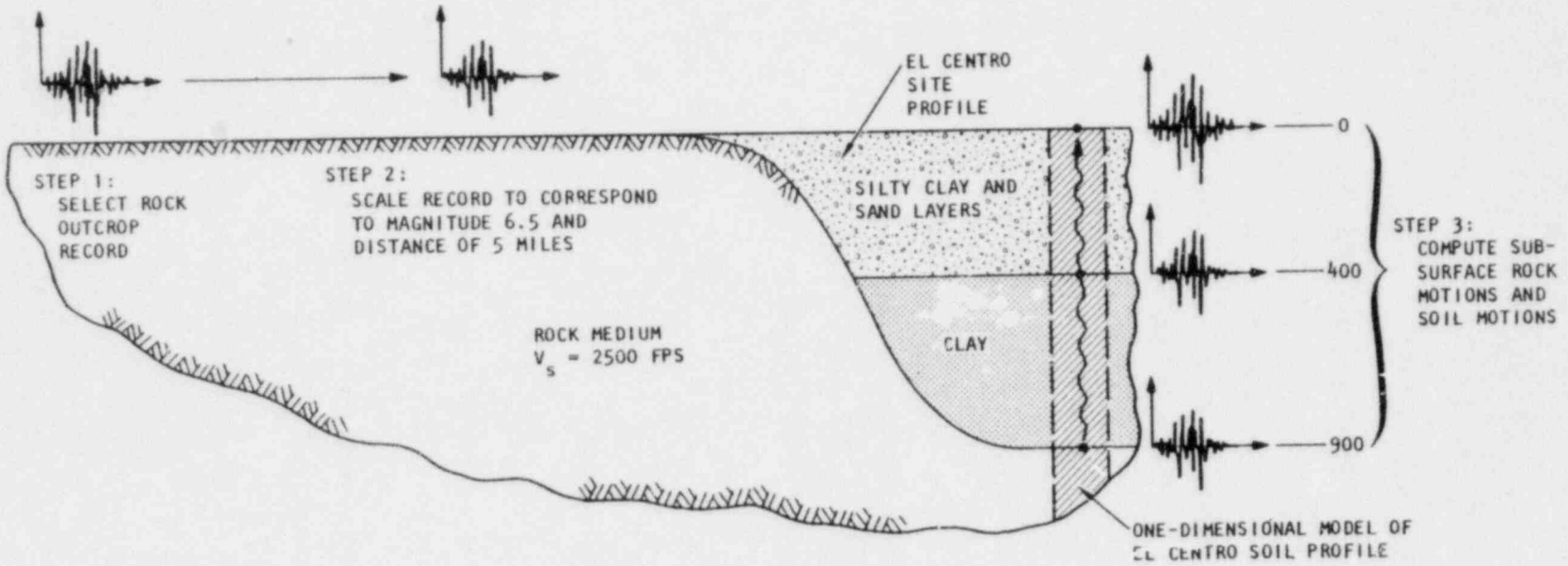

(a) Use of scaled rock outcrop motions

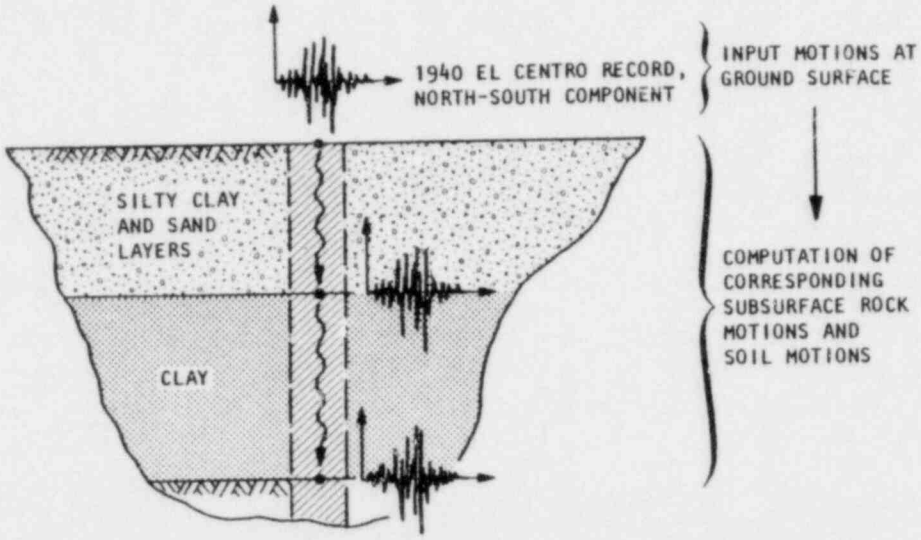

(b) Use of deconvolution of ground surface motions

FIGURE 4-1. FREE-FIELD ANALYSIS PROCEDURES USING *SHAKE* CODE

4.1.1.1 Selection of a Rock Outcrop Record (Step 1)

The record selected to represent rock outcrop motions for these calculations corresponds to the north-south component of the rock outcrop record measured at Helena, Montana, on October 31, 1935. The site of the Helena accelerograph was located 5 mi from the epicenter of the earthquake, which had a Richter magnitude of 6.0.

The acceleration, velocity, and displacement time histories for this Helena record are shown in Figure 4-2a and the Fourier amplitude spectrum, which depicts the frequency content of the record, is provided in Figure 4-2b. These figures indicate that (1) the record has a very short duration of strong shaking, a feature that will reduce the computer time required for the soil/structure interaction calculations; and (2) the significant frequencies for the record fall below 10 Hz, a factor that permits the use of a relatively low frequency cutoff in the Fast Fourier transform analysis in SHAKE and FLUSH codes. Therefore, it is seen that there are significant cost advantages associated with the use of the Helena record in these analyses.

4.1.1.2 Scaling of the Rock Outcrop Record (Step 2)

To scale the Helena record to correspond to a Magnitude 6.5 earthquake centered 5 mi from the site, the empirical curves developed by Schnabel and Seed (1972) are employed (Fig. 4-3). These curves define peak horizontal accelerations as a function of earthquake magnitude and epicentral distance for rock outcrop motions. They were developed from observations of prior records and from computations of rock motions.

The Schnabel-Seed curves indicate the peak rock outcrop acceleration caused by a Magnitude 6.5 earthquake centered 5 mi from the site is 0.47 g. The Helena record, which originally had a peak acceleration of 0.145 g, was therefore scaled by a factor of $\frac{0.47}{0.145} = 3.24$ to raise its peak acceleration to the Schnabel-Seed value.

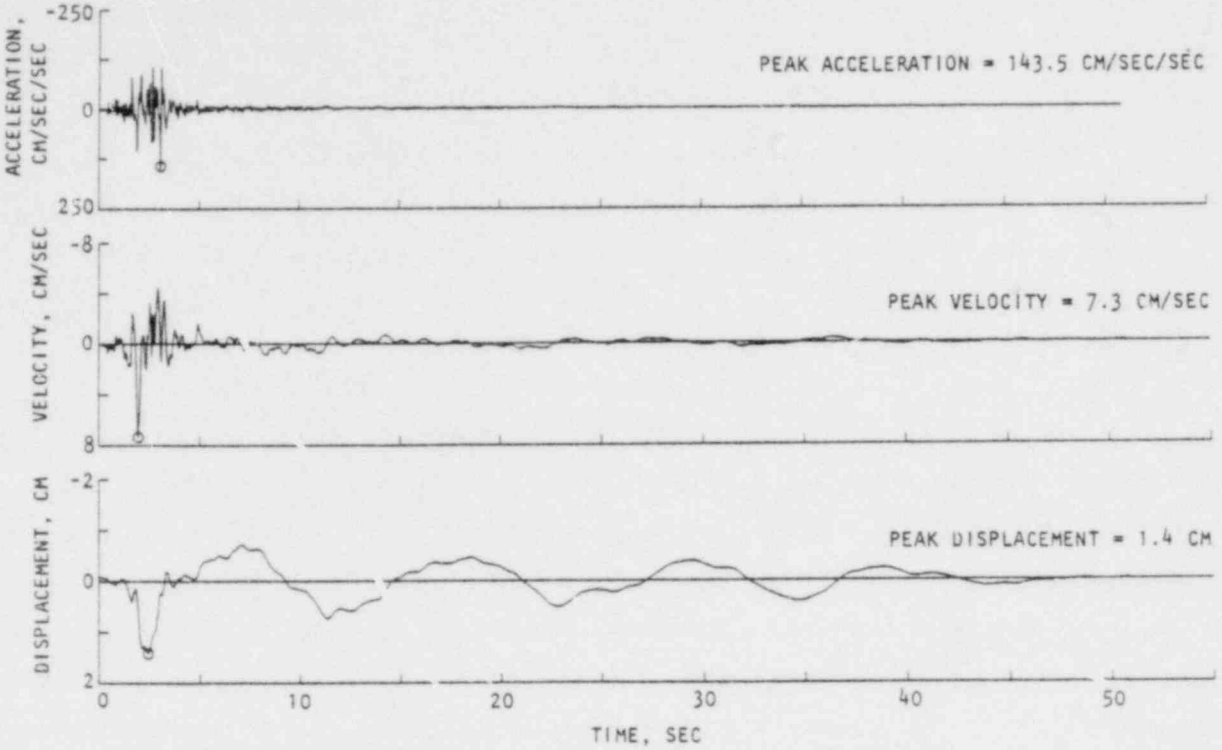

(a) Motion time histories

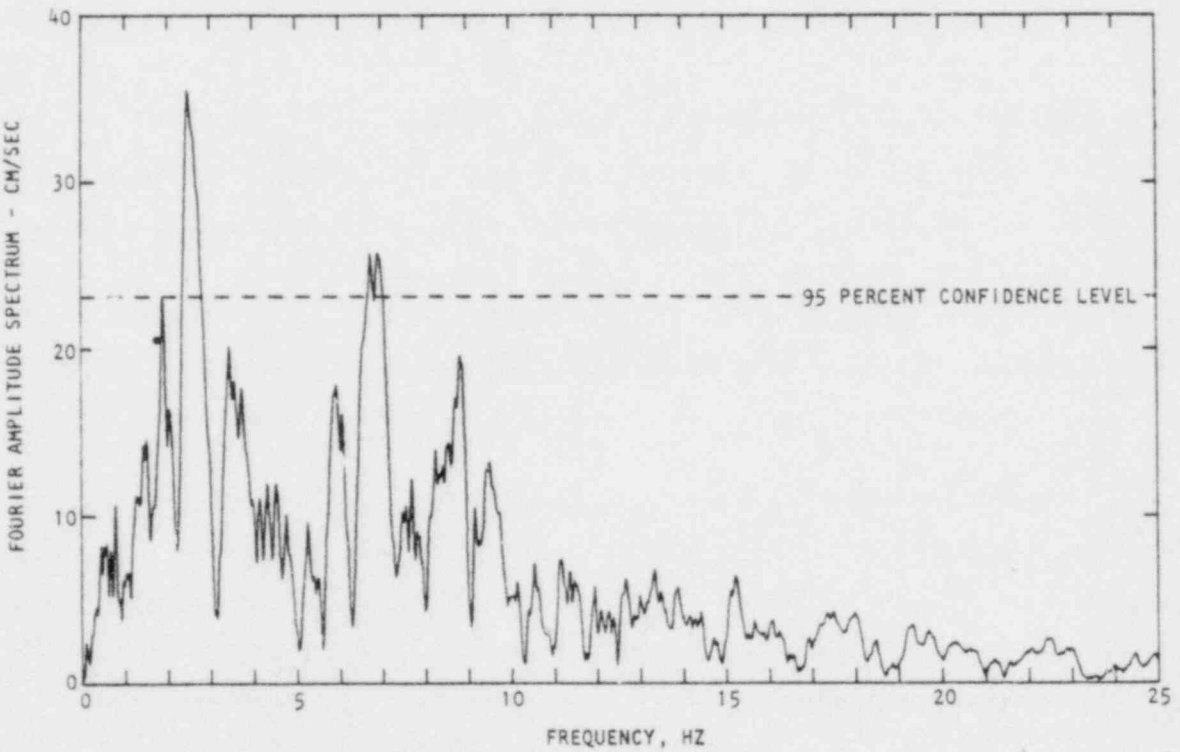

(b) Fourier amplitude spectrum of acceleration

FIGURE 4-2. NORTH-SOUTH COMPONENT OF ROCK OUTCROP MOTIONS RECORDED AT HELENA MONTANA ON OCTOBER 31, 1935 (CIT, 1969-1972)

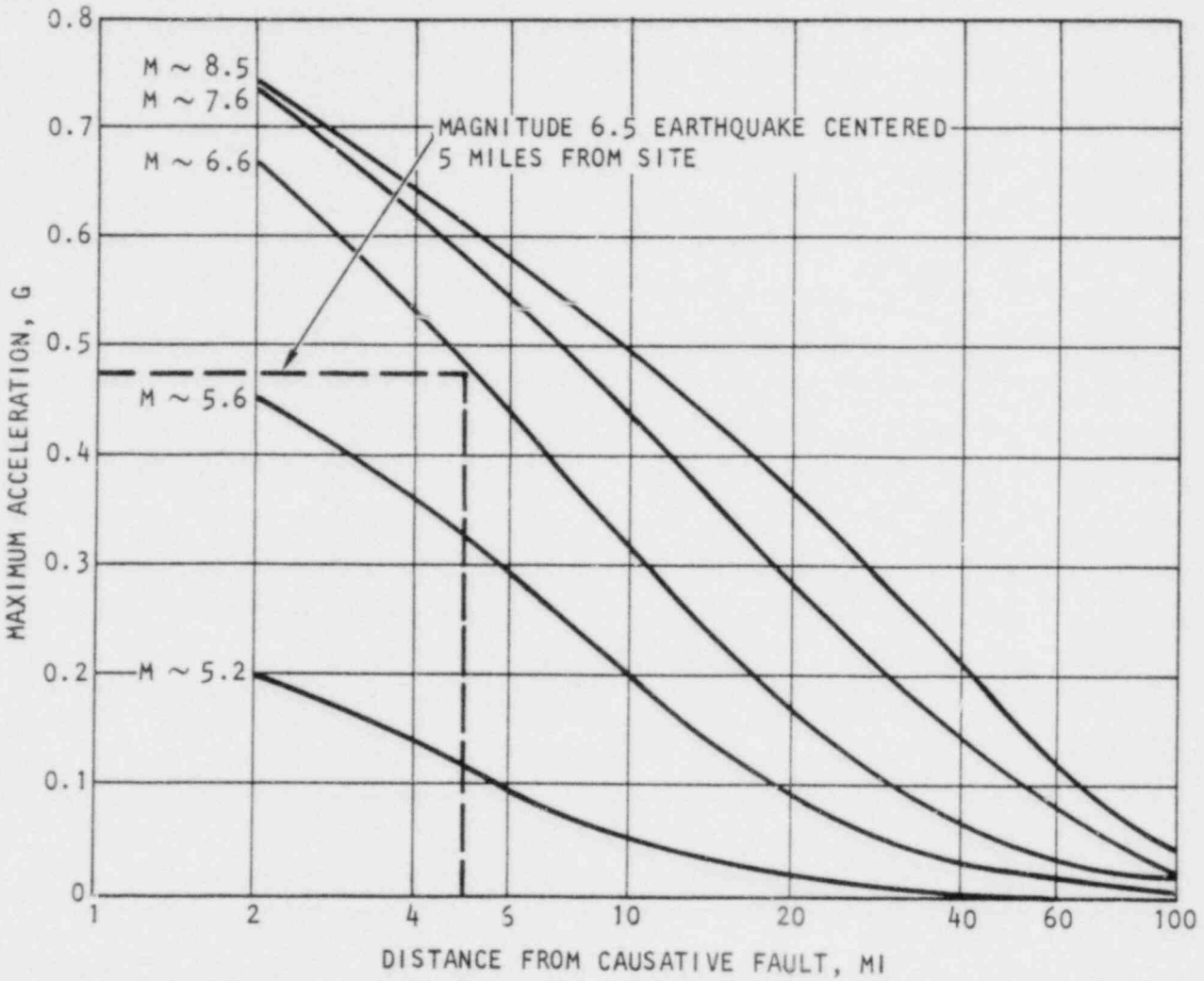

FIGURE 4-3. PEAK ACCELERATION-MAGNITUDE-DISTANCE CORRELATIONS FOR ROCK OUTCROP MOTIONS (Schnabel and Seed, 1972)

4.1.1.3 Computation of Subsurface Rock Motions and Soil Motions (Step 3)

A total of three different computations were carried out using the scaled Helena rock motions. These cases are carried out to determine the sensitivity of the ground surface motions to variations in soil properties at depths greater than 400 ft. This, in turn, is intended to provide a justification for locating the rigid base of the FLUSH soil/structure interaction model at a depth of 400 ft. The computed motions also represent possible base input motions and free-field surface motions for use in conjunction with the soil/structure interaction analysis; this depends on the subsequent comparisons with the deconvolution results.

The three cases are depicted in Table 4-1 and Figure 4-4. Case 1 has been carried out using the 900-ft SHAKE model shown in Table 3-1, and has served to provide computed motions at the 400-ft depth and at the ground surface. For this case, the soil medium immediately below the 400-ft depth is represented as a clay with strain-dependent properties and a small-strain shear wave velocity of 1900 fps. In Cases 2 and 3, the base of the model is moved to a 400-ft depth; subsurface soil motions computed at this depth in Case 1 are used as base input for Cases 2 and 3. Furthermore, in these latter two cases the soil medium below the 400-ft base is represented as an elastic half-space with a shear wave velocity of 2500 fps (Case 2) and 8000 fps (Case 3). Case 3 is therefore seen to simulate the location of the rigid base in the FLUSH model.

Results from these analyses are presented in Figures 4-5a and 4-5b and in Table 4-1. Figure 4-5a shows the Case 1 results in the form of 5% damped response spectra for the scaled Helena rock outcrop motions, for the computed motions at the 400-ft depth, and for the computed motions at the surface of the El Centro soil profile. Comparisons of these spectra indicate that

- The motions computed at the surface of the soil profile exhibit higher spectral amplitudes at low frequencies and lower spectral amplitudes at high frequencies than do the scaled rock outcrop motions.

TABLE 4-1. SUMMARY OF FREE-FIELD *(SHAKE)* ANALYSES USING INPUT MOTIONS AT THE BASE

Case No.	Effect Investigated	Earthquake Input				Soil Model*		Calculated Output Motions	
		Record	Peak Acceleration g	Scaled to g	Where Applied	Depth to Base ft	Half-Space V_s, fps	Peak Acceleration g	Where Calculated
1	Basic case for derivation of input motions for the 400-ft finite element (FLUSH) model.	Helena, Montana Oct 1935 N-S Component	0.146	0.47	At Base	900	2,500	0.279	Ground Surface
2	Use of motions obtained from Case 3 at -400 ft as input to a model with half-space V_s = 2,500 fps	Motion obtained from Case 1 at -400 ft	0.162	0.162	At Base	400	2,500	0.279	Ground Surface
3	Effect of using a stiff half-space at -400 ft on surface motions.	Motion obtained from Case 1 at -400 ft	0.162	0.162	At Base	400	8,000	0.279	Ground Surface

*See Table 3-2 for description of model.

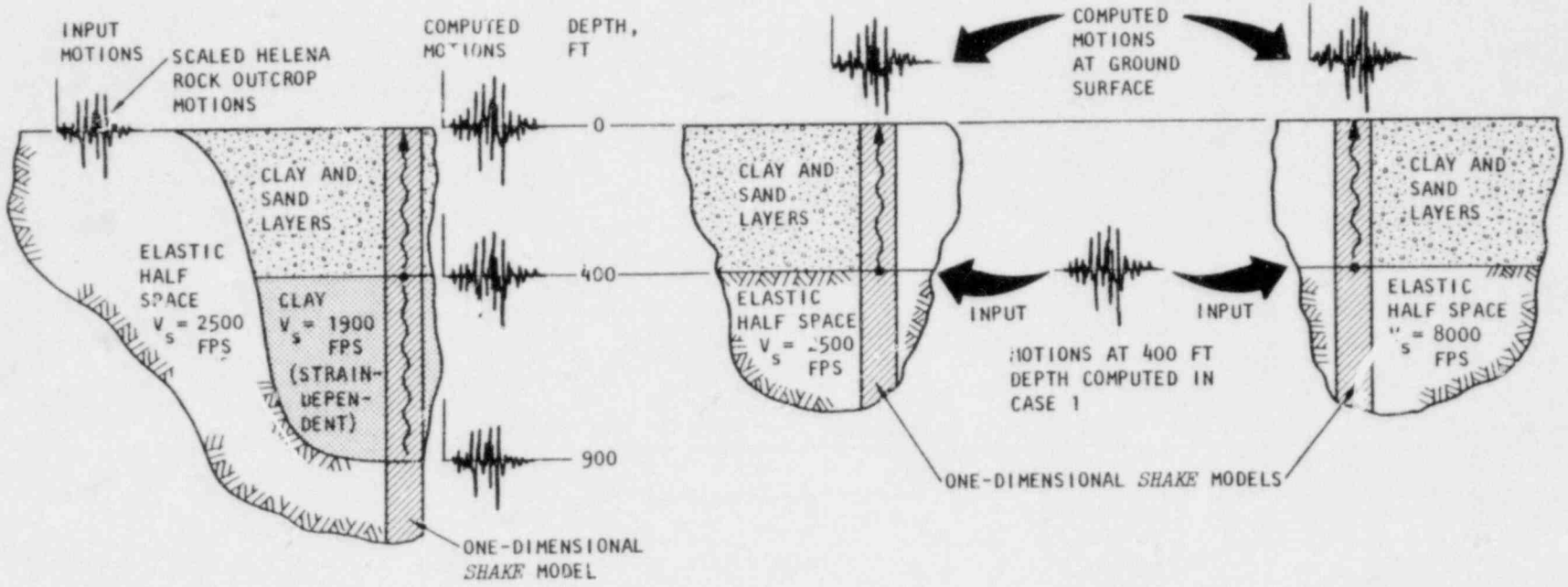

FIGURE 4-4. SENSITIVITY STUDY--EFFECT OF ASSUMED PROPERTIES OF DEEP SOIL LAYERS ON COMPUTED MOTIONS AT GROUND SURFACE

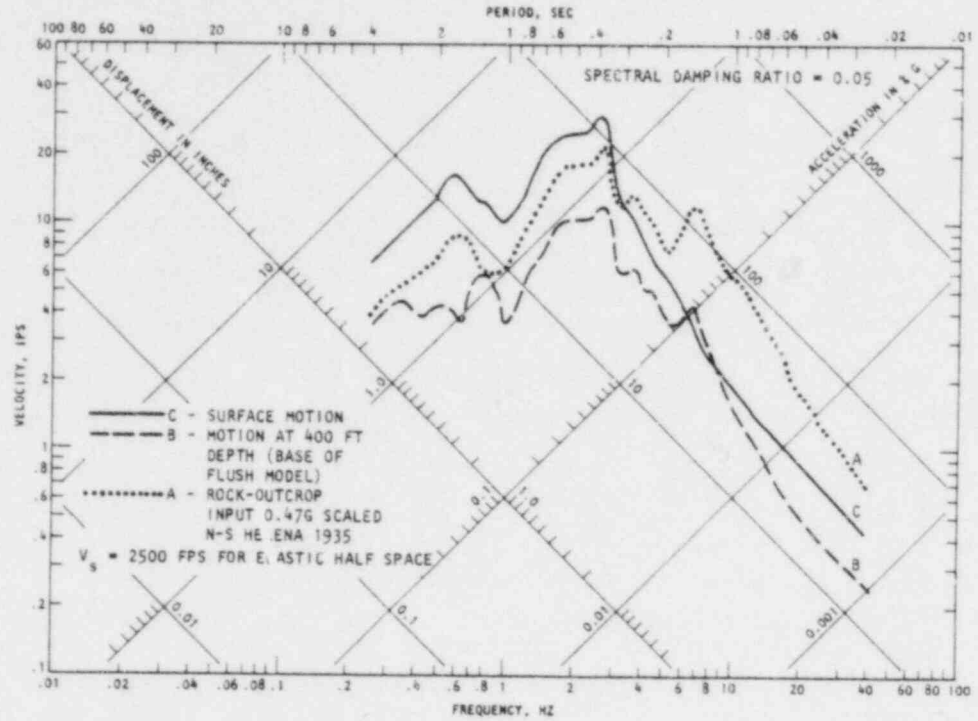

(a) Case 1 results

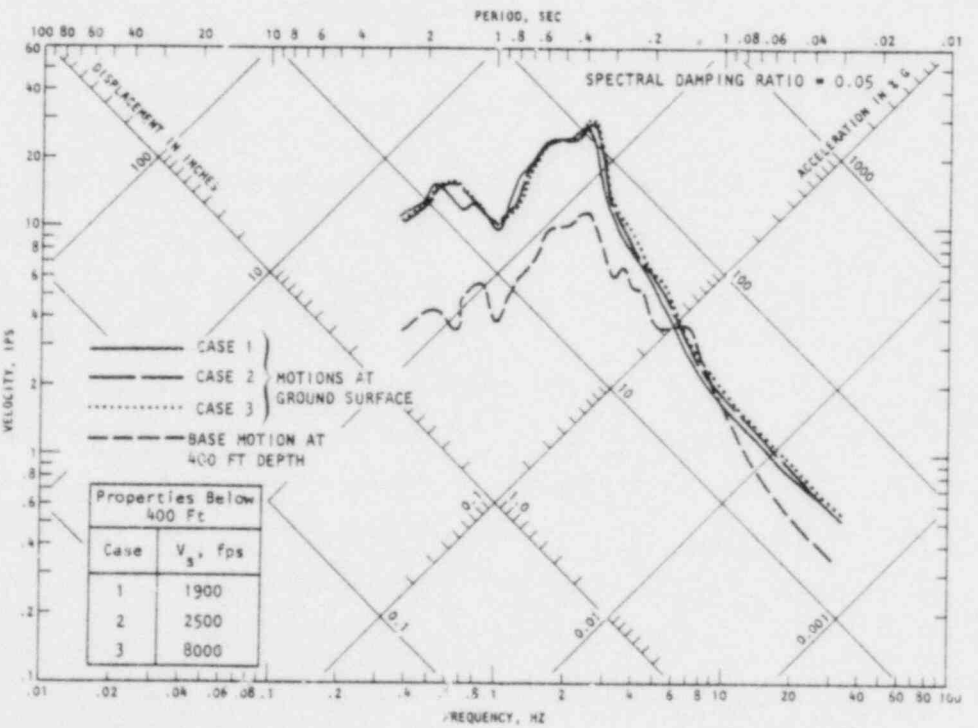

(b) Comparison of results from Cases 1, 2, and 3

FIGURE 4-5. COMPUTATION OF FREE-FIELD MOTIONS FROM SCALED ROCK-OUTCROP MOTIONS

- The motions computed at the surface of the soil profile exhibit spectral amplitudes that are amplified relative to those of the motions at the 400-ft depth. This amplification is significant over the entire frequency range of the calculations.

Figure 4-5b shows comparisons of response spectra from the ground surface motions computed by all three cases. These results indicate that the ground surface motions are virtually identical for the three cases; i.e., the near-surface motions are not sensitive to the properties of the soil medium below a depth of 400 ft. Therefore the use of a rigid base at a 400-ft depth in the FLUSH model should not affect the soil/structure system response to any significant degree.

4.1.2 USE OF DECONVOLUTION PROCEDURES

The second approach evaluated for defining subsurface base input motions for the soil/structure interaction analyses consists of the use of deconvolution procedures (Sec. 3.2.1.3). In the application of these procedures for this investigation, the north-south accelerogram recorded at El Centro on May 18, 1940 has been input at the ground surface in the 900-ft SHAKE model of the El Centro site (Table 3-2).

Results of this calculation are denoted under Case 4 in Table 4-2. These results indicate that the computed motions are well behaved within the clay layers that comprise the upper portion of the El Centro site. However, within the two sand layers at the site, the computed motions experience sudden and drastic increases. For example, in Layer 5 (Table 3-2) the peak acceleration increases from 0.20 g at the top of the layer (depth = 60 ft) to 1.50 g at its base (depth = 114 ft). Similarly, Layer 8 experiences an increase in the peak acceleration of from 2.67 g at its top (depth = 218 ft) to 131.2 g at its base (depth = 288 ft). Below Layer 8, the computed motions become unstable.

TABLE 4-2. RESULTS OF *SHAKE* DECONVOLUTION OF 1940 N-S EL CENTRO GROUND MOTIONS

Depth, ft	Case 4*		Case 5†	
	Peak Acceleration, g	Comments	Peak Acceleration, g	Comments
0	0.33	Input N-S component of 1940 El Centro deconvolved to the base.	0.33	Input N-S component of 1940 El Centro deconvolved to the base.
6	0.31		0.31	
16	0.25		0.25	
32	0.24		0.24	
60	0.20		0.20	
114	1.50	Sudden change from sand to clay	0.21	
166	1.61		0.20	
218	2.67		0.33	
288	131.20		0.42	
400	Very large	Sudden change from sand to clay	0.77	
400			0.77	
Outcrop	Very large		1.03	

*7 clay layers and 2 sand layers (see upper 400 ft of Table 3-2).

†9 clay layers--2 sand layers replaced by clay layers.

Note: The motions resulting from these cases were not used as base input for the FLUSH soil/structure interaction calculations. See text for explanation.

It is emphasized that the classification and soil properties used to represent Layers 5 and 8 in the El Centro site model have been defined from the SW/AA geotechnical investigations at the site, which were carried out using the latest sampling and testing techniques. Nevertheless, since these layers appeared to be the source of the numerical problems encountered in the Case 4 calculations, it was decided to change their classification from sand to clay and then repeat the deconvolution analysis. In this way, the entire site profile would be represented as consisting of clay layers; i.e., sudden changes in the strain-dependent material property curves that occur at the interfaces between the sand and clay layers would be eliminated. Results from this second deconvolution calculation, provided under Case 5 in Table 4-2, indicate that the sudden increase in the computed motions at Layers 5 and 8 have been virtually eliminated. However, the computed peak acceleration on rock outcropping (1.03 g) still appears to be very high, and is more than twice the rock outcrop acceleration indicated by the Schnabel-Seed empirical curves of Figure 4-3 (0.47 g).

4.1.3 ASSESSMENT OF FREE-FIELD ANALYSIS RESULTS

The results presented in Section 4.1.2 indicate that the deconvolution procedure is quite sensitive to certain details of the site model and is prone to numerical instabilities when applied to the El Centro site; potential difficulties of this type have previously been pointed out by Schnabel et al. (1972). However there are also certain physical reasons why the deconvolution procedure may not be adequate. For example, in this application, the procedure has been used in conjunction with the 1940 El Centro north-south accelerogram, which was applied as input at the ground surface of the *SHAKE* site model; this implicitly assumes that these particular motions are due solely to vertically incident shear waves. However other types of waves that approach the accelerograph station at various angles of horizontal and vertical incidence would also have contributed to the nature of this accelerogram. Furthermore, the accelerogram could have been influenced by the presence of the structure, as is being investigated in this study. The lack of consideration of these factors in the deconvolution approach may have contributed to the numerical problems described in Section 4.1.2.

The computation of free-field motions from rock outcrop and subsurface rock motions, as described in Section 4.1.1, is also limited to consideration of only vertically incident shear waves. However, the approach does not force a particular set of *recorded* motions to conform to this assumption; rather it computes subsurface rock motions and soil motions that are consistent with this assumption, with the site model, and with the scaled rock outcrop motions used as input to the calculations. This may be why no numerical difficulties were encountered in the results presented in Section 4.1.1. Furthermore, for the purposes of this study, it is not important that the computed free-field motions correspond to actual measured records or real earthquake motions. It is only important that such motions serve as a basis for comparison with results from the soil/structure interaction analysis that are computed from the same assumptions, site material model, and subsurface base motions. In this way, the comparisons of the SHAKE and FLUSH code results, as described in the remainder of this chapter, represent an approximate but *self-contained* basis for evaluating soil/structure interaction effects that arise at El Centro due to vertically incident shear waves.

With the above discussion as background, the free-field results obtained in Section 4.1.1 are used in conjunction with the FLUSH code analyses, as described in Sections 4.3 and 4.4. In this, the motions computed at a 400-ft depth by this application of SHAKE code are applied as input motions at the rigid base of the FLUSH soil/structure model (Spectrum B, Fig. 4-5a). Also, the motion computed in the structure basement by the FLUSH code analyses are compared to the free-field ground surface motions computed by SHAKE code as described in Section 4.1.1 (Spectrum C, Fig. 4-5a). Finally, the strain-dependent shear moduli and damping ratios in each sublayer, as obtained from the final iteration of this SHAKE code analysis, are used as initial properties for the first iteration of the soil/structure interaction analysis; this provides a basis for assessing the extent to which the variations in properties due solely to the presence of the structure affect the soil/structure system response (see Secs. 4.3 and 4.4).

4.2 ASSESSMENT OF MESH SIZE AND FREQUENCY CUTOFF IN FINITE ELEMENT ANALYSIS

Prior to performing the soil/structure interaction analyses, it is necessary to first determine (1) the adequacy of the finite element mesh (Fig. 3-4); and (2) an appropriate cutoff frequency for the analyses. These assessments are based on a one-dimensional free-field finite element analysis carried out using the FLUSH code. This finite element model has the following features: (1) the depth (400-ft) and the subsurface horizontal input motions along the rigid base were identical to those employed in the SHAKE Case 3 analysis (Table 4-2); (2) the vertical dimensions of the soil elements are identical to those employed in the two-dimensional FLUSH model of the soil/structure system; and (3) the cutoff frequency is set at 10 Hz, in order to reduce computer costs and because the Fourier spectra of the scaled Helena rock outcrop motions did not exhibit significant amplitudes above this frequency.

The above assessment is based on a comparison of the free-field ground surface motions computed by the one-dimensional FLUSH model with the corresponding results from the SHAKE Case 3 analysis (see Table 4-3, Case 6). In this regard, it is recalled that the SHAKE Case 3 results are based on a 20-Hz cutoff frequency and on a sufficient number of sublayer divisions to assure an accurate solution using the SHAKE continuum solution (Schnabel et al., 1972). Results of this comparison, in terms of 5% damped response spectra of these motions, are provided in Figure 4-6. The comparison indicates that the SHAKE code and FLUSH code surface motions are nearly identical. On this basis, the 10-Hz cutoff and the soil element sizes used in the FLUSH code model are judged to be satisfactory for use in the soil/structure interaction analyses.

TABLE 4-3. *FLUSH* FINITE ELEMENT ANALYSIS CASES

Case No.	Type of Analyses	Number of Iterations	Purpose of Analysis	Comments
6	Free Field	3	Check adequacy of 1) Mesh size 2) Cutoff frequency of analysis (10 Hz)	Results same as SHAKE Case 3 • Mesh size adequate • Frequency cutoff OK
7	Plane Strain	1	Check effect of non-linearities on response for single and multiple iterations	Results compare well with Case 8 Nonlinearities of building interaction are secondary
8	Plane Strain	4	Basic case for studying effects of building interaction	Differs from free field
9	Modified Two-Dimensional	1	Check effect of non-linearities on response for single and multiple iterations	Results compare well with Case 10 Nonlinearities of building interaction are secondary
10	Modified Two-Dimensional	3	Evaluate effect of refining two-dimensional model on building interaction	Building interaction effects are less than those reported for Case 8 Differs from free field

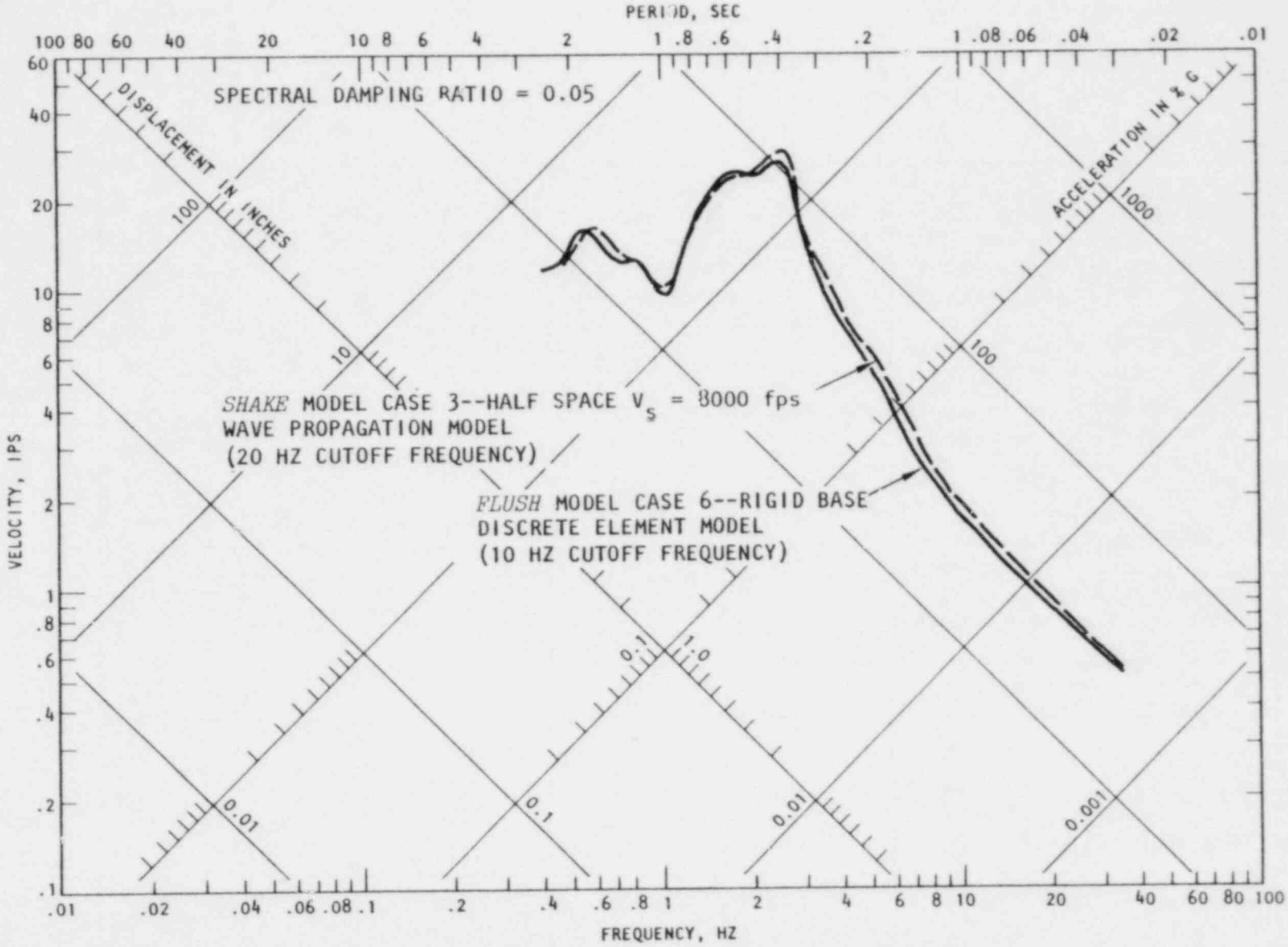

FIGURE 4-6. COMPARISON OF GROUND SURFACE RESPONSE SPECTRA OF FREE-FIELD MOTIONS CALCULATED BY 400 FT DEEP *SHAKE* AND *FLUSH* MODELS

4.3 SOIL/STRUCTURE SYSTEM RESPONSE

4.3.1 FORM OF RESULTS

The results of the analyses using the plane strain and modified two-dimensional models of the soil/structure system (see Secs. 3.3.1.3b and c) are described in this section. Both analyses are based on the same grid configuration, which is shown in simplified form in Figure 4-7 for ready reference to the analysis results. The various node points at which the system response is monitored are shown in this figure. Referring to Figure 2-5c, Node Point 100 corresponds to the instrument location at the time of occurrence of the 1940 Imperial Valley earthquake. Node Point 180 is representative of the present location of the instrument, which was moved to the other end of the Terminal Substation Basement in March 1955.* The remaining node points in the structure represent the response of the structure at the base of the foundation block (Node 146) and on the first floor level (Node 135). Nodes 69 and 149 indicate the response of the soil medium in the vicinity of the structure. Node Point 19 defines the response along the ground surface at a location relatively far from the structure; therefore the response at this node point should be quite similar to the free-field motions, unless the response is distorted by signals reflected from the side boundary of the grid.

---

*The extent to which Node Point 180 represents the present instrument location must be evaluated on the basis of the modeling procedure used. In the modified two-dimensional model, the entire width of the building is considered in representing the structure element properties (Sec. 3.3.1.3c); therefore, for this case, Node 180 can be considered representative of the present instrument location. This is not entirely true for the plane strain model which is based on particular cross sections of the structure that corresponds to the original instrument location (see Fig. 2-5c); this cross section is different from that of the present location of the instrument (Sec. 3.3.1.3b). It is judged, however, that the structure response will not be overly sensitive to the differences between these cross sections.

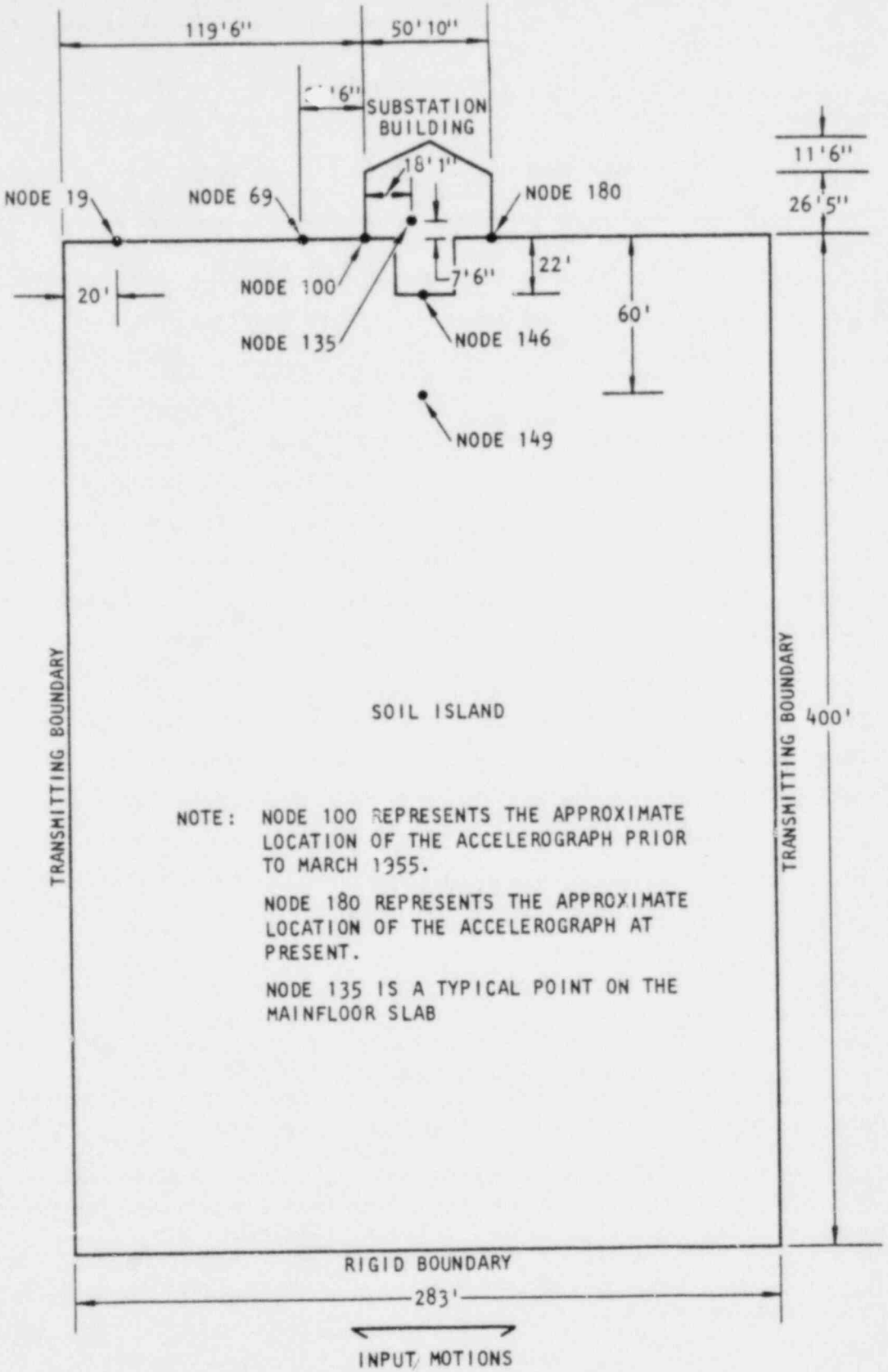

FIGURE 4-7. SOIL/STRUCTURE MODEL FOR *FLUSH* ANALYSIS
(Simplified from Figure 3-4)

The plane strain and modified two-dimensional results are provided as 5% damped response spectra at the above node point locations. These spectra are compared to each other and to the free-field ground surface spectrum to provide a means for assessing the nature of the soil/structure interaction at El Centro, as represented by the FLUSH code analysis. In addition, the structure response after one iteration of the FLUSH code analysis (which uses strain-dependent soil properties from the final iteration of the free-field analysis) is compared to the response after several additional FLUSH iterations (which uses strain-dependent soil properties that have been adjusted to account for the presence of the structure). The purpose of this comparison is to test a hypothesis by Kausel et al. (1976) which suggests that the nonlinearities induced in the soil by the presence of the structure are of secondary importance when compared to the nonlinearities induced solely by the incident seismic waves.

4.3.2 DESCRIPTION AND DISCUSSION OF RESULTS

The various finite element analysis results are tabulated in Table 4-3 as Cases 7 and 8 for the plane strain analysis and as Cases 9 and 10 for the modified two-dimensional (2-D) calculations. Cases 7 and 9 correspond to the results from a single iteration for each set of calculations, whereas Cases 8 and 10 represent the results from a sufficient number of iterations to assure adequate convergence of the equivalent linear properties in each soil element.

The comparisons of the system response from one iteration and from multiple iterations are depicted in Figures 4-8 and 4-9 and in Table 4-4. These results indicate that, for both the plane strain and modified 2-D analyses, the additional iterations exert only minor influences on the computed soil/structure response. They tend to support the above-indicated hypothesis of Kausel et al. (1976) regarding the relative lack of importance on the nonlinearities induced in the soil solely by the presence of the structure.

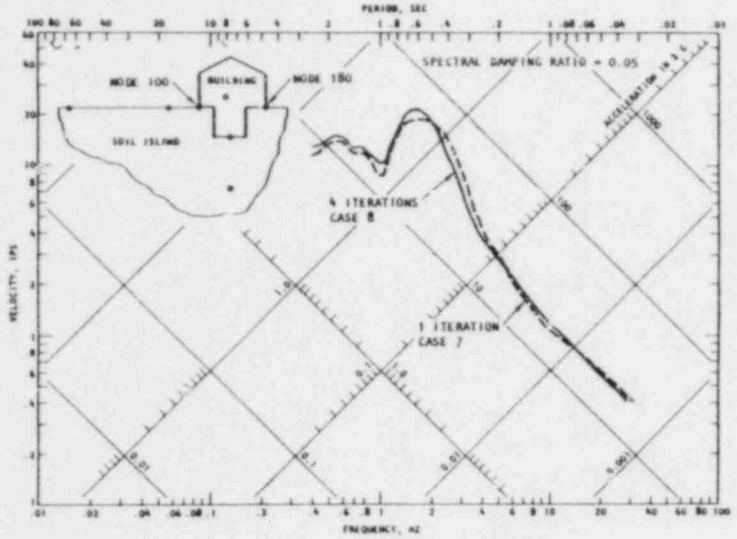

(a) Nodes 100 and 180

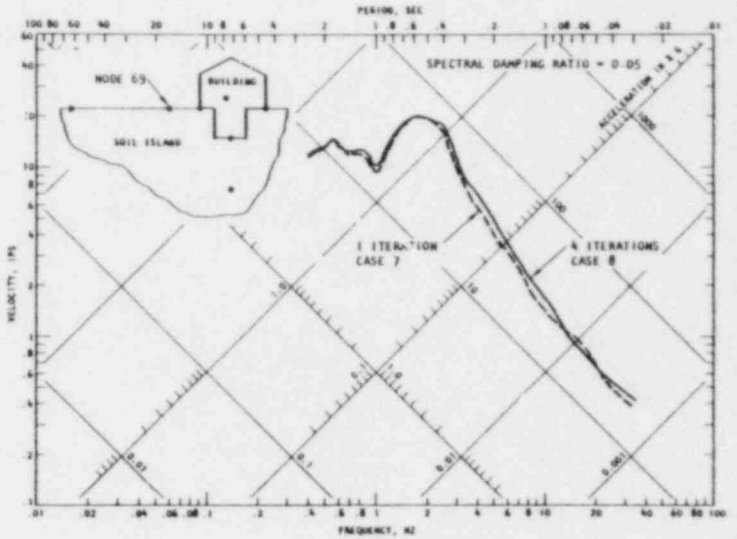

(b) Node 69

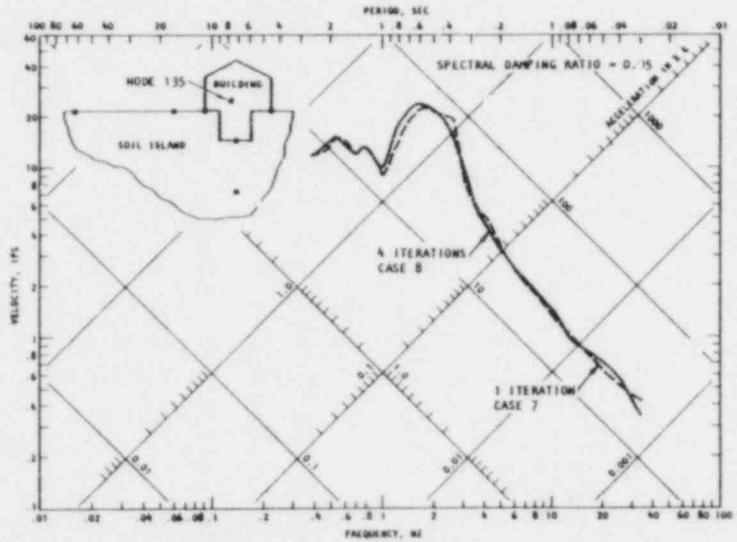

(c) Node 135

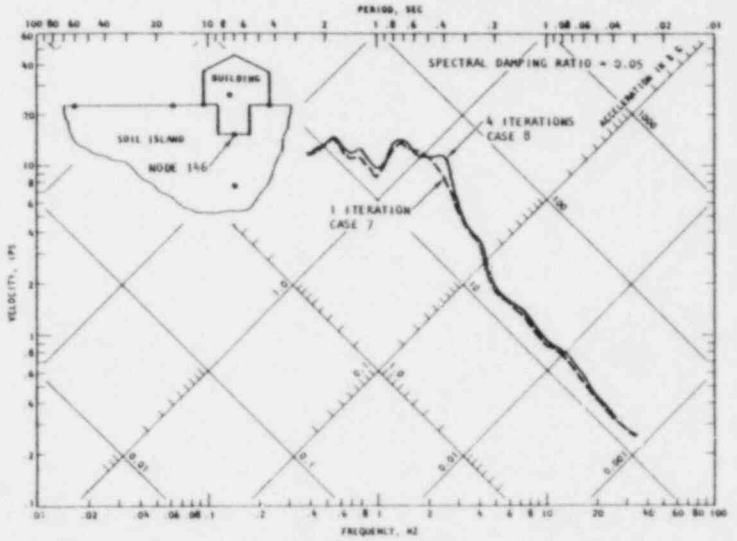

(d) Node 146

FIGURE 4-8. INFLUENCE OF NUMBER OF ITERATIONS ON RESPONSE OF SOIL/STRUCTURE SYSTEM -- PLANE/STRAIN ANALYSIS

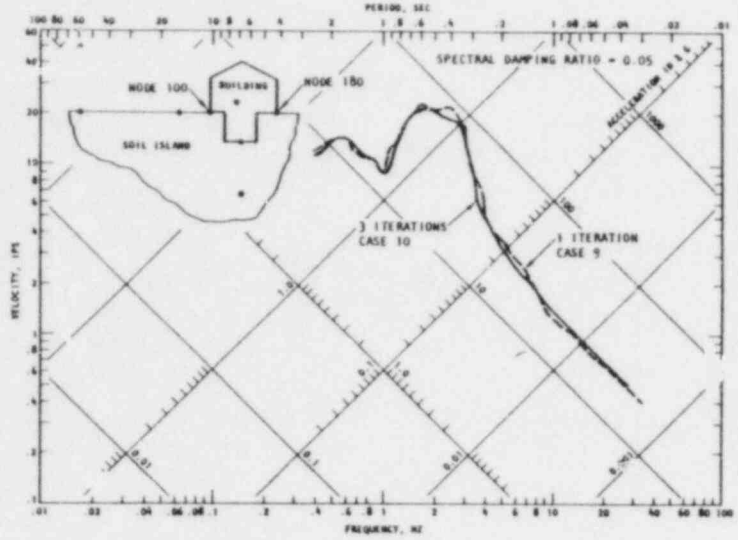

(a) Nodes 100 and 180

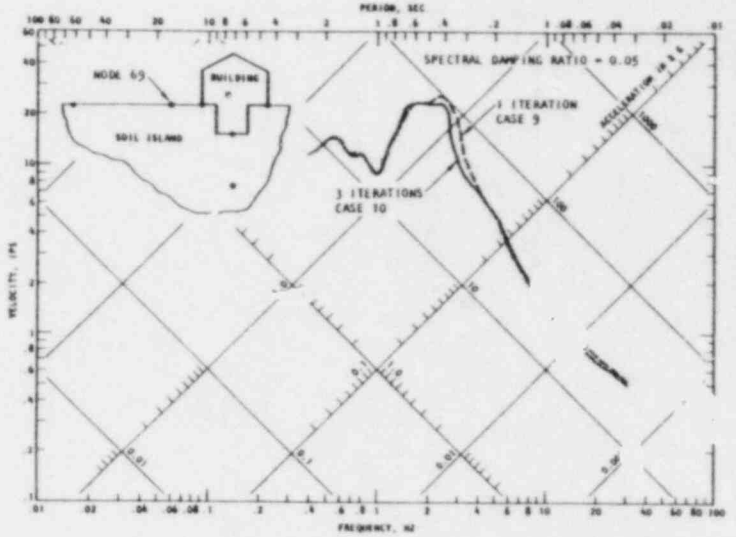

(b) Node 69

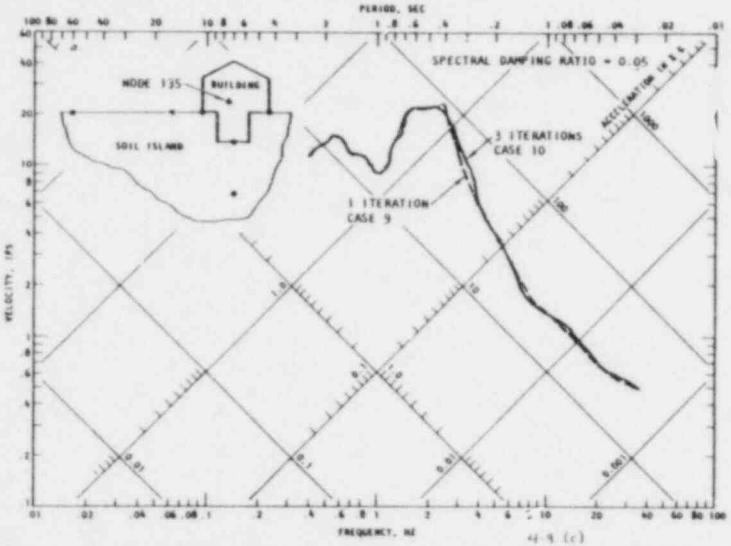

(c) Node 135

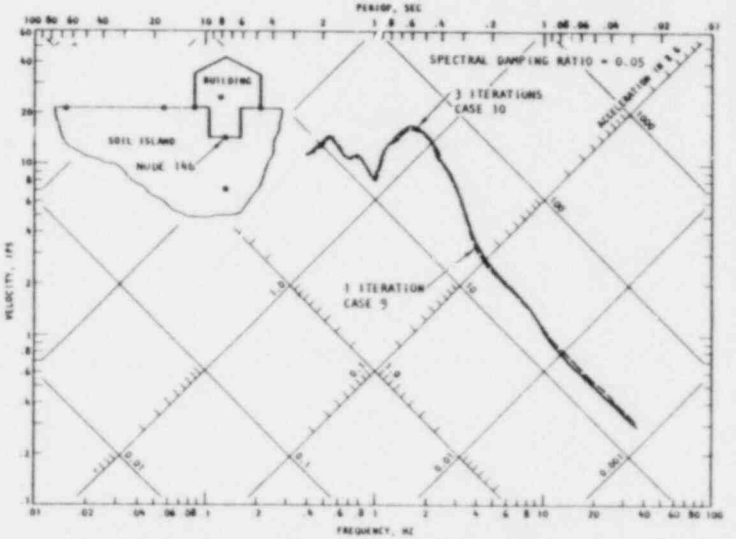

(d) Node 146

FIGURE 4-9. INFLUENCE OF NUMBER OF ITERATIONS ON RESPONSE OF SOIL/STRUCTURE SYSTEM--
MODIFIED 2-D ANALYSIS

TABLE 4-4. COMPARISON OF PEAK HORIZONTAL GROUND SURFACE ACCELERATIONS AT SELECTED NODAL POINTS

Nodal Point	Peak Horizontal Ground Surface Accelerations, g			
	Plane Strain		Modified Two-Dimensional	
	Case 7	Case 8	Case 9	Case 10
	One Iteration	Four Iterations	One Iteration	Three Iterations
19*	0.256	0.266	0.275	0.272
69	0.217	0.217	0.260	0.245
100	0.191	0.190	0.217	0.218
135	0.233	0.239	0.237	0.240
146	0.135	0.137	0.172	0.174
149	0.117	0.120	0.127	0.132
180	0.191	0.190	0.218	0.219

*Free-field-response peak ground surface accelerations = 0.272g

The most important results from these calculations correspond to the comparisons between the free-field ground surface motions and the computed motions at the former and present accelerograph locations within the building (Nodes 100 and 180). These comparisons are shown in Figure 4-10a and Table 4-5 and indicate the following trends:

- The structure response spectra at the two accelerograph locations are identical to one another and fall below the free-field ground surface response spectrum at frequencies greater than about 1.5 Hz.

- The accelerograph motions computed from the plane strain analysis are somewhat lower than those computed from the modified 2-D analysis. At frequencies of 2 Hz or greater, the plane strain analysis results show the spectral accelerations of the free field to exceed those of the structure (at the accelerograph locations) by factors ranging from 1.33 to 2.29. The corresponding factors from the modified 2-D results range from 1.19 to 1.69 (see Table 4-5).

Another comparison of note is that of the free-field ground surface response spectrum, as computed from the SHAKE calculations, to that at Node 19 in the FLUSH soil/structure grid, which is a point along the ground surface that is far from the structure. Figure 4-10b shows these spectra to be nearly identical, indicating that the overall width of the finite element soil/structure grid was adequate and that the transmitting boundary was working well for both the plane strain and the modified 2-D analyses.

The FLUSH results also provide comparisons of computed responses at various locations within the building (Fig. 4-11) and within the soil medium (Fig. 4-12). These comparisons indicate that

- Within the structure, the response spectra along the first-floor level (Node 135) and at the corners of the basement (Nodes 100 and 180) are quite similar. At frequencies above

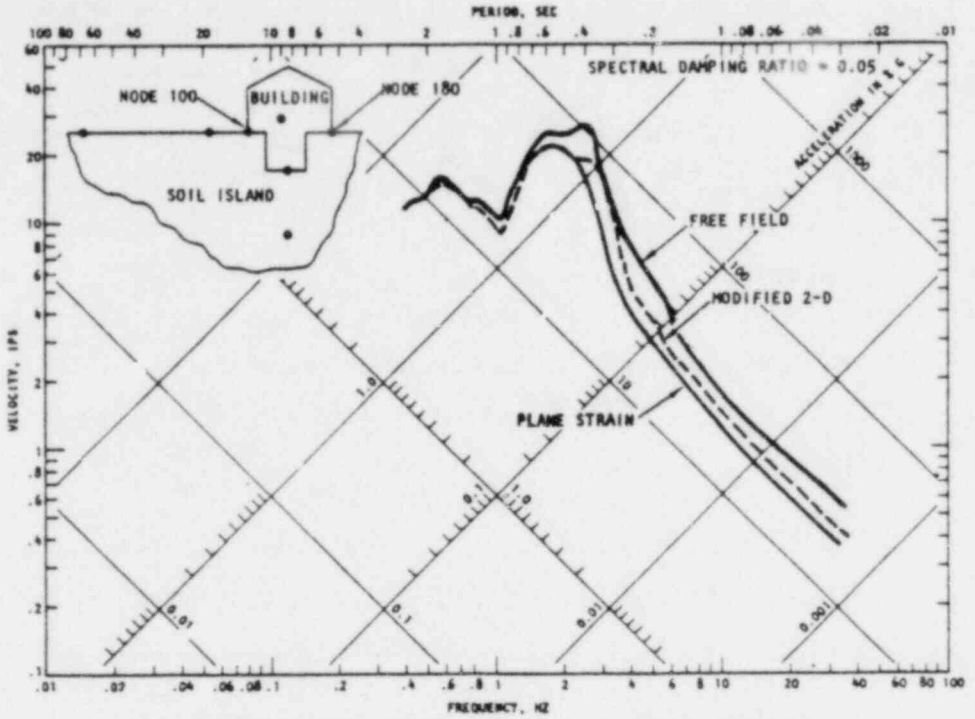

(a) Comparisons with structure response at accelerograph locations (Nodes 100 and 180)

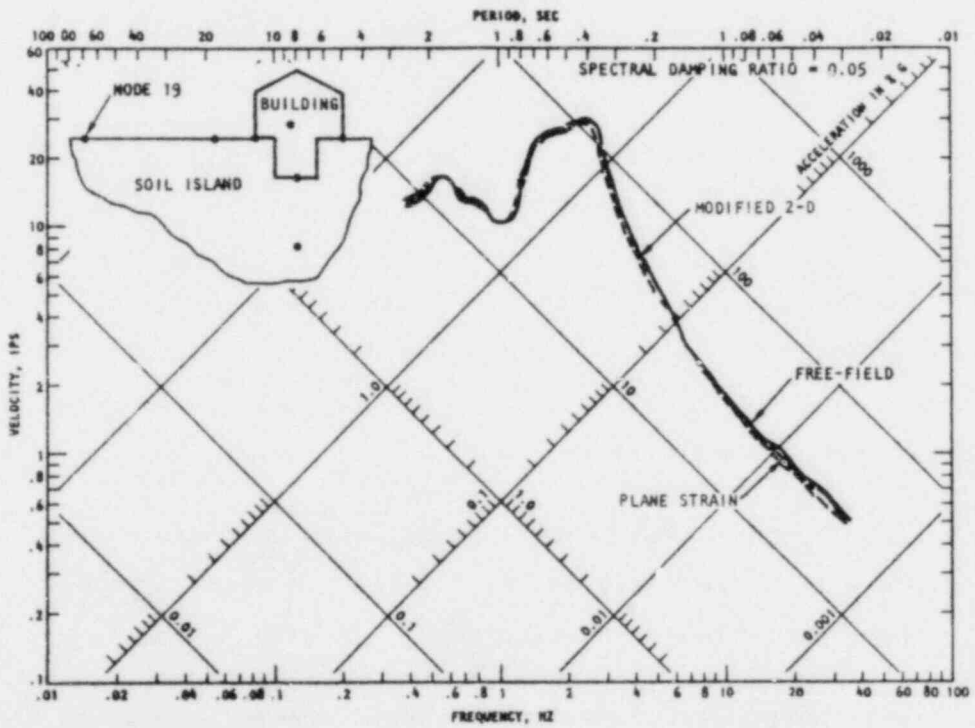

(b) Comparison with soil response at node 19

FIGURE 4-10. COMPARISONS OF FREE-FIELD GROUND SURFACE RESPONSES AND COMPUTED SOIL/STRUCTURE SYSTEM RESPONSE

TABLE 4-5. EFFECT OF SOIL/STRUCTURE INTERACTION ON MOTIONS ALONG BASEMENT OF EL CENTRO TERMINAL SUBSTATION BUILDING--*SHAKE/FLUSH* RESULTS

Frequency, Hz	Absolute Horizontal Spectral Acceleration, g				
	Finite Element FLUSH Model (Nodal Points 100 and 180)				
	Case 3 Free-Field (1-D SHAKE Model)	Case 8 Structure (Plane Strain)	Case 3 / Case 8 or Free Field / Structure (Plane Strain)	Case 10 Structure (Modified 2-D)	Case 3 / Case 10 or Free Field / Structure (Modified 2-D)
0.40	0.076	0.078	0.97	0.076	1.00
0.50	0.112	0.119	0.94	0.111	1.01
0.80	0.161	0.175	0.92	0.158	1.02
1.0	0.152	0.165	0.92	0.146	1.04
1.6	0.606	0.562	1.08	0.539	1.12
2.0	0.797	0.601	1.33	0.661	1.21
2.5	1.076	0.511	2.11	0.787	1.37
3.2	0.613	0.343	1.79	0.462	1.33
3.6	0.648	0.283	(2.29)	0.384	(1.69)
4.0	0.513	0.255	2.01	0.334	1.54
5.0	0.465	0.230	2.02	0.284	1.64
8.0	0.281	0.198	1.42	0.236	1.19
10.0	0.282	0.195	1.45	0.228	1.24

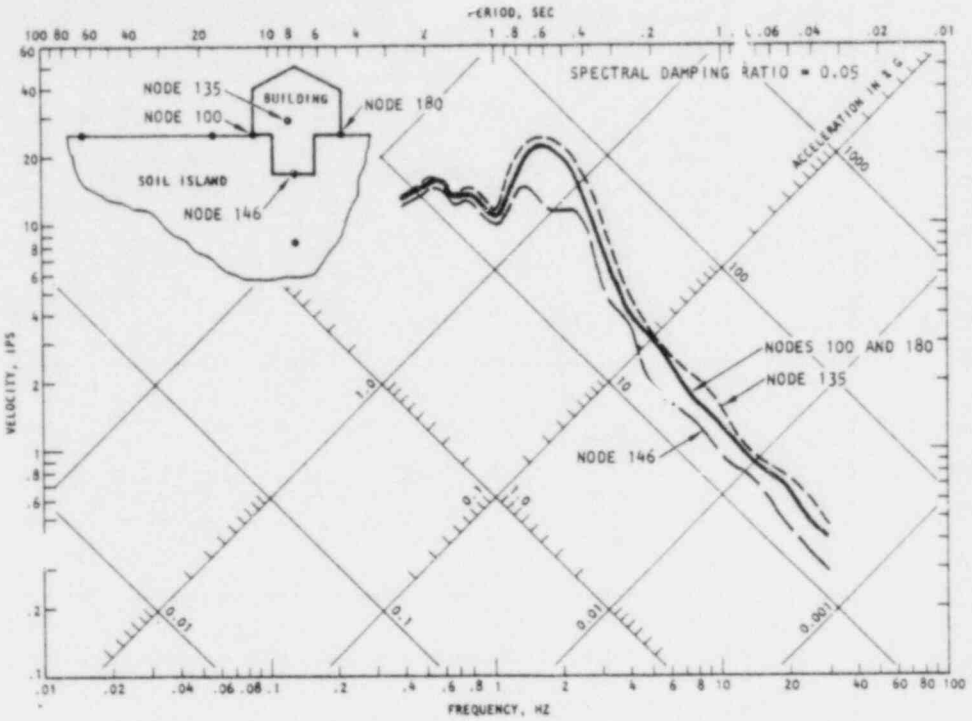

(a) Plane strain analysis results

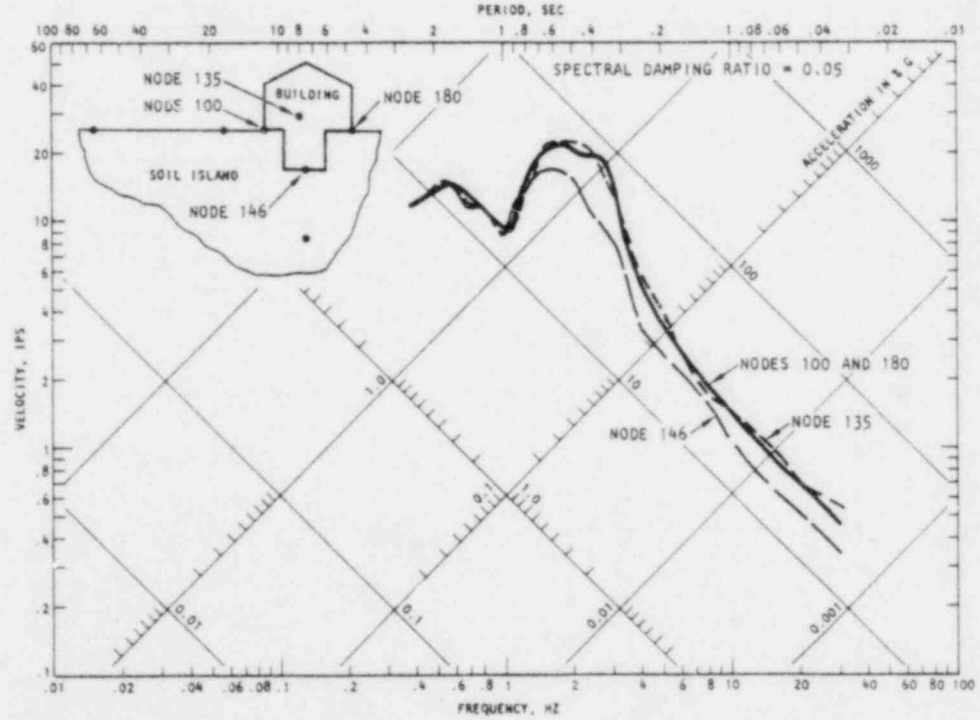

(b) Modified 2-D analysis results

FIGURE 4-11. RESPONSE SPECTRA OF MOTIONS WITHIN STRUCTURE

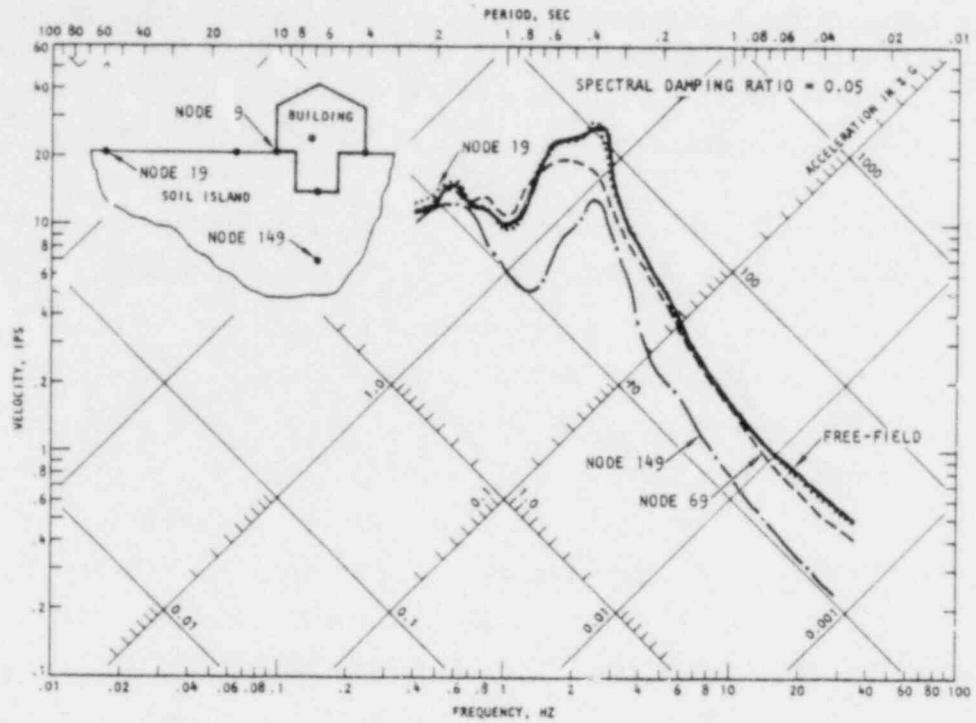

(a) Plane strain analysis results

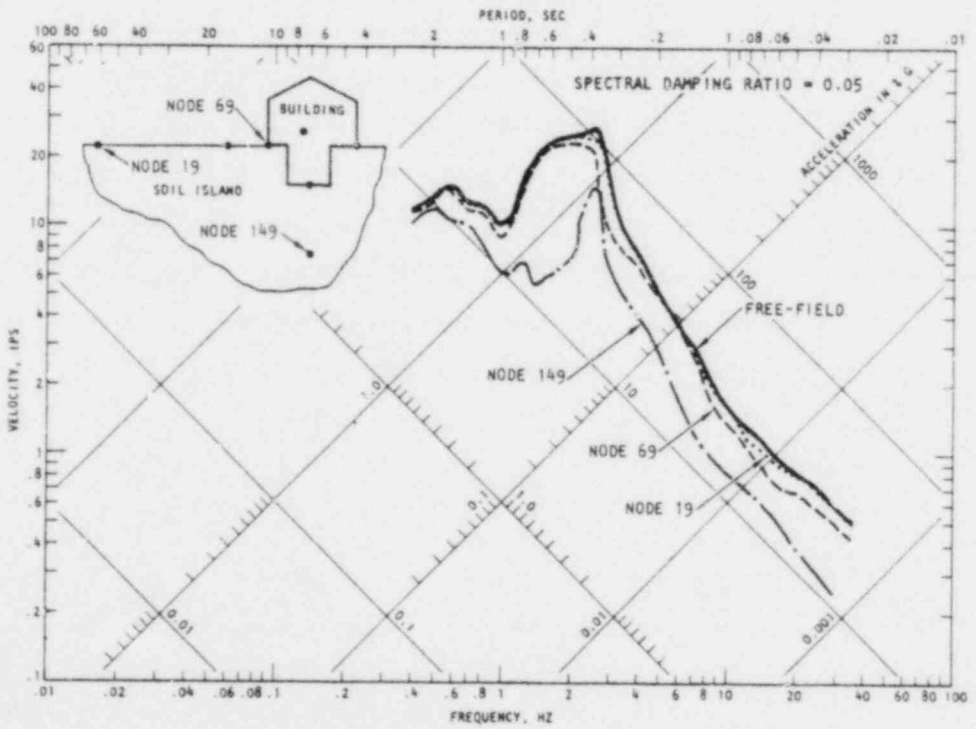

(b) Modified 2-D analysis results

FIGURE 4-12. RESPONSE SPECTRA OF MOTIONS WITHIN SOIL MEDIUM

about 1 Hz, these spectral amplitudes at these locations exceed those at the base of the foundation block (Node 146) probably because of the significant mass of the block.

- Within the soil medium, the ground surface response at Node 19, a point far from the structure, has been previously indicated to be nearly identical to the free-field ground surface response. However, the response at Node 69, a point along the ground surface only 25 ft from the structure, falls below that of the free field at frequencies ranging from about 1.5 Hz to 6 Hz, because of soil/structure interaction effects. The soil response spectrum at Node 149, 38-ft below the foundation block and 60-ft below the ground surface, falls well below the ground surface response spectra at all frequencies; this is probably due primarily to the depth dependence of the computed free-field motions, although soil/structure interaction may have had some effect on this particular comparison.

The above trends hold for both the plane strain and the modified 2-D results. Comparisons of response spectra computed from these two sets of results at the various structure and soil node points are provided in Figure 4-13. These comparisons indicate that, as previously noted for Nodes 100 and 180, the plane strain analysis resulted in slightly less intense structure motions than did the modified 2-D analysis. However, the motions at Nodes 69 and 149 in the soil medium are nearly identical for the two cases.

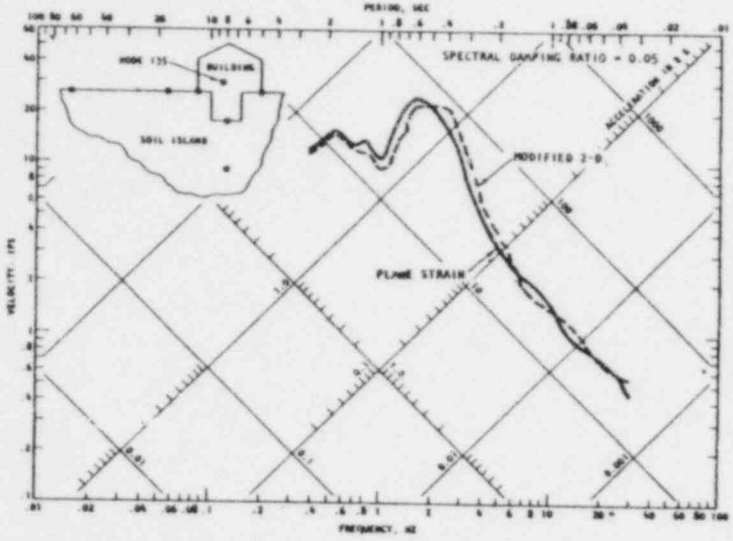

(a) First floor of building (Node 135)

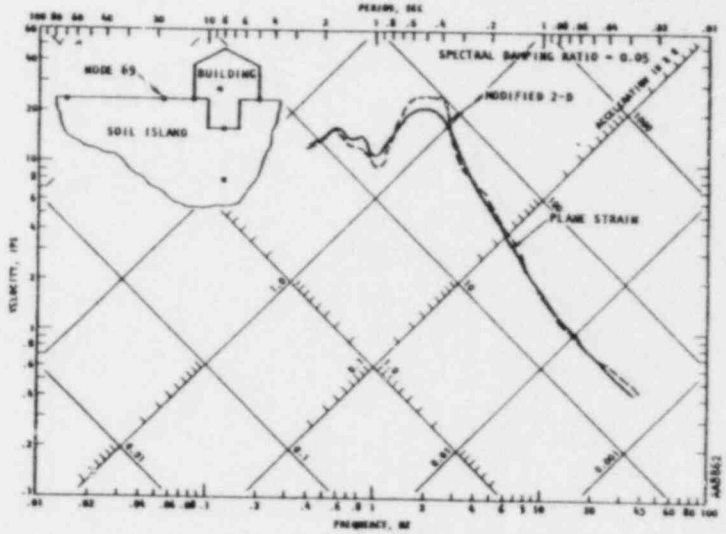

(b) Along ground surface near structure (Node 69)

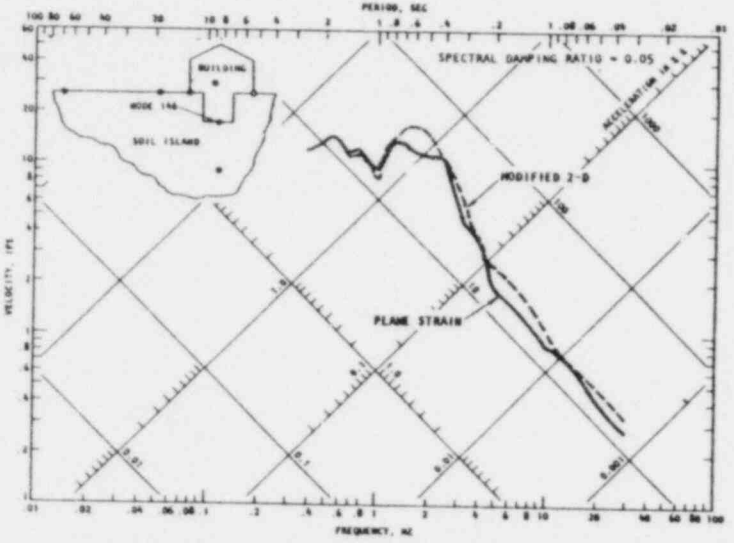

(c) Base of foundation block (Node 146)

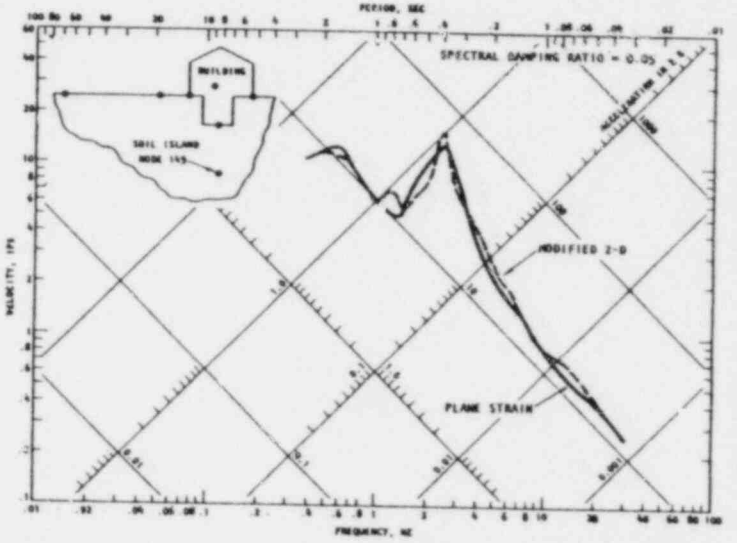

(d) Soil medium below structure (Node 149)

FIGURE 4-13. COMPARISONS OF RESPONSE SPECTRA FROM PLANE/STRAIN AND MODIFIED 2-D ANALYSIS RESULTS

CHAPTER 5

ANALYSIS RESULTS USING *TRI/SAC* CODE

5.1 SYSTEM PARAMETERS

As noted in Chapter 3, the TRI/SAC assessments of soil/structure interaction effects at the El Centro Terminal Substation accelerograph site involve first a free-field response calculation, then a soil/structure system response calculation, and finally a comparison of response results from these calculations at corresponding locations in the grid. Both the free-field and the soil/structure system calculation use identical two-dimensional models of the soil medium and identical input motions along the left boundaries of each grid. The input motions, soil properties, and damping parameters used in these calculations are given below; the structure properties are described in Chapter 3.

5.1.1 INPUT MOTIONS

The input motions applied uniformly along the left boundary of the two grids correspond to the first 3 sec of the S45E and vertical components of motion recorded at the Santa Barbara, California, Courthouse during the Santa Barbara earthquake of 30 June 1941 (Fig. 5-1). These particular motions were selected for the following reasons:

- The site at which these motions were recorded is a deep alluvium site that is reasonably similar to the El Centro Terminal Substation site.
- The ground shaking represented by these motions is reasonably strong, with peak horizontal and vertical accelerations of about 0.18 g and 0.07 g, respectively.

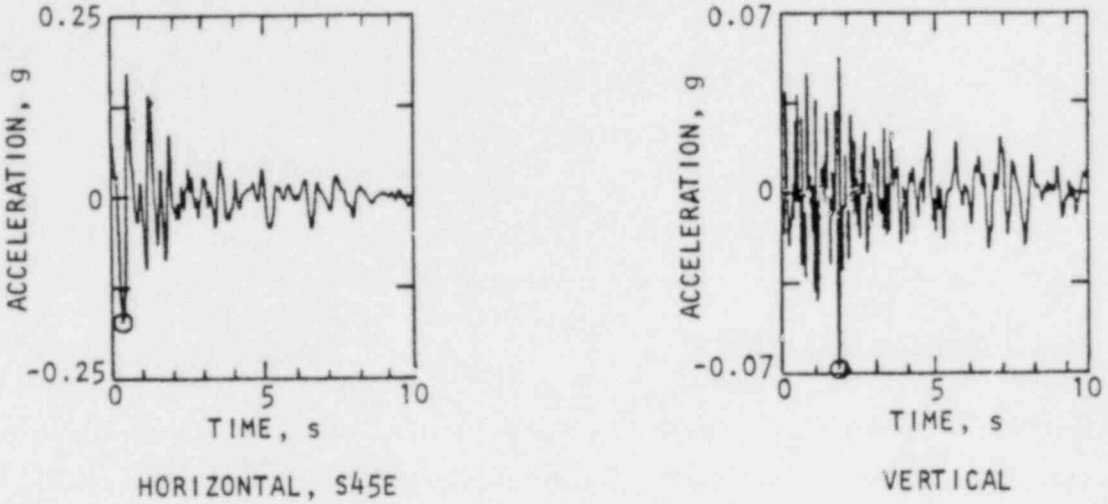

(a) Accelerograms (first 3 seconds used in calculation)

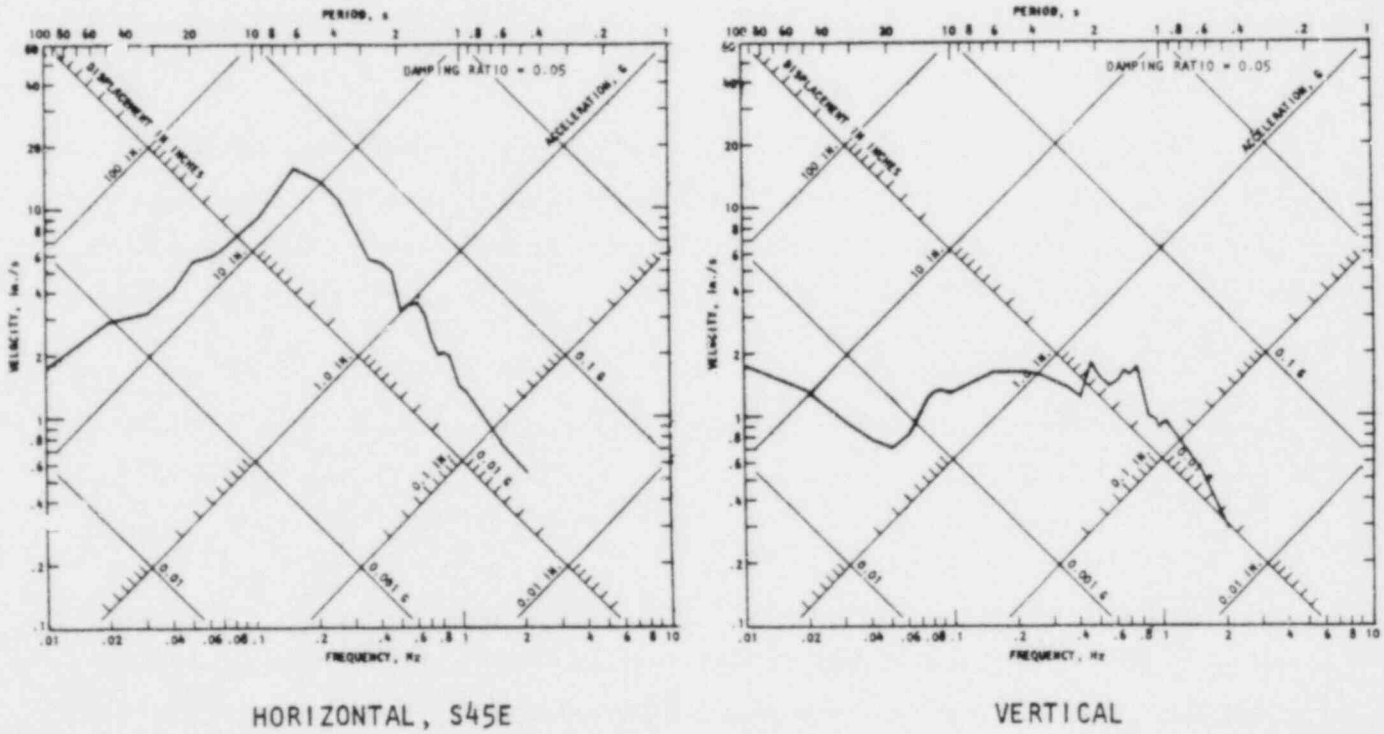

(b) Response spectra for 3 seconds of motion

FIGURE 5-1. INPUT MOTIONS FOR *TRI/SAC* ANALYSIS — 30 JUNE 1941 SANTA BARBARA, CALIFORNIA RECORDS

- Much of the significant strong motion represented by these acceleration records occurs over a short time span (Fig. 5-1). Therefore, the 3-sec duration considered in these calculations to reduce computer costs encompasses most of the strong shaking recorded during this earthquake event, at least in the moderate-to-high frequency range. (However, this short duration will result in some truncation of the system response at low frequencies).

5.1.2 SOIL PROPERTIES

Because the TRI/SAC code is linear, it is not possible to establish properties of the soil elements that are consistent with the strain levels developed in the elements during the particular shaking induced by the input motions described above. An iterative approach could, in theory, be used in conjunction with TRI/SAC in much the same manner as FLUSH; however, because of the structure of the TRI/SAC code, costs associated with such an approach would be prohibitive. Therefore, it is necessary to estimate linear soil properties that, although not fully compatible of the earthquake-induced soil strain levels, provide at least a general approximation of the behavior of the El Centro site during a reasonably strong earthquake.

With these considerations in mind, the iterated soil properties from the SHAKE code calculations described in Chapter 4 (see Case 1 of Table 4-1) have been used as the basis for estimating linear soil properties for the TRI/SAC calculations. As shown in Table 5-1, the shear moduli of the soil layers in the TRI/SAC model are essentially identical to the iterated shear moduli of the upper soil layers in the SHAKE model. However the TRI/SAC representation of the damping in the soil medium in terms of the iterated SHAKE results is less straightforward; this is because SHAKE defines a damping ratio, λ, for each soil layer whereas TRI/SAC represents damping only for the combined soil/structure system in terms of a Rayleigh damping matrix. The determination of this overall system damping is discussed in the next subsection.

TABLE 5-1. SOIL PROPERTIES USED IN *TRI/SAC* CALCULATIONS

Iterated Properties from SHAKE Code (Case 1, Table 4-1)[1]				Assumed Properties for TRI/SAC Calculations[1,2]		
Layer No. (Fig. 3-8)	Thickness, ft	Shear Modulus, kip/ft^2	Damping Ratio	Layer No.	Thickness, ft	Shear Modulus, kip/ft^2
1	6	217.8	0.048	1	6	218.0
2	10	222.6	0.063	2	10	224.0
3	16	349.9	0.064	3	16	350.0
4	28	1499.5	0.050	4	28	1500.0
5	54	808.5	0.126	5	54	817.0

Notes:

[1]Unit weight taken at 0.12 kip/ft^3 for upper 5 layers in SHAKE model and for all layers in TRI/SAC model

[2]Damping for TRI/SAC model is assumed to be represented by Rayleigh damping coefficients $\alpha = 0.317$ and $\beta = 0.0027$ (see Fig. 5-2)

5.1.3 DAMPING PARAMETERS

The TRI/SAC code represents damping for the soil/structure system as

$$[C] = \alpha[M] + \beta[K] \tag{5-1}$$

where [C], the Rayleigh damping matrix for the system, is expressed as a weighted sum of the system mass matrix [M] and stiffness matrix [K]. Thus it is seen that two parameters, α and β, must serve to represent the damping characteristics of the entire soil/structure system. These damping characteristics can be defined from α and β either by using Equation 5-1 directly or, alternatively, by expressing Equation 5-1 in terms of modal damping ratios, ξ_n, and corresponding frequencies, ω_n, i.e.,

$$\xi_n = \frac{\alpha}{2\omega_n} + 2\beta\omega_n \tag{5-2}$$

Equation 5-2 shows that α and β can be defined to represent desired damping ratios for two modes of vibration of the soil/structure system; damping ratios for other modes are computed using Equation 5-2, once α and β are specified.

With this as background, it is necessary to estimate α and β such that the overall damping characteristics in the various soil layers as well as the structure are appro'mated. This has been done by considering basic concepts described by Roesset et al. (1973), who showed that the total damping ratio in a given mode of a soil/structure system can be estimated as the weighted sum of the damping ratios of the individual system components; the weighting factors correspond to the strain energy of that component in that mode. On this basis, since the modes of interest for this study correspond to those featuring the primary response of the structure, the upper layers of the soil medium will be of greatest importance and will undergo the greatest amount of energy in these modes. Therefore the damping of these upper layers,

which from the SHAKE calculations (Table 5-1) vary from 0.046 to 0.064, will have the greatest influence on the overall system damping. Considering these soil damping levels together with an estimated structure damping ratio of about 0.05 in these predominant modes, the overall system damping ratios for these modes should be on the order of about 0.05.

This line of reasoning was used to establish α and β for the TRI/SAC soil/structure model. The predominant modes of the system were assumed to fall in a frequency range of about 0.5 Hz to 5 Hz, and α and β were selected to provide damping ratios of about 0.05 or less in this range. The resulting frequency-dependent damping ratios are shown in Figure 5-2 and are seen to vary from about 0.03 to 0.05 in the 0.5 Hz to 5 Hz frequency range. Beyond this range, the damping ratios take on larger values.

For the free-field grid, the same values of α and β were used. The rationale for this was that (1) it was desired to keep the material properties of the free-field grid and the soil/structure grid as nearly similar as possible; (2) the damping ratio of the structure and of the upper soil layers are reasonably similar so that, by deleting the structure and using the same reasoning as outlined in the above paragraphs, the overall damping of the free-field grid should be similar to that of the soil/structure grid.

5.2 FREE-FIELD RESPONSE

The first set of calculations to be presented correspond to the computed free-field motions. Two sets of free-field results are presented--the first showing how the motions vary with distance from the left boundary, and the second showing the depth dependence of the computed free-field motions. These free-field responses, as well as the soil/structure system responses presented in Section 5.3, are provided as response spectra for a damping ratio of 0.05.

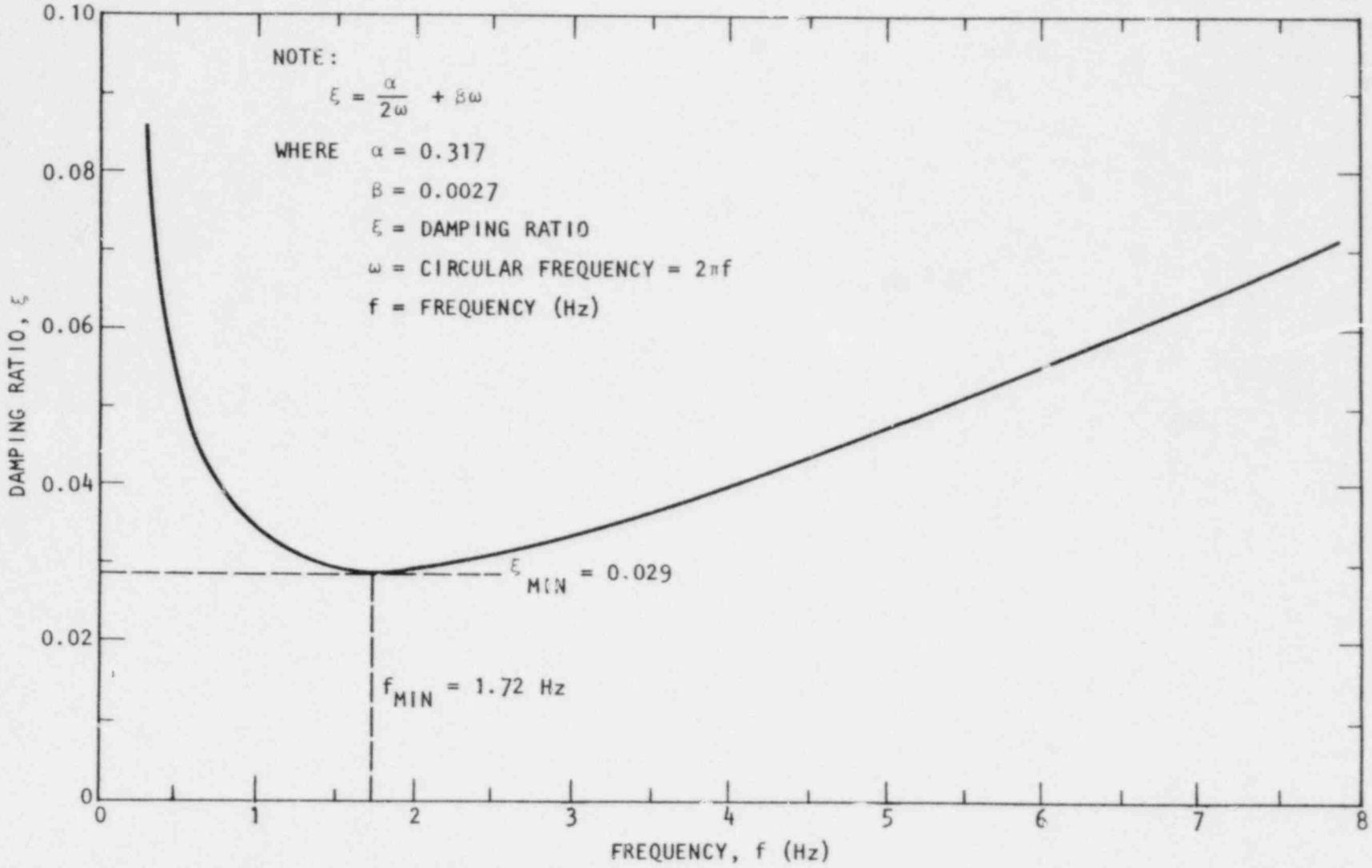

FIGURE 5-2. DAMPING CHARACTERISTICS OF SOIL/STRUCTURE SYSTEM

5.2.1 VARIATION WITH DISTANCE FROM LEFT BOUNDARY

The variation of free-field motions with distance from the left boundary is shown in Figures 5-3 and 5-4 for horizontal and vertical motions respectively. These figures contain several comparisons of free-field response spectra at various distances from the left boundary; the comparisons are provided at depths of 0, 24, 44, and 72 ft below the ground surface.

5.2.1.1 Horizontal Motions

The variation of the horizontal free-field motions with distance from the left boundary is shown from Figure 5-3 to have the following trends:

- The shapes of the spectra of the computed free-field horizontal motions are generally similar to those of the horizontal input motions at the left boundary.

- The amplitudes of horizontal motion computed 170 ft from the left boundary generally fall slightly below those at shorter distances (see discussion in Sec. 5.2.3). Otherwise, there are no consistent trends regarding distance effects.

5.2.1.2 Vertical Motions

The influence of distance from the left boundary on the computed vertical free-field motions is seen from Figure 5-4 to be as follows:

- The shapes of the spectra of the computed free-field vertical motions are markedly different from those of the vertical input motions at the left boundary. This is particularly true near the ground surface, where the upper soil layers appear to significantly amplify the vertical ground motions.

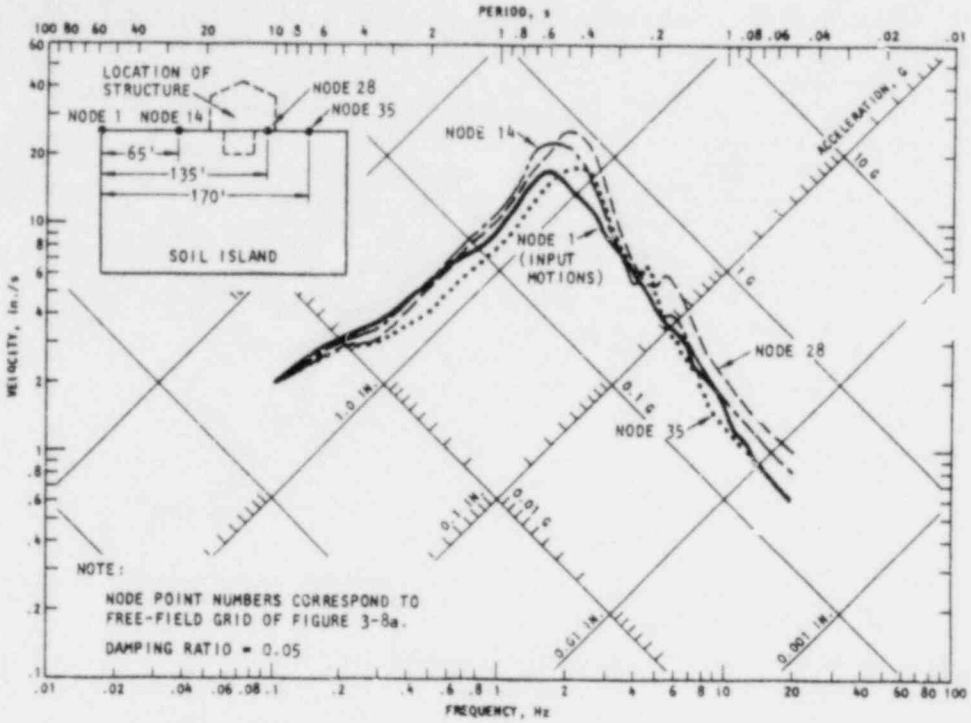

(a) Depth below ground surface = 0 feet

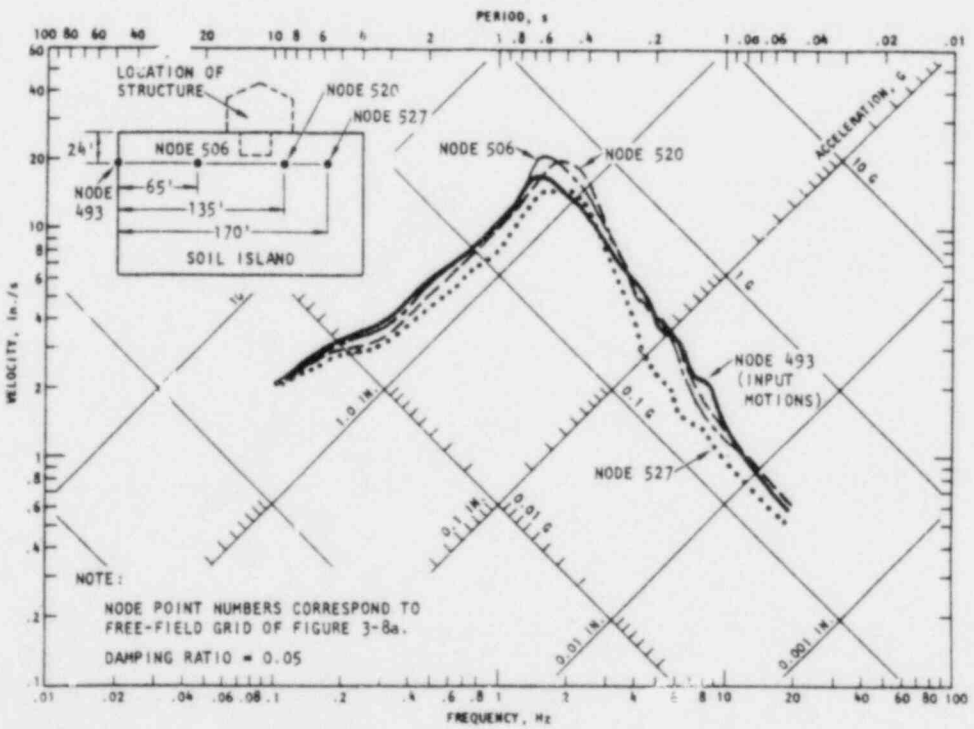

(b) Depth below ground surface = 24 feet

FIGURE 5-3. VARIATION OF COMPUTED FREE-FIELD HORIZONTAL MOTION WITH DISTANCE FROM LEFT BOUNDARY OF GRID

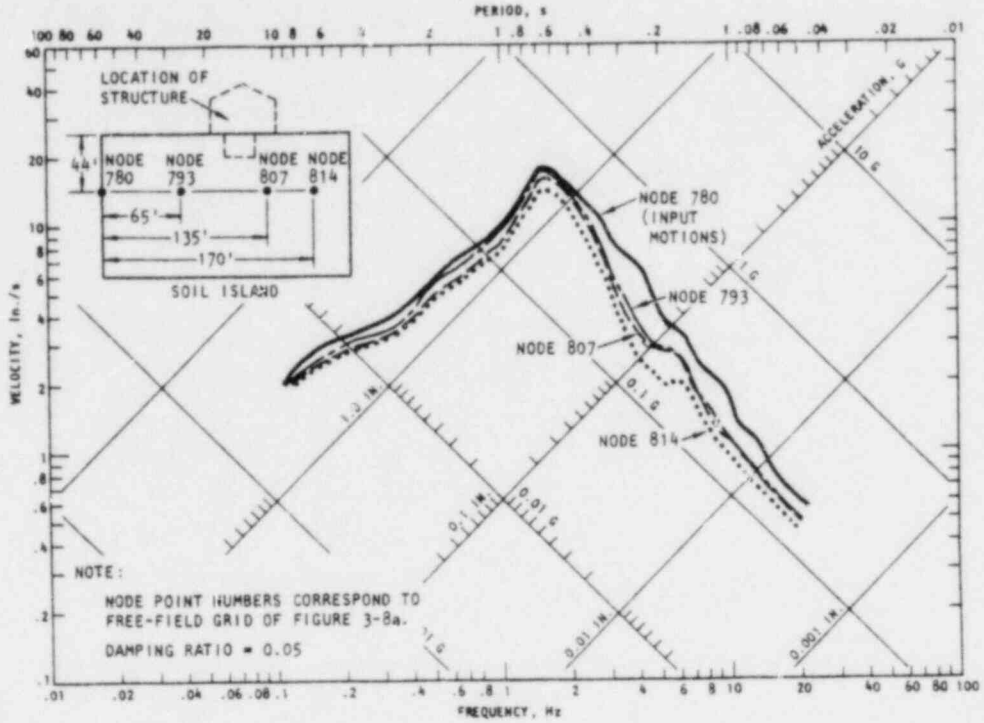

(c) Depth below ground surface = 44 feet

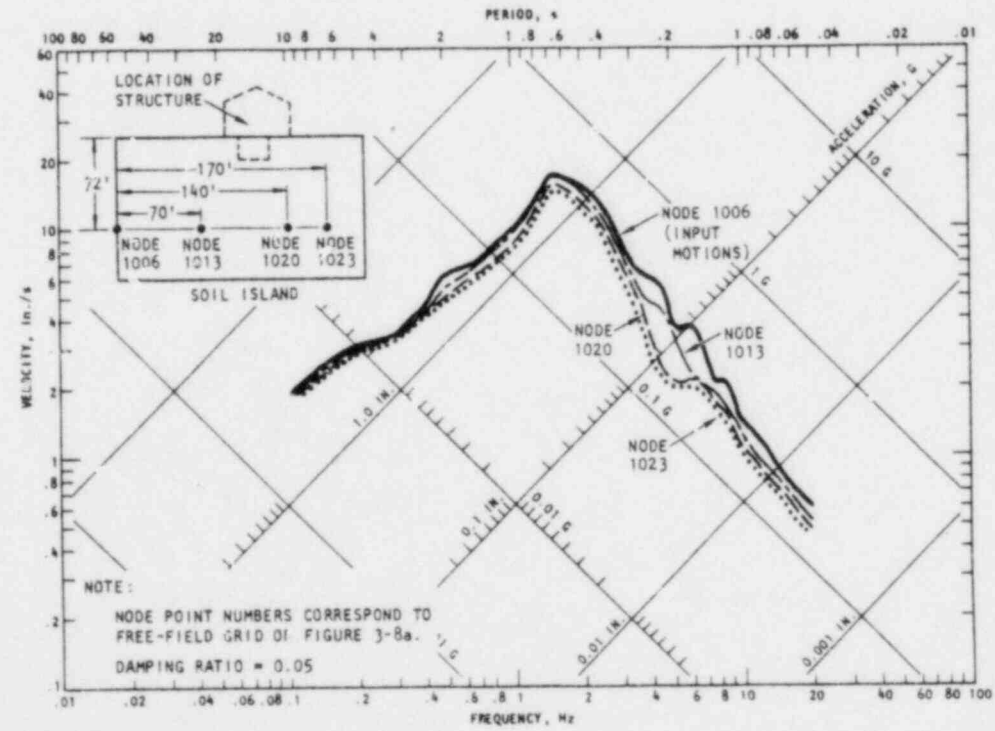

(d) Depth below ground surface = 72 feet

FIGURE 5-3. (CONCLUDED)

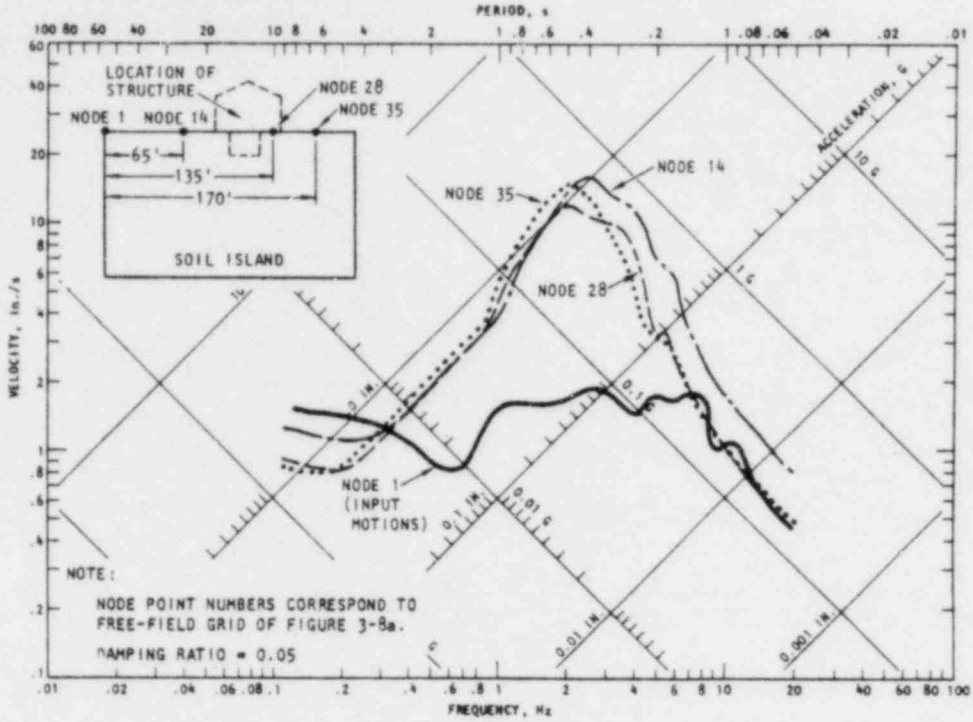

(a) Depth below ground surface = 0 feet

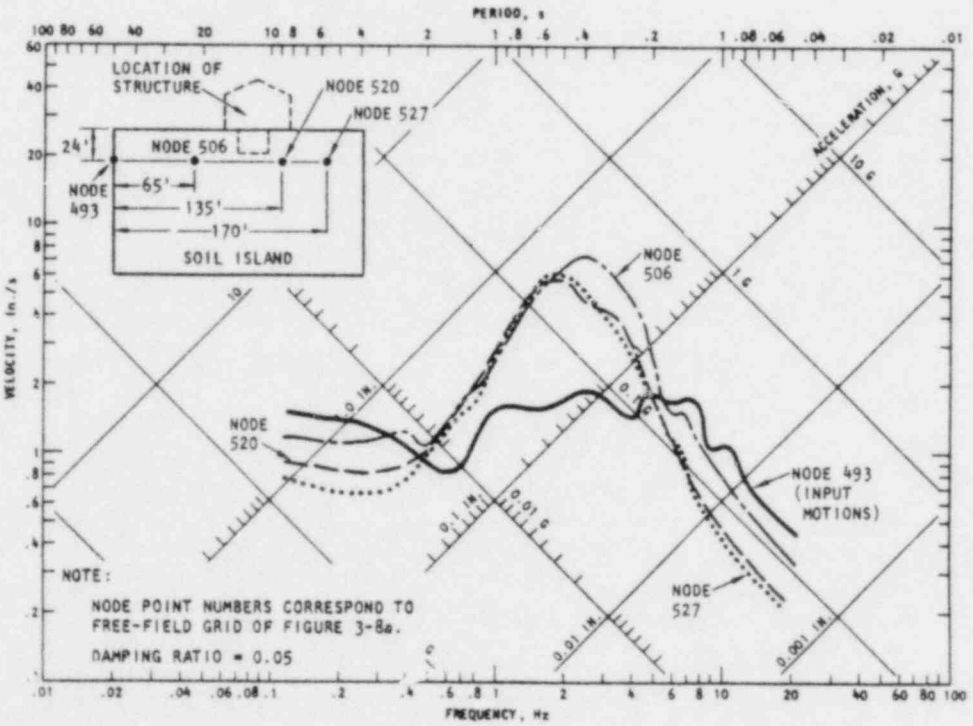

(b) Depth below ground surface = 24 feet

FIGURE 5-4. VARIATION OF COMPUTED FREE-FIELD VERTICAL MOTION WITH DISTANCE FROM LEFT BOUNDARY OF GRID

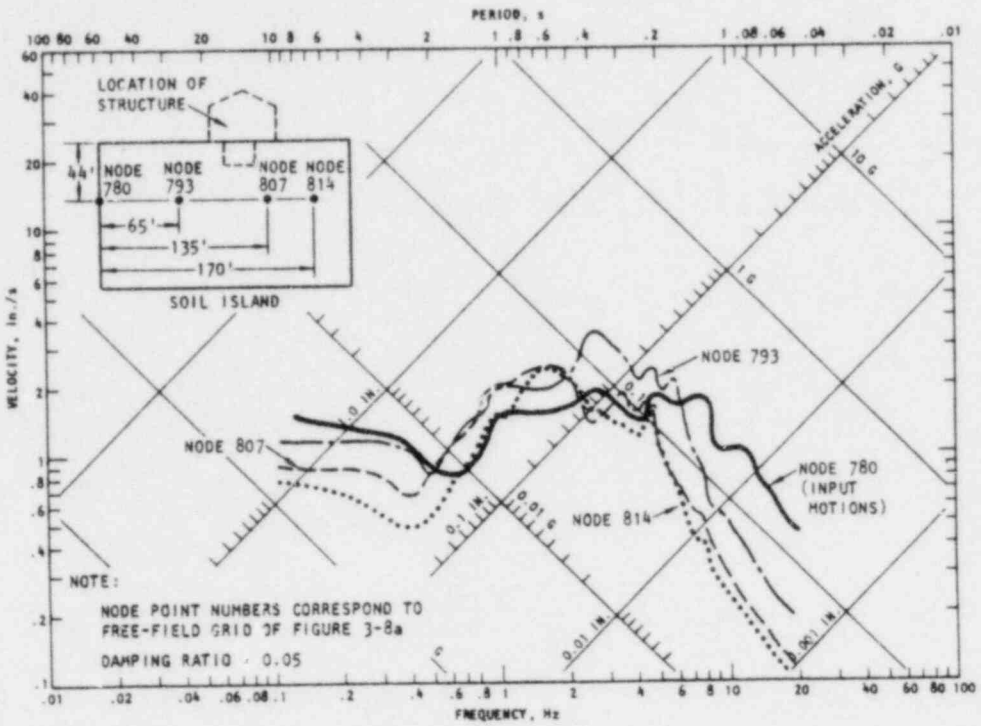

(c) Depth below ground surface = 44 feet

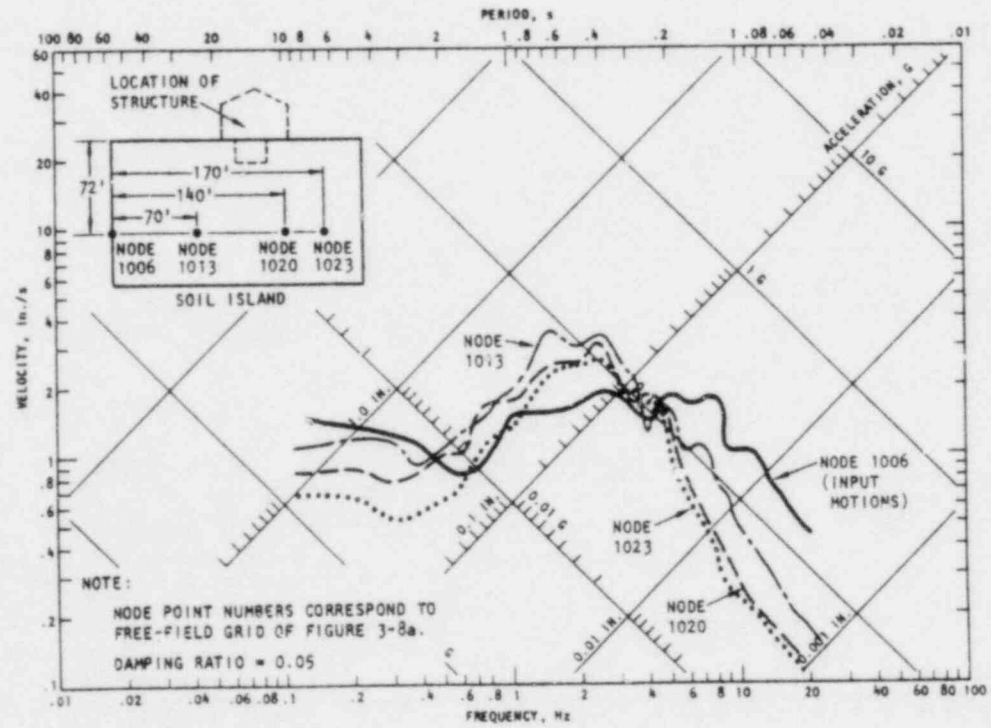

(d) Depth below ground surface = 72 feet

FIGURE 5-4. (CONCLUDED)

- At shallow depths, the greatest differences between vertical motion spectra at a given depth are seen to exist in the comparisons of spectra at 0 ft and 65 ft from the left boundary. These differences become much smaller with increasing distance from the left boundary.

5.2.2 VARIATION WITH DEPTH BELOW GROUND SURFACE

The variation of free-field motion with depth below the ground surface is shown in Figures 5-5 and 5-6 for horizontal and vertical motions respectively. These figures correspond to a cross plotting of the results given in Figures 5-3 and 5-4, in order to clearly show depth-dependent effects. They contain several comparisons of free-field response spectra at various depths; these comparisons are provided at distances of 30, 100, 135, and 170 ft from the left boundary.

5.2.2.1 Horizontal Motions

The variations in the free-field horizontal response spectra with increasing depth below the ground surface are shown in Figure 5-5 to be as follows:

- The variation of the spectra with depth is small when the distance to the left boundary of the free-field grid is short (e.g., 30 ft) and becomes greater at larger distances from that boundary.

- The depth-dependent effects on the low-frequency motions (below 2 Hz) is generally small. Differences between such motions at the ground surface and at a 72 ft depth are typically less than 10% at any given distance from the left boundary.

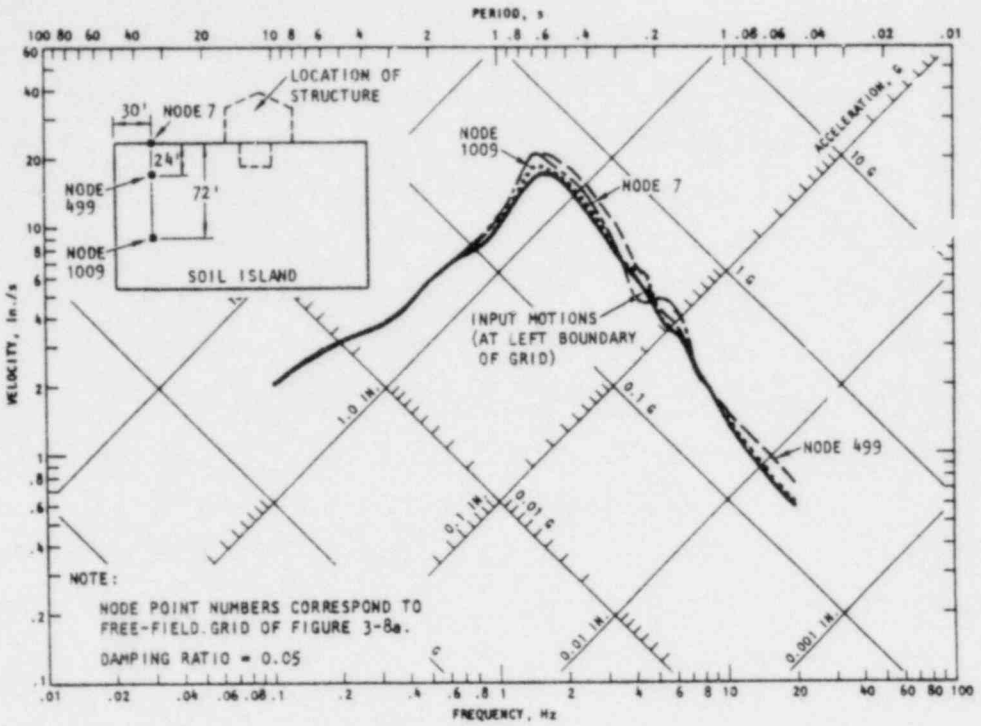

(a) Distance from left boundary of grid = 30 feet

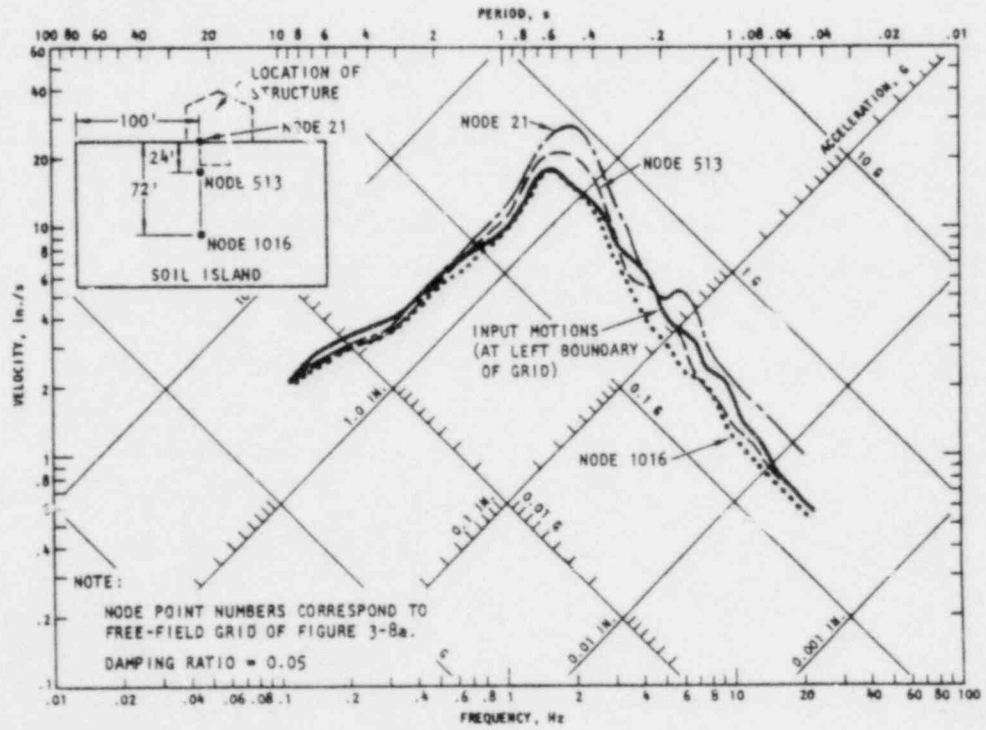

(b) Distance from left boundary of grid = 100 feet

FIGURE 5-5. VARIATION OF COMPUTED FREE-FIELD HORIZONTAL MOTION WITH DEPTH BELOW GROUND SURFACE

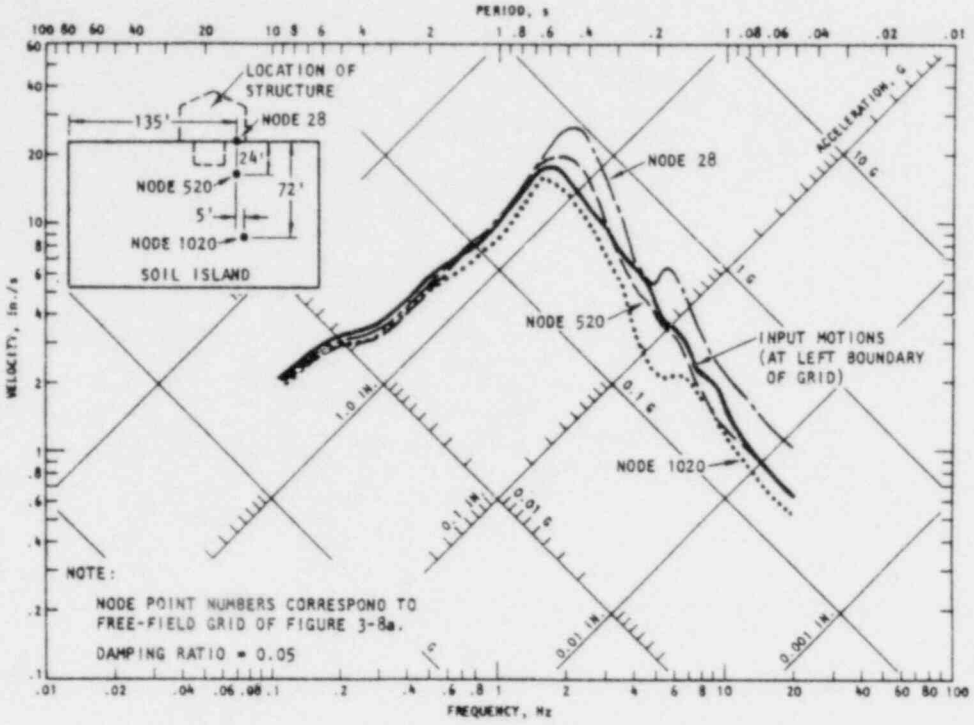

(c) Distance from left boundary of grid = 135 feet

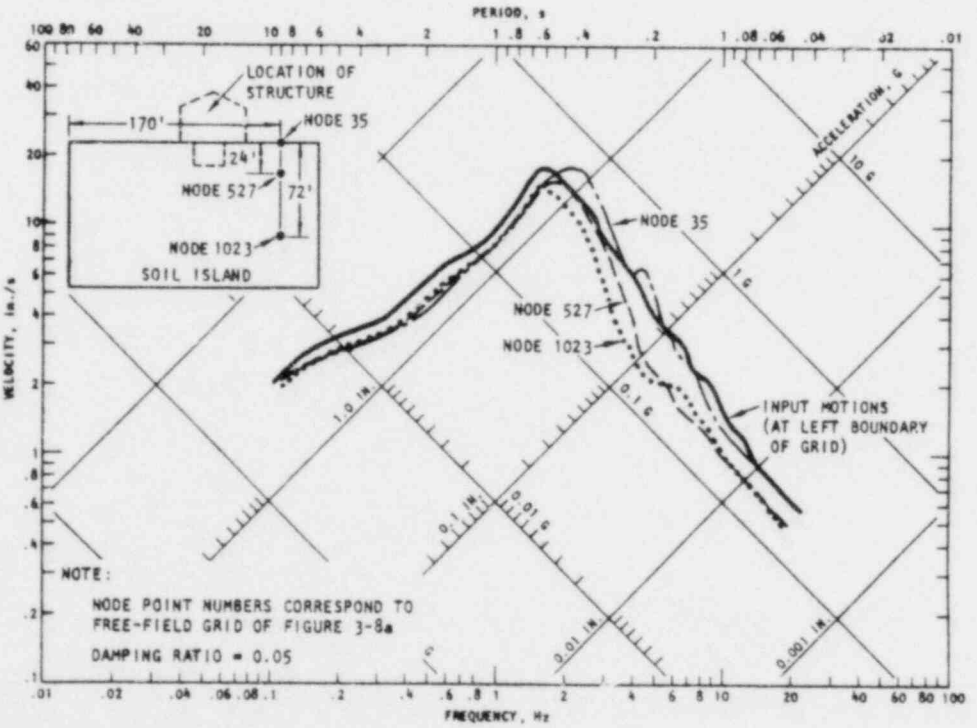

(d) Distance from left boundary of grid = 170 feet

FIGURE 5-5. (CONCLUDED)

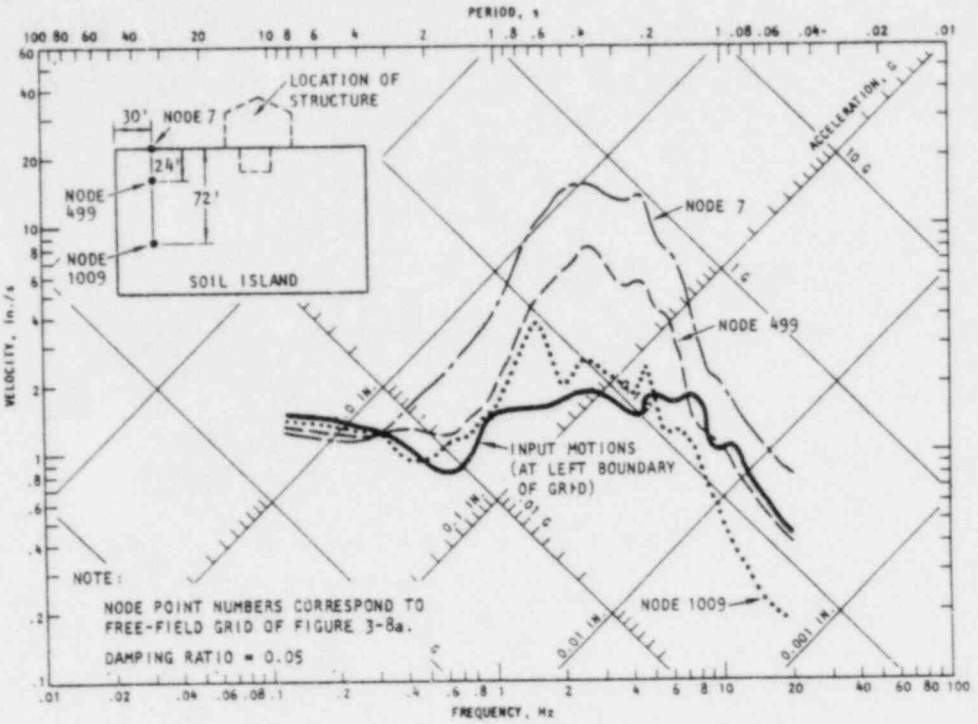

(a) Distance from left boundary of grid = 30 feet

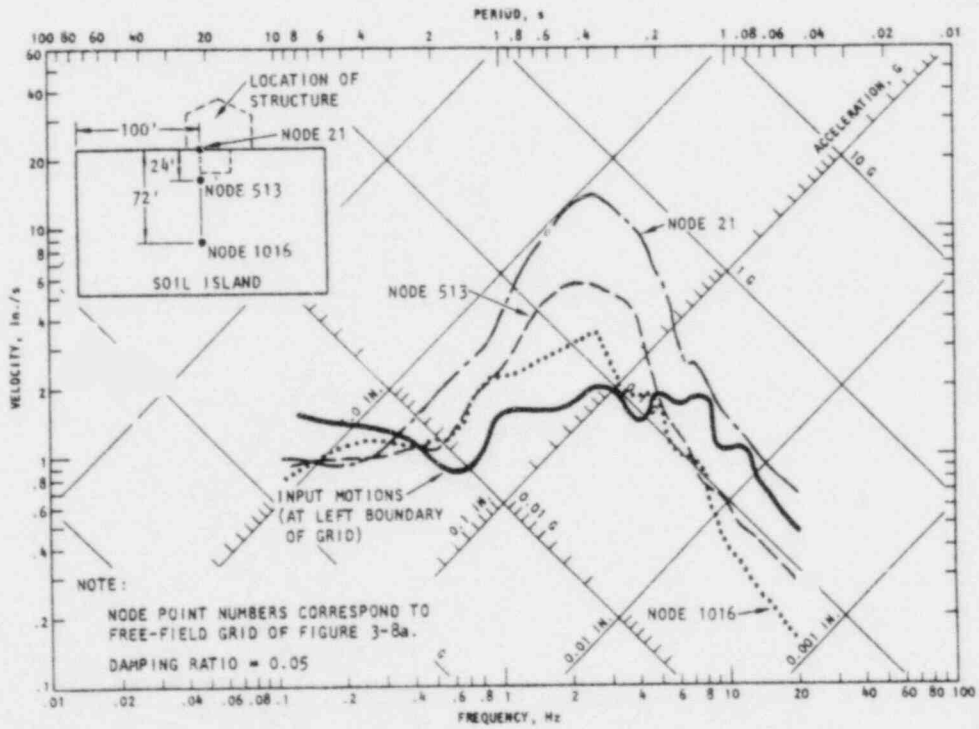

(b) Distance from left boundary of grid = 100 feet

FIGURE 5-6. VARIATION OF COMPUTED FREE-FIELD VERTICAL MOTION WITH DEPTH BELOW GROUND SURFACE

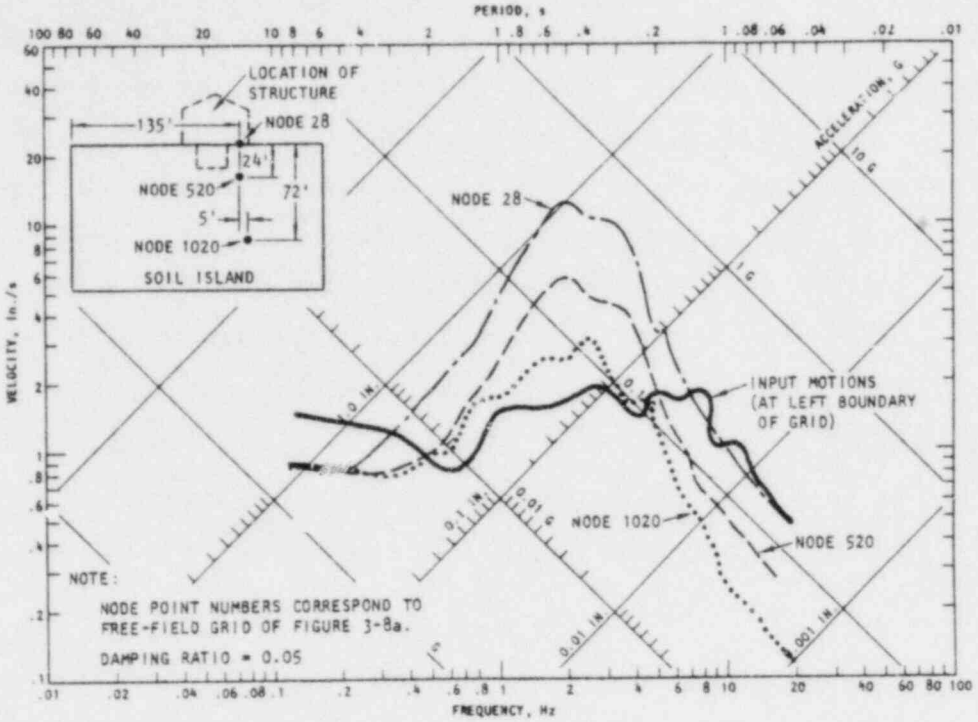

(c) Distance from left boundary of grid = 135 feet

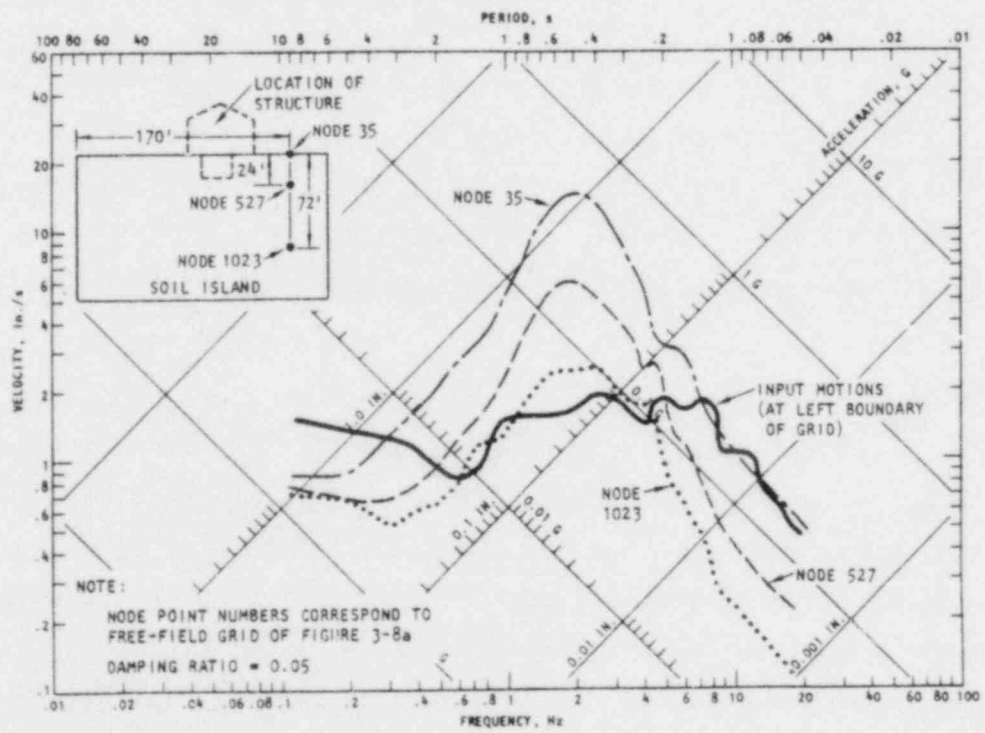

(d) Distance from left boundary of grid = 170 feet

FIGURE 5-6. (CONCLUDED)

- The depth-dependent effects on the higher-frequency motions (above 1 Hz) are greater than for lower-frequency motions. Spectral amplitudes at the ground surface are shown in Figure 5-5 to exceed those at a 72-ft depth by factors typically ranging from 40% to 100% at distances from the left boundary of 100 ft or greater; isolated instances of even larger differences are observed over a narrow frequency range centered at about 6 Hz.

5.2.2.2 Vertical Motions

The variation of the free-field vertical response spectra with increasing depth below the ground surface is shown in Figure 5-6 to be as follows:

- The variation of the spectra with depth is substantial over the entire length of the free-field grid (even when the distance to the left boundary is small) and over the entire frequency range of the spectra.

- At a given distance from the left boundary, Figure 5-6 shows that spectral amplitudes at the ground surface typically exceed those at a 72 ft depth by factors ranging from about 3 to 7. Such differences are much greater than those described for horizontal motions in Section 5.2.2.1.

5.2.3 GENERAL DISCUSSION OF FREE-FIELD RESULTS

As previously noted, the free-field motion results presented above and the soil/structure system results presented in Section 5.3 are based on the same soil model and input motions along the left boundary. A fully consistent basis for assessing *relative* effects of soil/structure interaction is thereby provided by such results; however the *absolute* values of the free field and soil/structure system responses are undoubtedly influenced by certain computational aspects of the TRI/SAC code and input parameters. Two such computational aspects are discussed with regard to the free-field results in the paragraphs that follow.

5.2.3.1 Computational Stabilization of Input Motions

The attenuation of the free-field motions with distance from the left boundary is undoubtedly influenced by the fact that the input motions applied along the left boundary are *assumed* and therefore are not fully compatible with the properties of the TRI/SAC soil model. Prior experience has shown that in such instances, which are typical of most finite element calculations of this type, the input motions will be modified to be more nearly consistent with the site model as they propagate across the grid. When, with increasing distance from the left boundary, the computed soil motions no longer change markedly, these computed motions are regarded as "stabilized" (AJA, 1971). Observation of Figures 5-3 and 5-4 indicates that this type of stabilization may have occurred for the vertical motions in the upper soil layers, but not in the lower layers. Except for the nodes 170 ft from the left boundary (which may be influenced by reflections from the nearby right boundary, as discussed below) some degree of stabilization appears to have occurred in the horizontal motions below the ground surface, but not on the ground surface. Therefore, it is seen that the attenuation effects observed in Figures 5-3 and 5-4 are undoubtedly influenced by this *computational* stabilization process, as well as by the actual *physical* nature of the soil profile.

5.2.3.2 Energy-Absorbing Boundary Dampers

As noted in Section 3.3.2, the right boundary of the TRI/SAC grid employs viscous dampers to simulate an infinitely long soil profile by absorbing signals that might be reflected from this artificial boundary. However, it is well known that such dampers are an imperfect absorber of such reflected energy; as a result, the computed response of node points located in the vicinity of the right boundary may be influenced by reflected signals not fully absorbed by these damper elements. This may account for some of the differences in free-field motions observed in Sections 5.2.1 and 5.2.2 between node points 135 ft and 170 ft from the left boundary.

5.3 SOIL/STRUCTURE SYSTEM RESPONSE

Two sets of TRI/SAC results that depict the nature of the computed soil/structure interaction effects at the Terminal Substation site are presented. The first and most important from these calculations involve comparisons of spectra of motions along the Terminal Substation basement with spectra of free-field motions at the corresponding locations. The second set of results compare spectra of motions in the soil medium, with and without the structure.

5.3.1 TERMINAL SUBSTATION BASEMENT RESPONSE

Spectra from motions at several different locations along the Terminal Substation basement are provided. These locations extend along the entire length of the basement slab, including Nodes 61 and 70 (Fig. 3-3b) which correspond to the former and present locations respectively of the accelerograph in the basement and Node 63, which is along an edge of the foundation block. These results are described in the paragraphs that follow.

5.3.1.1 Horizontal Response

Comparisons of horizontal response spectra at Nodes 61, 63, and 70 along the basement slab with free-field motions at the corresponding locations in the finite element grid are shown in Figure 5-7. These figures show that, at each node, the free field and basement responses at frequencies below about 1.5 Hz are nearly identical. At higher frequencies, the free-field motions exceed the horizontal motions of the basement slab by factors as high as 64% but most typically about 25% to 35% (Table 5-2). It is noted that these trends are very similar to those observed from the SHAKE/FLUSH results, as presented in Chapter 4.

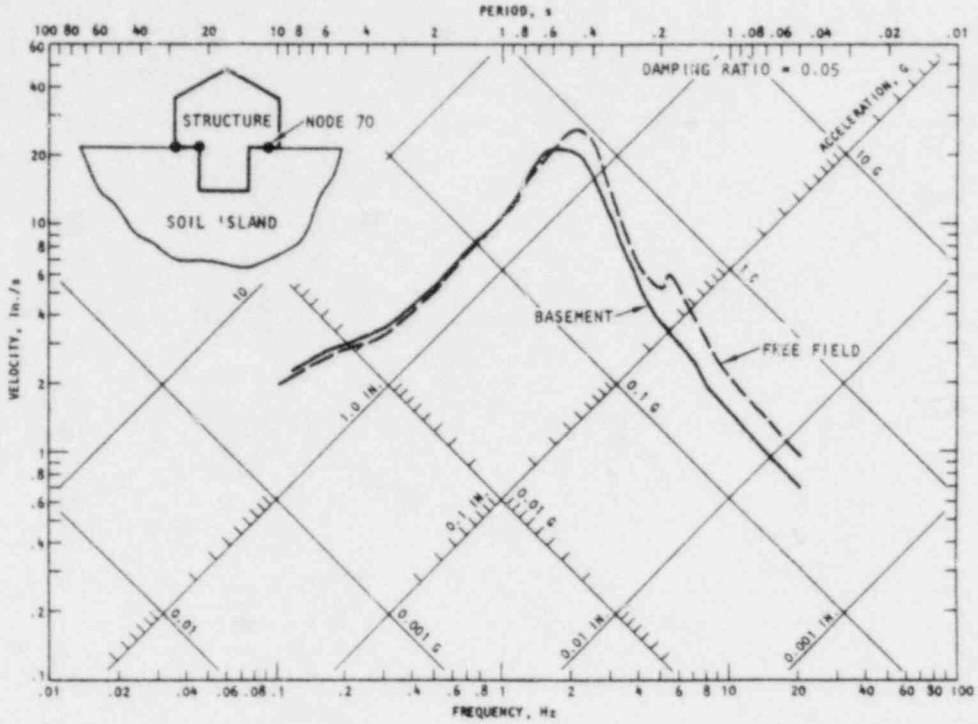

(a) Node 70 (present accelerograph location)

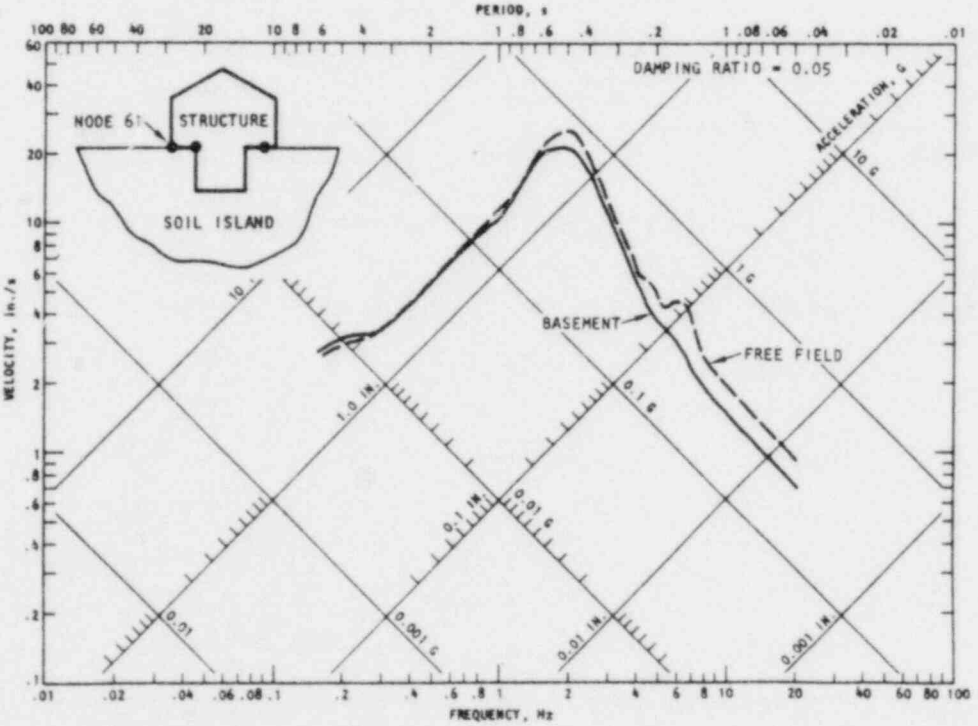

(b) Node 61 (former accelerograph location)

FIGURE 5-7. COMPARISONS OF HORIZONTAL RESPONSE SPECTRA OF BASEMENT AND FREE FIELD

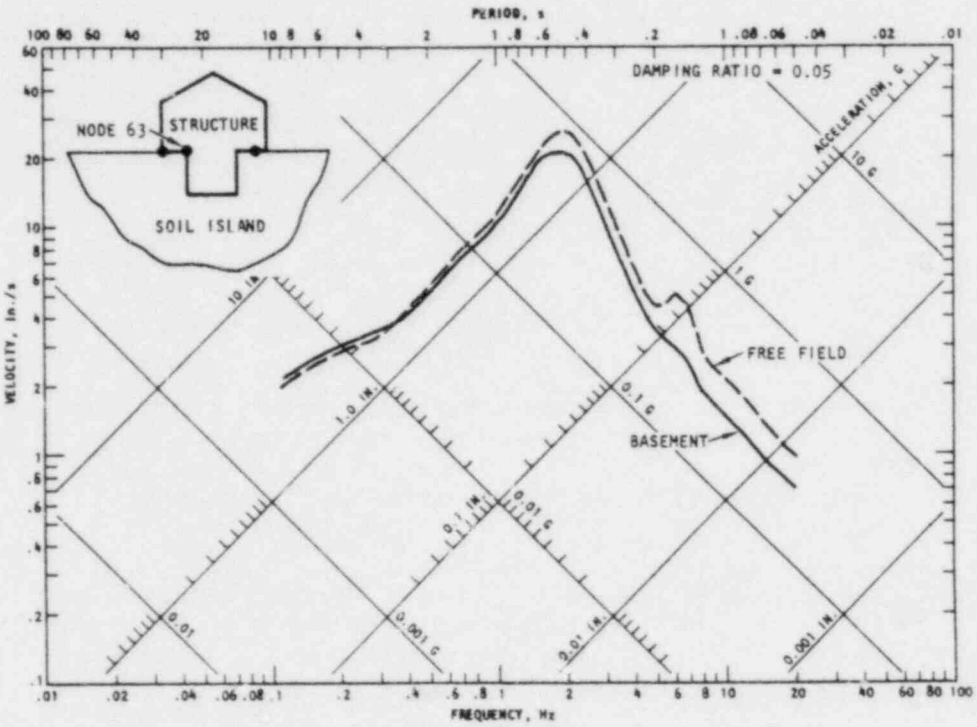

(c) Node 63 (edge of foundation block)

FIGURE 5-7. (CONCLUDED)

TABLE 5-2. EFFECT OF SOIL/STRUCTURE INTERACTION ON SPECTRAL ACCELERATIONS ALONG BASEMENT OF EL CENTRO TERMINAL SUBSTATION BUILDING--*TRI/SAC* RESULTS

Frequency, Hz	Node 61 (at former accelerograph location)						Node 63 (along edge of foundation block)						Node 70 (at present accelerograph location)					
	Horizontal			Vertical			Horizontal			Vertical			Horizontal			Vertical		
	Free-Field	Structure	Free-Field / Structure	Free-Field	Structure	Free-Field / Structure	Free-Field	Structure	Free-Field / Structure	Free-Field	Structure	Free-Field / Structure	Free-Field	Structure	Free-Field / Structure	Free-Field	Structure	Free-Field / Structure
0.4	0.028	0.027	1.04	0.0092	0.0068	1.35	0.028	0.027	1.03	0.0092	0.0062	1.48	0.025	0.027	0.93	0.0092	0.0076	1.21
0.5	0.046	0.042	1.10	0.015	0.010	1.50	0.046	0.042	1.10	0.015	0.010	1.50	0.040	0.044	0.91	0.015	0.012	1.25
0.8	0.120	0.110	1.10	0.036	0.024	1.50	0.120	0.110	1.09	0.036	0.024	1.50	0.110	0.110	1.00	0.037	0.030	1.23
1.0	0.190	0.180	1.06	0.060	0.039	1.54	0.190	0.180	1.06	0.062	0.040	1.55	0.180	0.180	1.00	0.070	0.054	1.30
1.5	0.540	0.500	1.08	0.200	0.120	1.67	0.540	0.500	1.08	0.200	0.130	1.54	0.460	0.500	1.00	0.200	0.180	1.11
2.0	0.820	0.670	1.22	0.400	0.200	2.00	0.820	0.670	1.22	0.400	0.220	1.82	0.830	0.670	1.24	0.400	0.300	(1.33)
2.5	0.800	0.620	1.29	0.600	0.250	(2.40)	0.800	0.620	1.29	0.550	0.250	(2.20)	0.900	0.620	1.45	0.420	0.320	1.31
3.0	0.650	0.500	1.30	0.650	0.340	1.91	0.650	0.500	1.30	0.600	0.320	1.88	0.680	0.500	1.36	0.480	0.380	1.26
[illegible]	0.360	0.290	1.24	0.550	0.400	1.38	0.360	0.290	1.24	0.500	0.250	2.00	0.400	0.290	1.38	0.250	0.250	1.00
7.0	0.440	0.280	(1.57)	0.300	0.100	1.67	0.440	0.280	(1.57)	0.300	0.140	2.14	0.460	0.280	(1.64)	0.180	0.170	1.06
10.0	0.320	0.230	1.39	0.260	0.140	1.86	0.320	0.230	1.39	0.240	0.120	2.00	0.340	0.230	1.48	0.160	0.120	1.33

Note: Spectral accelerations of free field and structure given in units of g.

Further insight into these comparisons is provided from separate plots of the free field and basement horizontal response spectra at locations along the length of the basement. These plots, given in Figure 5-8, show that the free-field spectra at the Node 61 and 63 locations are nearly identical to each other. In addition, at frequencies below 1.5 Hz, these spectra are seen to slightly exceed the free-field spectra at the Node 70 location whereas, at higher frequencies, they fall slightly below the Node 70 spectra (Fig. 5-8a). In contrast, the spectra of basement motions are essentially identical at all locations along the length of the basement, probably because of the high in-plane stiffness of the basement slab (Fig. 5-8b). Because of these factors, Table 5-2 shows that at lower frequencies, the ratio of the free-field response to the structure response is typically slightly higher at Nodes 61 and 63 than at 70 whereas, at frequencies above 1.5 Hz, the reverse is true.

5.3.1.2 Vertical Response

Comparisons of vertical response spectra at Nodes 61, 63, and 70 along the basement slab with the corresponding free-field motions are shown in Figure 5-9. These comparisons, unlike those for the horizontal motions, show that the free-field vertical response exceeds the basement response over the entire frequency range of the spectra. Table 5-2 shows that the ratios between the free-field and basement vertical motions (1) are much greater than the corresponding ratios involving horizontal motions; and (2) are largest at Nodes 61 and 63 where they range from 1.35 to 2.40. Discussions of these comparisons follows:

a. Differences between Horizontal and Vertical Response Results

One particularly interesting aspect of these vertical motion results is how they differ from the horizontal motion results presented in the previous subsection. For vertical motions, as stated above, the basement response is attenuated relative to the free-field response over the entire frequency range whereas, for horizontal motions, it was shown in Subsection 5.3.1.1 that such an attenuation is evident only at frequencies greater than about 1.5 Hz.

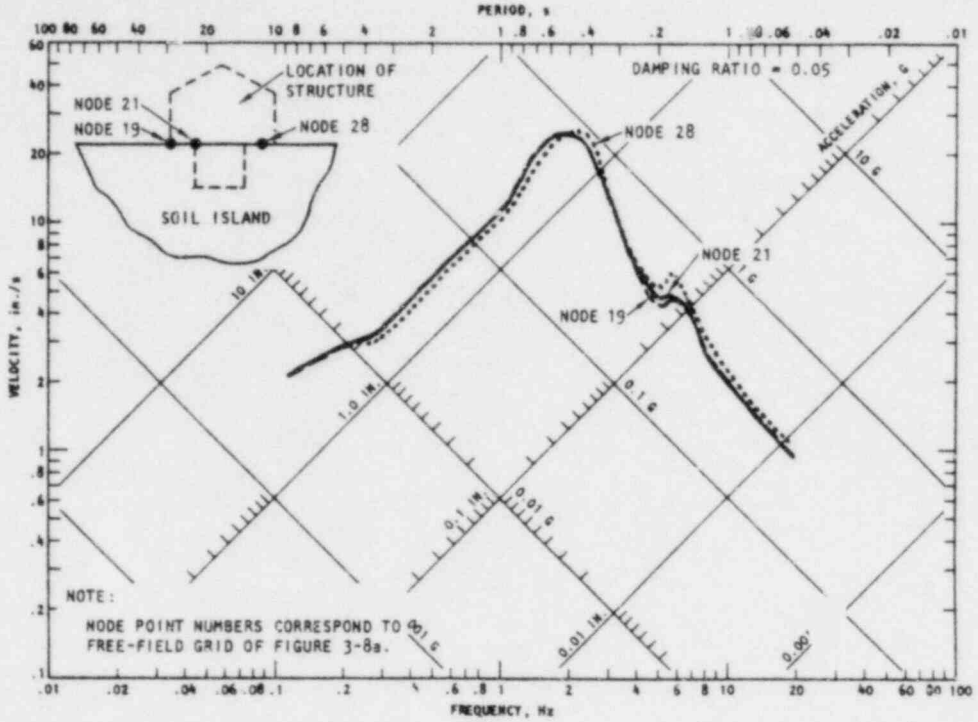

(a) Free-field motions

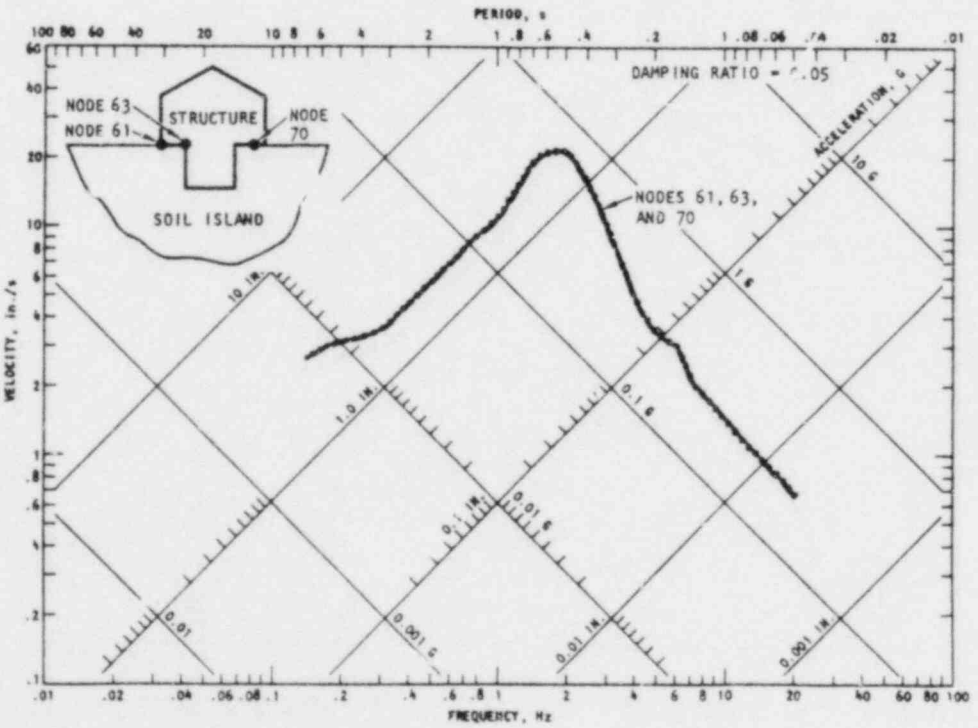

(b) Basement motions

FIGURE 5-8. FREE-FIELD AND BASEMENT HORIZONTAL RESPONSE SPECTRA ALONG LENGTH OF STRUCTURE

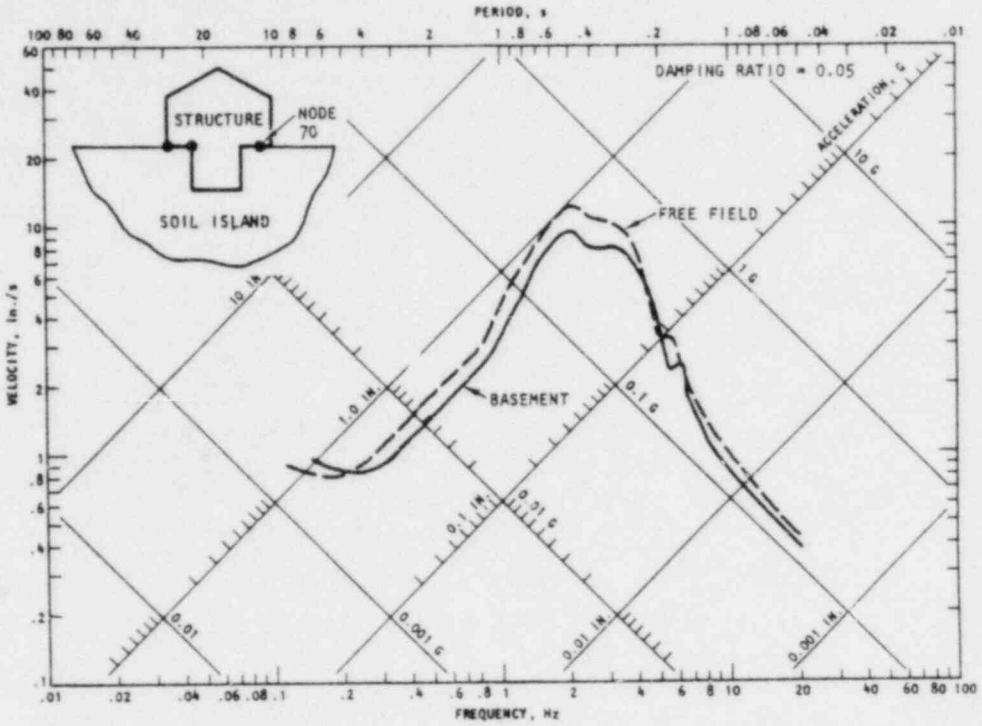

(a) Node 70 (present accelerograph location)

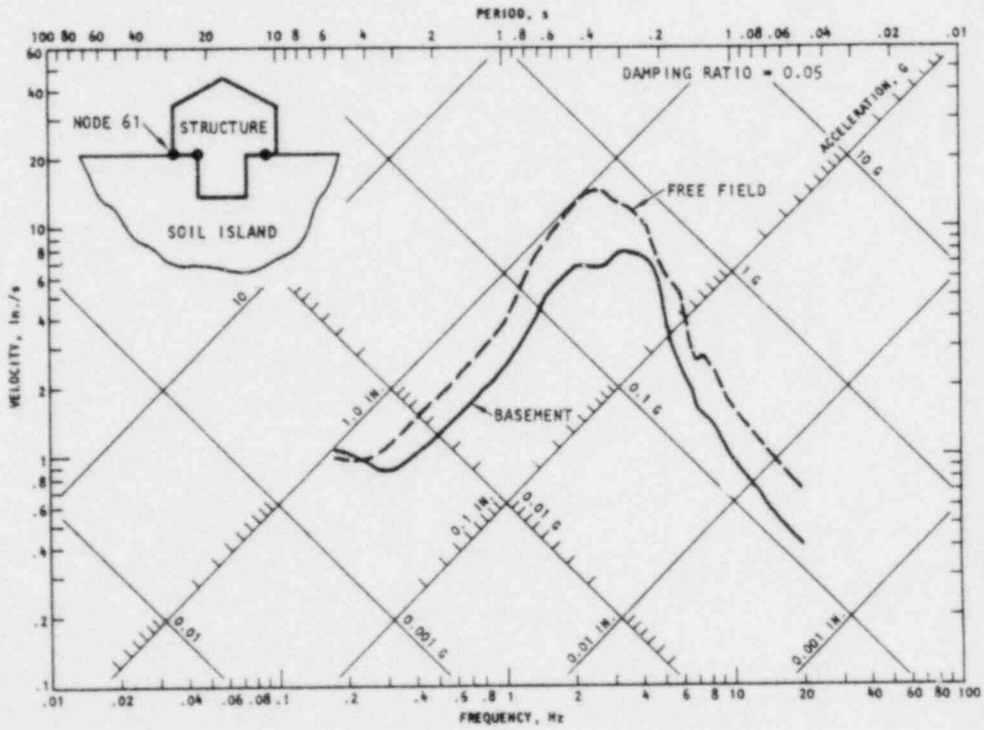

(b) Node 61 (former accelerograph location)

FIGURE 5-9. COMPARISON OF VERTICAL RESPONSE SPECTRA OF BASEMENT AND FREE FIELD

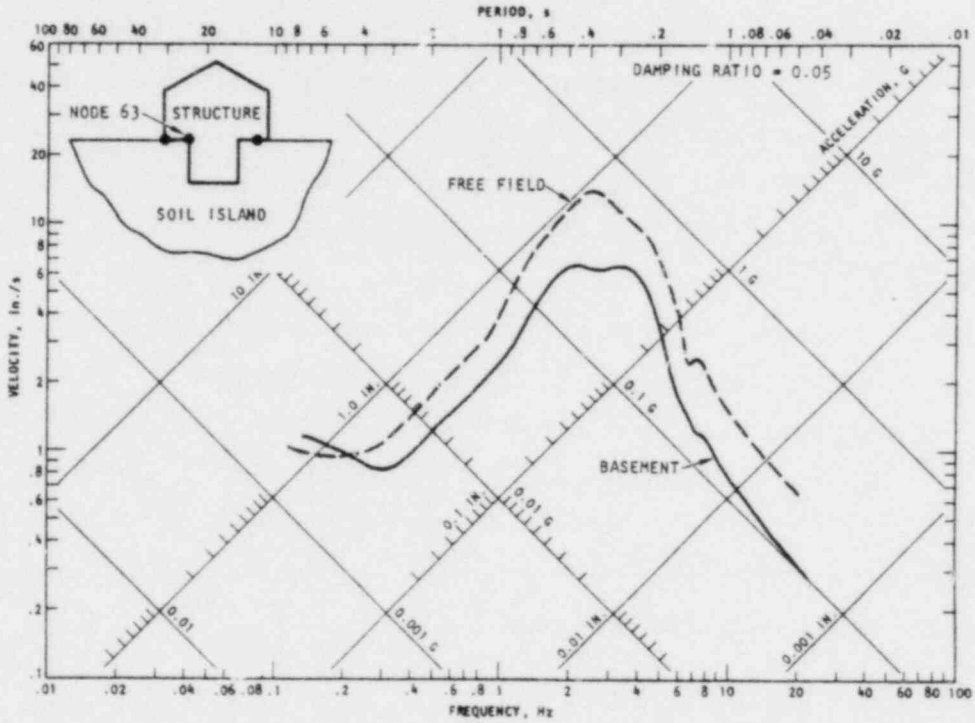

(c) Node 63 (edge of foundation block)

FIGURE 5-9. (CONCLUDED)

Reasons for these differences between the horizontal and vertical basement/free-field response comparisons at lower frequencies may be related to (1) the differences in the way the free-field horizontal and vertical motions attenuate with depth; and (2) the fact that for deeply embedded foundations, the seismic loads applied to the foundations are influenced not only by the free-field motions at the ground surface, but also by the free-field motions at depth. With these factors in mind, it was shown in Section 5.2.2.2 that the vertical free-field motions at lower frequencies attenuate substantially with depth. Therefore, the lower-frequency vertical loadings applied along the foundation block by these attenuated vertical free-field motions are undoubtedly lower than loadings that would result if no such depth-attenuation took place with depth. These reduced loadings undoubtedly contribute to the fact that the lower-frequency vertical motions of the basement are reduced relative to the free-field vertical motions *at the ground surface*. In contrast, for horizontal motions, the lower frequency free-field response *does not* attenuate substantially with depth and therefore applies significant horizontal forces along the embedded foundation block; this may contribute to the close comparisons between the horizontal basement response and free-field ground surface response observed at lower frequencies.

At higher frequencies, it is noted that for both horizontal and vertical motions, the basement response falls below that of the free field at the ground surface. This is undoubtedly caused by the significant mass of the foundation block, which tends to filter and reduce the effects of higher frequency seismic loadings. The somewhat larger differences between the vertical components of the free-field and basement response may be attributed to the reduced vertical loadings along the foundation block as described above.

b. Nature of Differences between Vertical Response at Various locations along Length of Basement

The vertical response spectral amplitudes tabulated in Table 5-2 and plotted in Figure 5-9 show that the differences between the free-field and basement responses are much greater at Nodes 61 and 63 of the basement

than at Node 70. To gain insight into reasons for this trend, Figure 5-10 shows comparisons of free-field vertical response spectra along the length of the basement, as well as comparisons of the basement motions themselves. Figure 5-10a provides the free-field comparisons and shows that, at frequencies below about 2 Hz, the free-field spectra are nearly identical all along the basement whereas, at higher frequencies, the free-field spectral amplitudes at the Node 70 location are attenuated by about 40% relative to those at the Node 61 and 63 locations. The basement spectrum comparisons, as given in Figure 5-10b, show that the basement response at Nodes 61 and 63 are generally quite similar, particularly at lower frequencies; however the most significant feature of this figure is that the Node 70 spectral amplitudes at frequencies below about 3 Hz have markedly larger values than do the corresponding spectral amplitudes for Nodes 61 and 63. At higher frequencies, the basement spectral amplitudes are seen in Figure 5-10b to be about the same all along the length of the basement slab.

These results show that, at lower frequencies, the fact that the free-field and basement responses compare closer at the Node 70 location than at the Node 61 and 63 locations is due to a larger basement response at Node 70. Conversely, at higher frequencies, the closer comparisons at Node 70 is caused by attenuated free-field motions at this location. These reduced higher-frequency free-field motions correspond to the distance-attenuation effects discussed in Section 5.2.3 with regard to physical phenomena and computational stabilization of the input motions. However, the lower frequency trends noted above, which are caused by the differences in basement response along the length of the basement slab, warrant further discussion.

The nature of the low frequency vertical response along the length of the basement slab is shown in Figure 5-11. In this, Figure 5-11a shows spectral amplitudes in the 0.4 Hz to 2 Hz range for several locations along the basement slab. Figure 5-11b uses results from these spectra to provide spectral displacement profiles of the basement slab at various frequencies in the 0.4 Hz to 2 Hz range. These profiles represent the deformed shape of

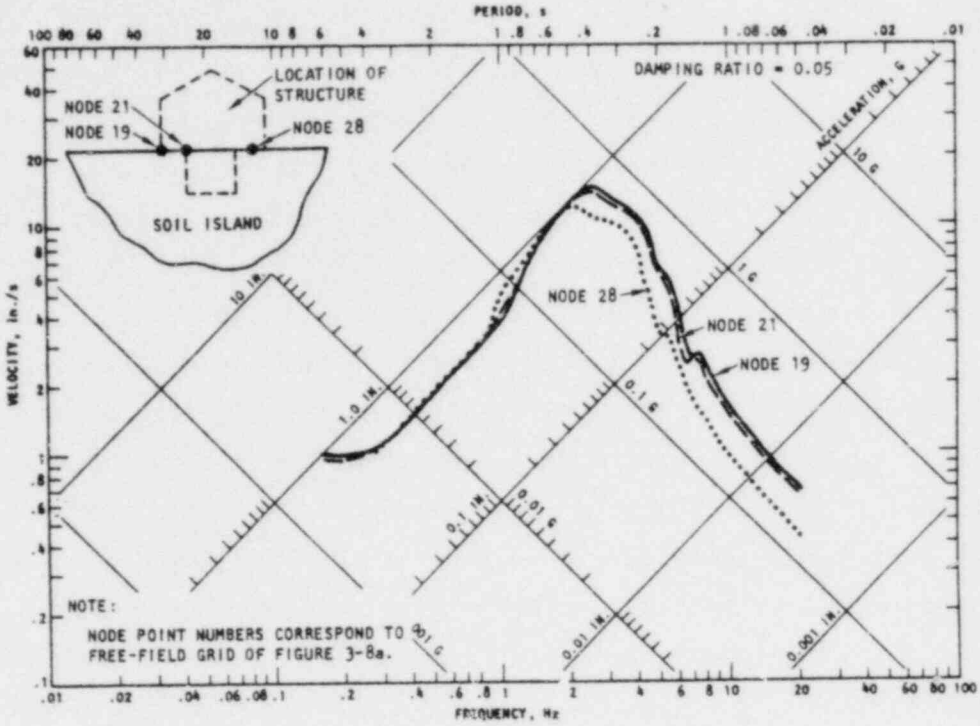

(a) Free-field motions

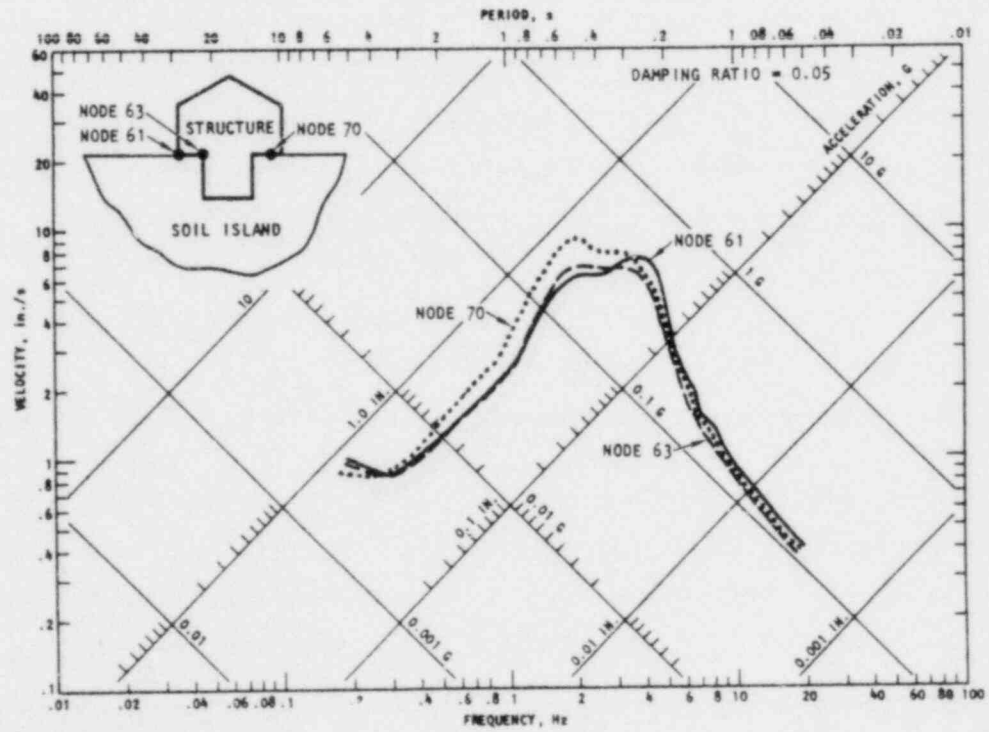

(b) Basement motions

FIGURE 5-10. FREE-FIELD AND BASEMENT VERTICAL RESPONSE SPECTRA ALONG LENGTH OF STRUCTURE

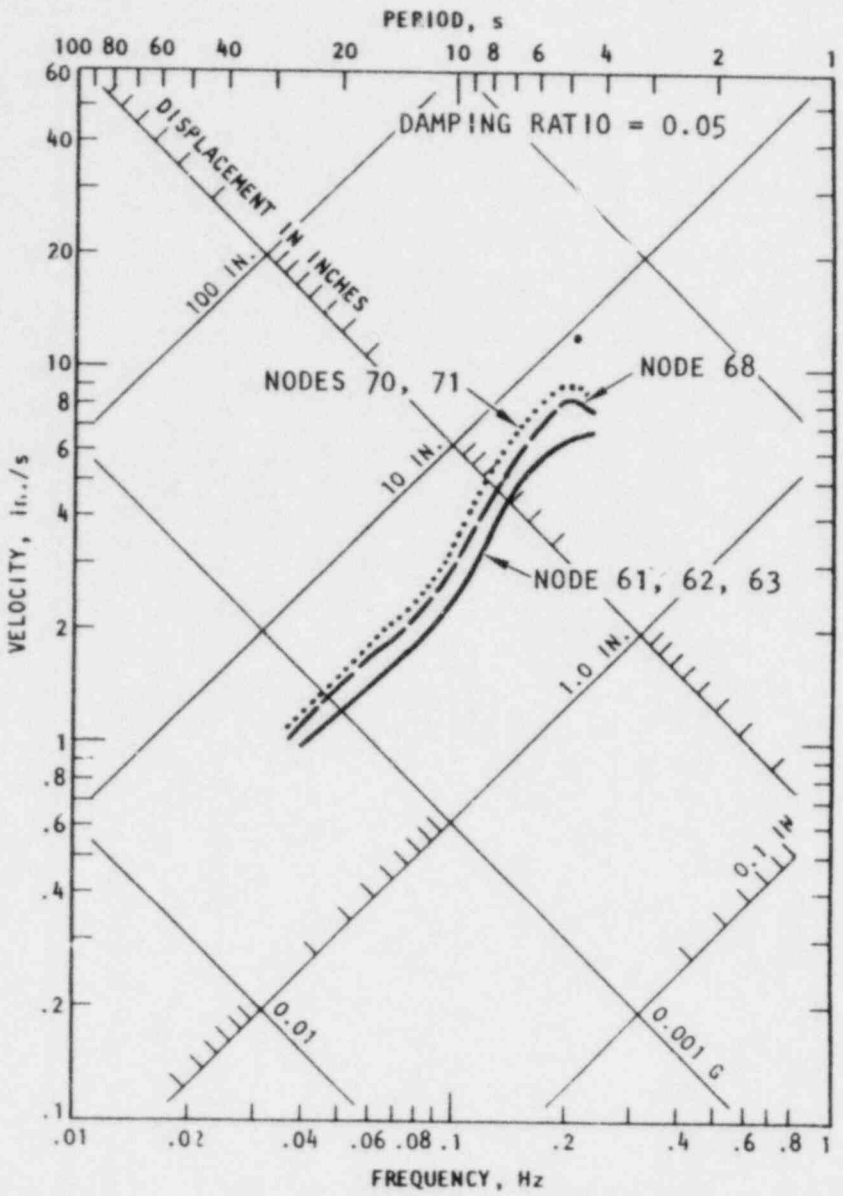

(a) Response spectra

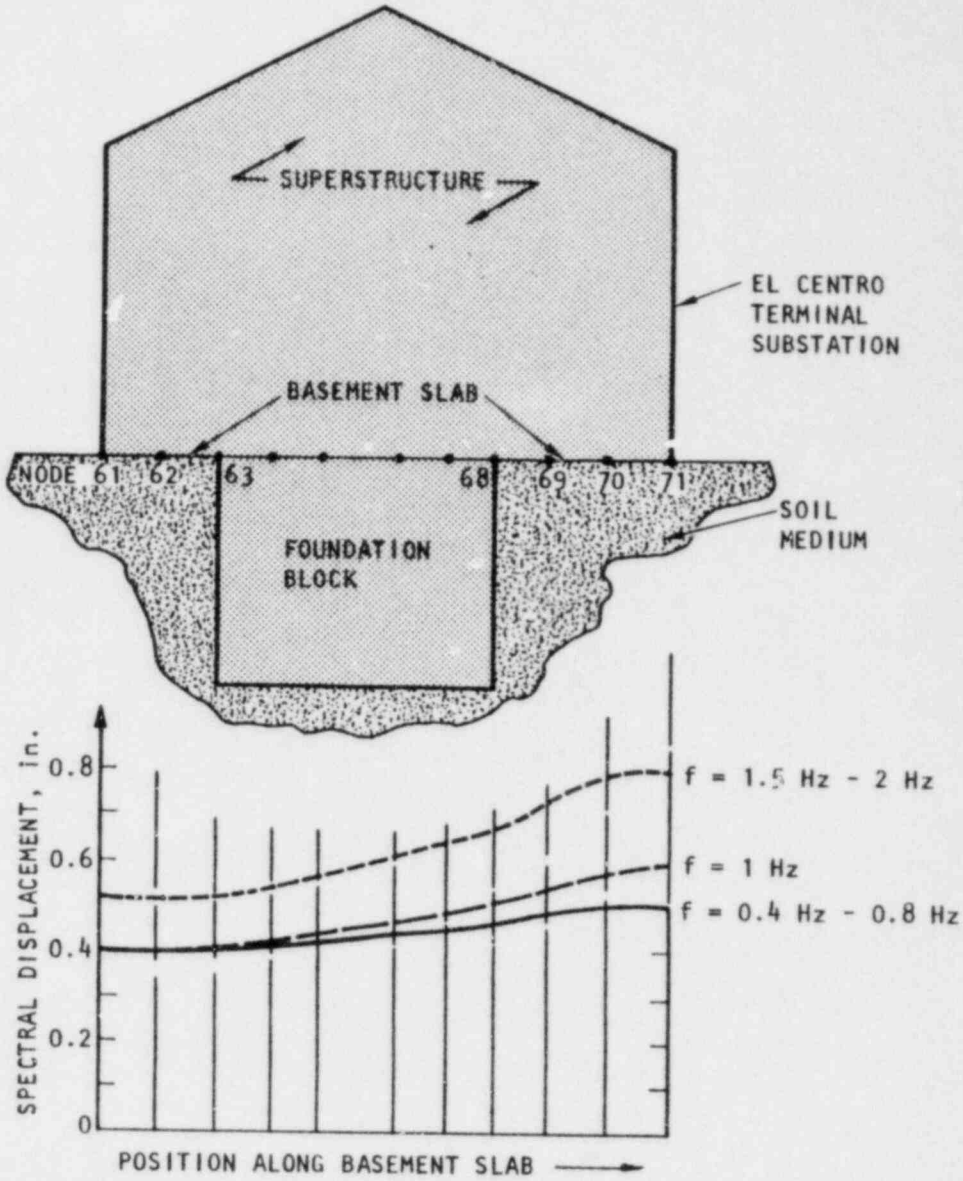

(b) Spectral displacement profiles

FIGURE 5-11. VERTICAL RESPONSE SPECTRAL AMPLITUDES OF BASEMENT SLAB FOR FREQUENCIES RANGING FROM 0.4 Hz TO 2 Hz

the basement at these frequencies only if the vertical responses at the various node points along the length of the basement are in phase with one another. Figure 5-12, which contains overlaid acceleration histories at several of these node points, shows that indeed this is the case. In fact, only slight time shifts between the major peaks in the acceleration histories are observed, and arise from the travel times of the waves along the length of the basement; effects of these slight time shifts will be negligible when lower frequency responses (i.e., displacements) are compared. Therefore, it is seen that the lower frequency vertical responses along the length of the basement slab are essentially in-phase, and the spectral displacement profiles provided in Figure 5-11b are a good representation of the deformed shapes of the basement slab at the frequencies indicated.

With this as background, the spectral displacement profiles (or, in this case, deformed shape plots) shown in Figure 5-11b indicate the nature of the lower-frequency vertical response of the basement. This response is comprised of some bending near Node 63 and Nodes 68 to 71, but is dominated by rigid body rotations about a center of rotation in the vicinity of Nodes 61 to 63. This location of the center of rotation is influenced by the position of the foundation block being offset toward Node 61 (relative to the midlength of the building) and is a major reason for the larger vertical displacements at Node 70 in this lower-frequency range.

In summary, it is seen that the major features of the comparisons of the vertical motions of the free field and the basement are influenced by several factors. At higher frequencies, the fact that the basement motions at Node 70 (the present accelerograph location) are closest to the free-field motions is due to the fact that the computed free-field motions in this frequency attenuate with distance along the length of the grid, while the motions along the length of the basement in this frequency range are reasonably similar. At lower frequencies, the more favorable comparisons between the Node 70 basement motions and the free field are due to amplifications of the basement motions near Node 70, that, in turn, are caused by building rotations and some local bending deformations of the basement slab.

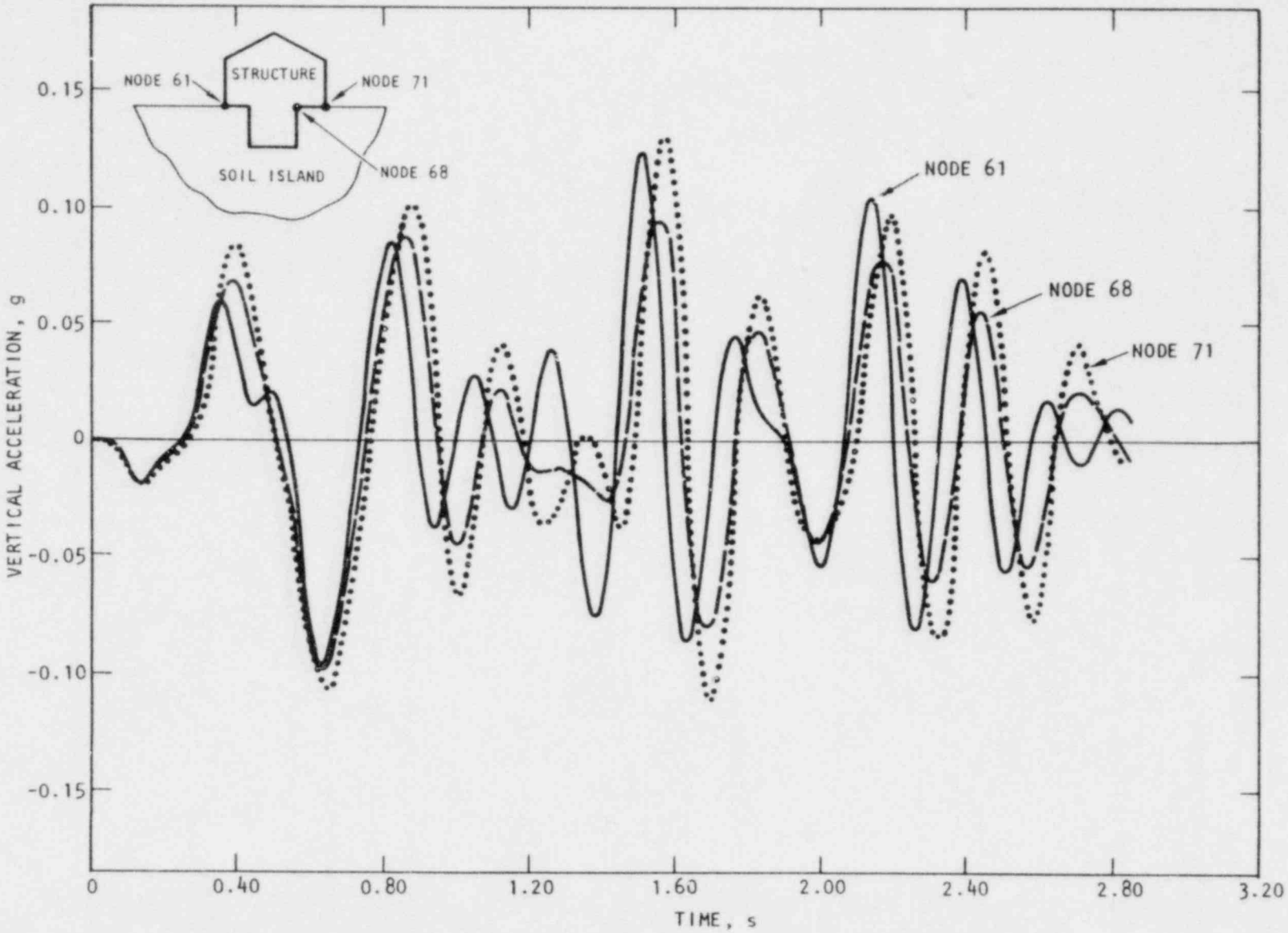

FIGURE 5-12. VERTICAL ACCELERATION TIME HISTORIES ALONG LENGTH OF BASEMENT

5.3.2 RESPONSE OF SOIL MEDIUM

The second and final set of results from the TRI/SAC soil/structure system response analysis involve assessment of soil/structure interaction effects on the response of the soil medium at the El Centro site. To carry out this assessment, motions computed in the soil medium with and without the Terminal Substation Building have been compared at the following four locations:

1. 25 ft to the left of the structure, along the ground surface (Node 56 of the soil/structure system grid in Fig. 3-8b)

2. 4 ft below the left edge of the foundation block (Node 555)

3. 10 ft to the right of the foundation block and 8 ft below the ground surface (Node 234)

4. 30 ft to the right of the right of the structure, along the ground surface (Node 77)

5.3.2.1 Horizontal Response

The horizontal response spectra at the above four soil locations are provided in Figure 5-13. This figure shows that, at frequencies below about 2 Hz, the horizontal motions at each of these locations are not influenced by soil/structure inateraction. At higher frequencies, the soil motions computed without the structure (i.e., from the free-field analysis) slightly exceed those computed with the structure (i.e., including soil/structure interaction effects). These differences between soil motions with and without the structure are small at Node 555 (24 ft below the ground surface) and reach values of about 25% at the other node points (which have shallower depths). These percent differences are of about the same order as those discussed earlier for the basement motions (Table 5-2).

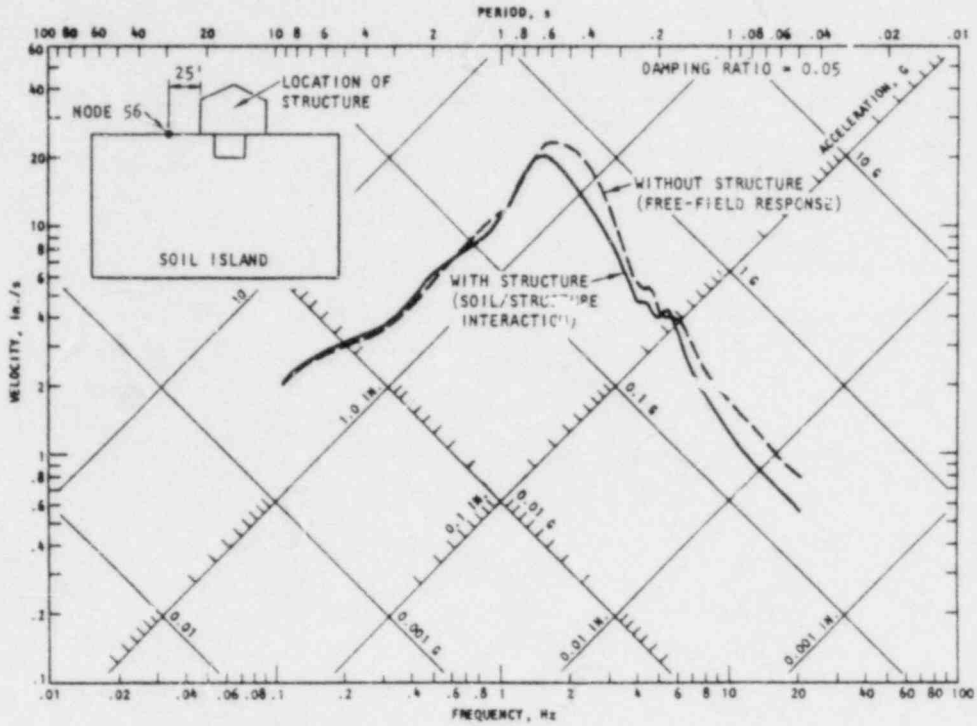

(a) Node 56

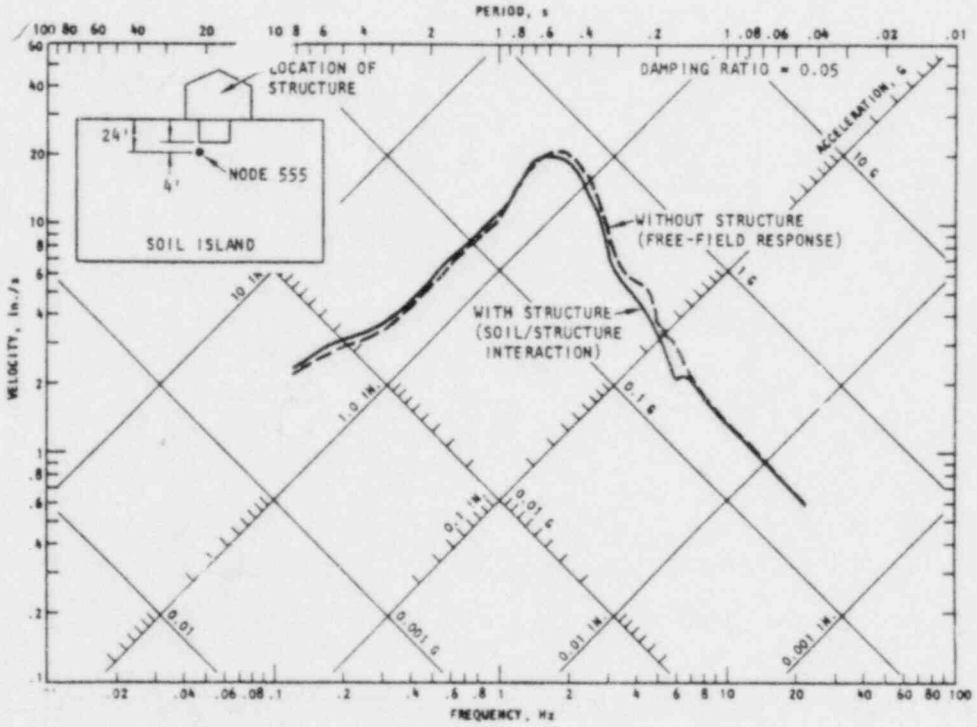

(b) Node 555

FIGURE 5-13. EFFECT OF SOIL/STRUCTURE INTERACTION ON HORIZONTAL RESPONSE OF SOIL MEDIUM

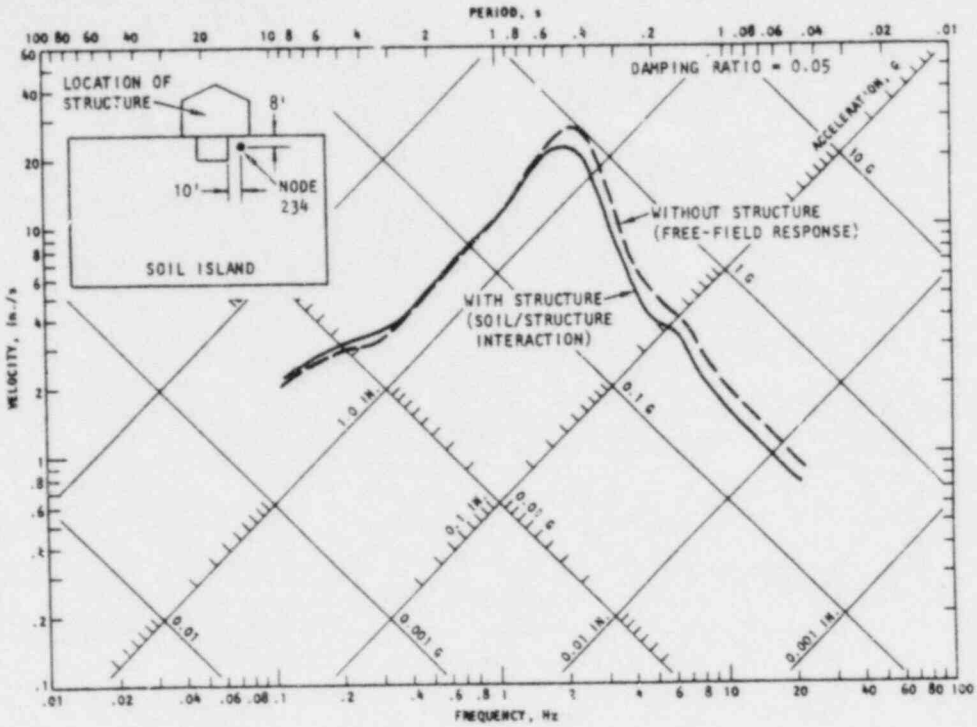

(c) Node 234

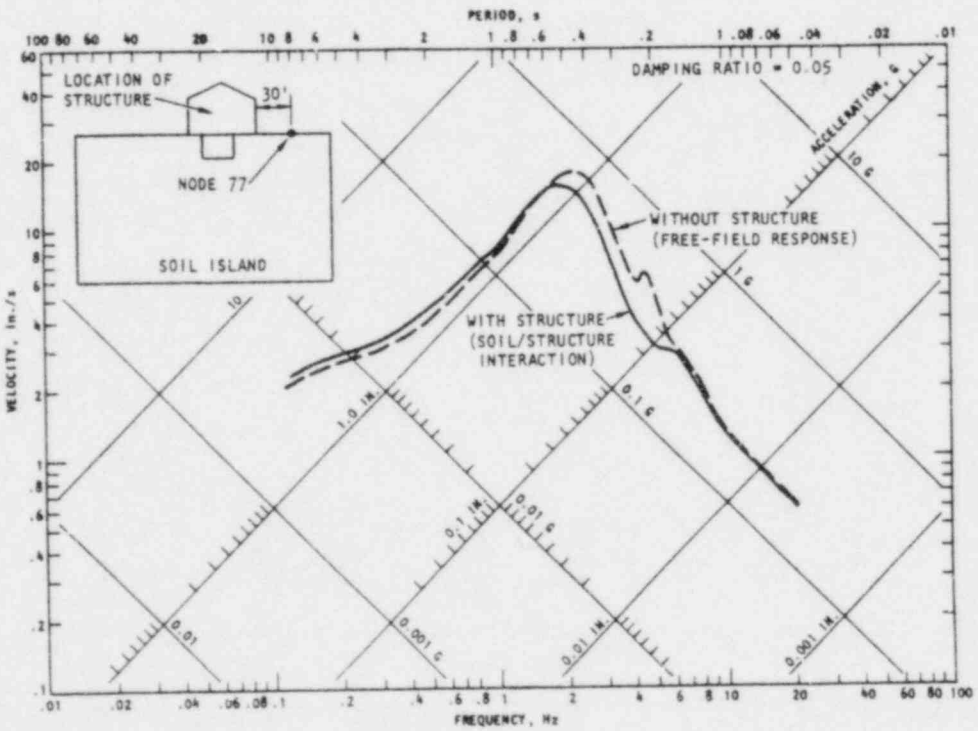

(d) Node 77

FIGURE 5-13. (CONCLUDED)

5.3.2.2 Vertical Response

The vertical response spectra at these soil locations are shown in Figure 5-14. These spectra show that, at the locations furthest from the structure (Nodes 56 and 77), the influence of soil/structure interaction on the vertical motions is much smaller than for horizontal motions, particularly for frequencies above about 2 Hz. At Node 555 (24 ft below the ground surface and 4 ft below the foundation block) the lower frequency soil motions (below about 4 Hz) computed without the structure exceed those computed with the structure by up to 20%. These differences at lower frequencies are somewhat greater than for the horizontal motions at this node point; at frequencies above 4 Hz the influence of soil/structure interaction is very small for vertical motions at Node 555, as it also was for horizontal motions. At Node 234 (8 ft beneath the right side of the structure) the influence of soil/structure interaction on the vertical motions is about the same as for horizontal motions; i.e., at lower frequencies this influence is small whereas at higher frequencies, the soil response computed without the structure exceeds that computed with the structure by about 25%.

In general, the influence of soil/structure interaction on the vertical soil motions is more localized and somewhat less than for horizontal motions. Also, this influence is considerably less than that observed for the vertical basement response (Table 5-2). However, this latter trend should be as previously interpreted in light of the fact that, as noted in Section 5.3.1.2, the vertical basement motions at these frequencies were compared with free-field vertical motions at the ground surface but were excited seismically by substantially attenuated vertical free-field motions along the 20 ft depth of the foundation block.

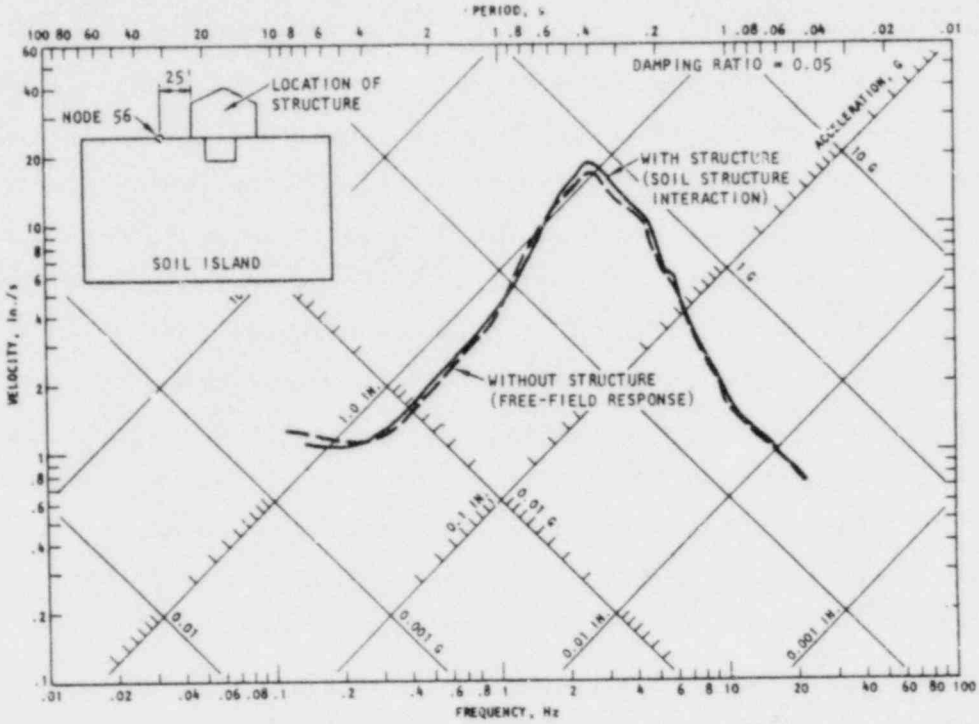

(a) Node 56

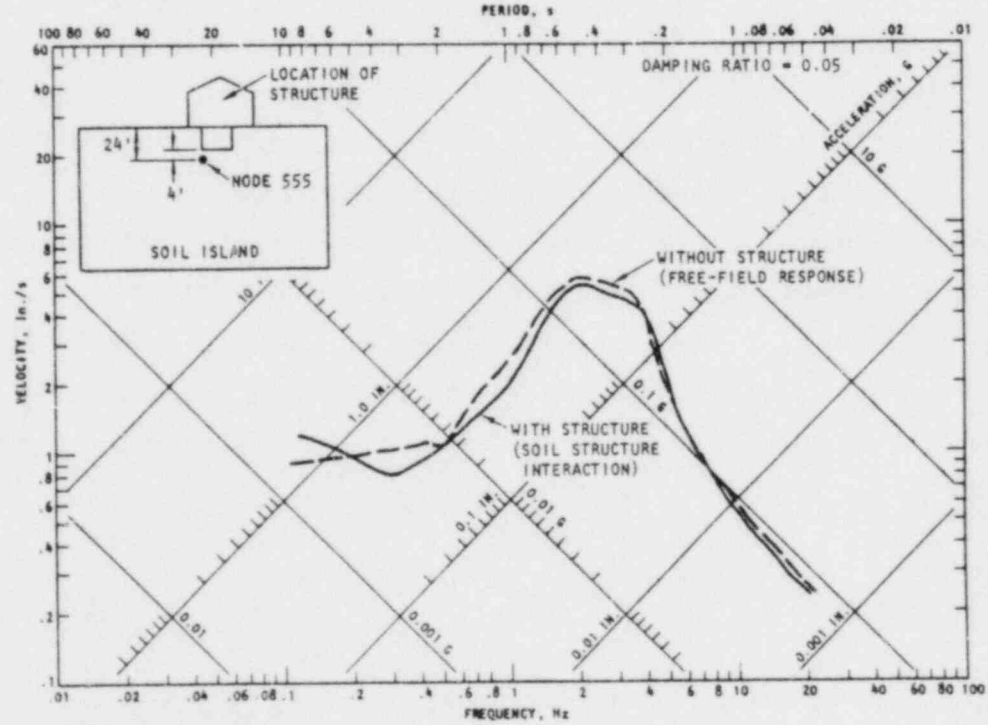

(b) Node 555

FIGURE 5-14. EFFECT OF SOIL/STRUCTURE INTERACTION ON VERTICAL RESPONSE OF SOIL MEDIUM

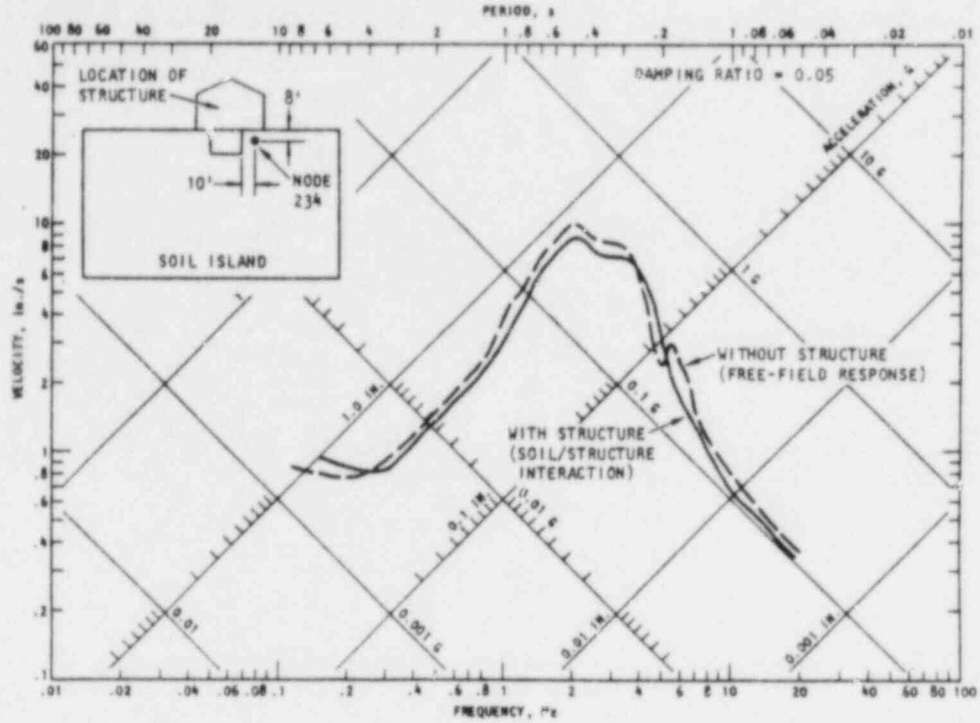

(c) Node 234

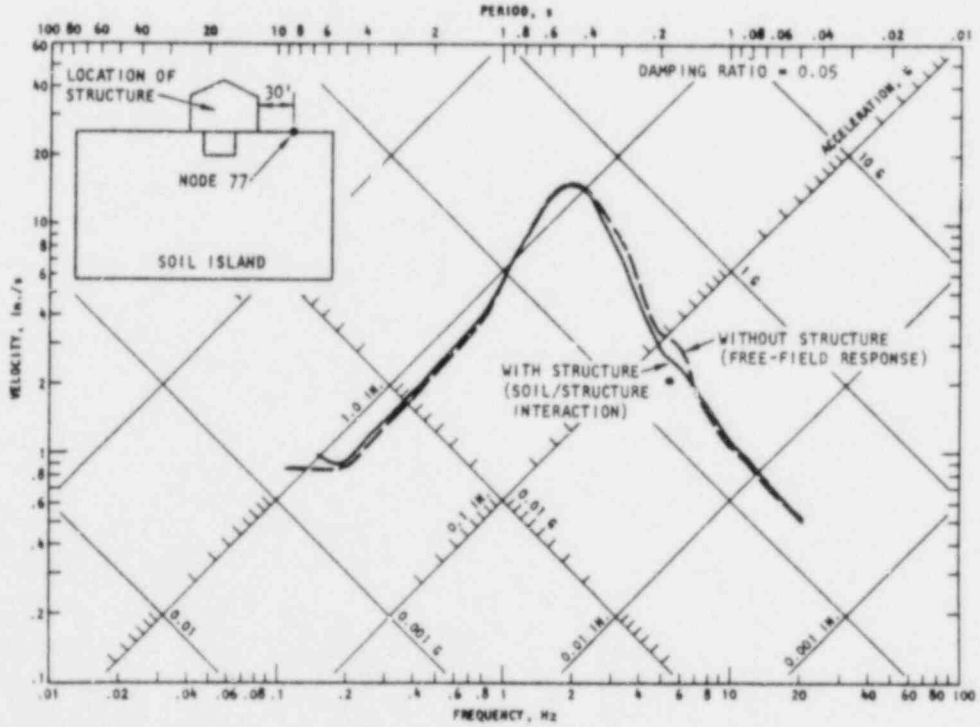

(d) Node 77

FIGURE 5-14. (CONCLUDED)

CHAPTER 6

REFERENCES

Agbabian-Jacobsen Assoc. (AJA) (1971). *Dynamic Analysis of Safeguard Structures*, R-6820-1400. El Segundo, CA: AJA, Apr.

Agbabian Assoc. (AA) (1976). *User's Guide for TRI/SAC Code*, 2nd rev. ed. R-7128-4-4102. El Segundo, CA: AA, May.

Calif. Div. of Mines (CDM) (1954). "Key Map for Mineral Localities in Southern California," in *Geology of Southern California* edited by R.H. Jahns. Chap. 6, p 6. Sacramento, CA: CDM. Sep.

Calif. Inst. of Tech. (CIT) (1969-1975). *Strong Motion Earthquake Accelerograms*, Volumes I-IV, Parts A-Y. Pasadena: CIT Earthquake Eng. Res. Lab.

Cooley, J.W. and Tukey, J.W. (1965) "An Algorithm for the Machine Computation of Complex Fourier Series, "*Math. of Computation*, 19: p 297, Apr.

Hudson, D.E. (1976) "Reading of Records--Data Processing for Ground Motions and Structural Response," Lecture presented at Earthquake Engineering Research Institute seminar on Interpretation of Strong Motion Records for Earthquake Design Criteria and Structural Response, Univ. of So. Calif., Apr.

Kanai, K. (1950) "The Effect of Solid Viscosity of Surface Layer on the Earthquake Movements," *Bull. Earthq. Res. Inst.* 28:1950.

Kausel, E.; Roesset, J.M.; and Christian, J.T. (1976) "Nonlinear Behavior in Soil/Structure Interaction," *Proc. ASCE Geotech. Div.* 102:GT11, Nov, pp 1159-1169.

Lysmer, J. and Kuhlemeyer, R.L. (1969) "Finite Dynamic Model for Infinite Media," *Proc. ASCE Eng. Mech. Div.* 95:EM4, Aug, pp 859-877.

Lysmer, J. and Richart, F.E., Jr. (1966) "Dynamic Response of Footings to Vertical Loading," *Proc. ASCE Soil Mech. Div.* 92:SM1, Jan.

Lysmer, J. et al. (1975) *FLUSH, A computer Program for Approximate 3-D Analysis of Soil/Structure Interaction Problems*, EERC-75-30. Berkeley, CA: Univ. of Calif. Earthquake Eng. Res. Center, Nov.

Perez, V. and Schwartz, S.B. (1973). *Strong Motion Seismograph Station Listing*, Open-File Report. Menlo Park, CA:U.S. Geol. Survey.

Roesset, J.M.; Whitman, R.V.; and Dobry, R. (1973). "Modal Analysis for Structures with Foundation Interaction," *Proc. ASCE Struct. Div.* 99:ST3, Mar.

Schnabel, P.B. and Seed, H.B. (1972) *Acceleration in Rock for Earthquakes in the Western United States,* EERC-72-2. Berkeley: Univ. of Calif. Earthquake Eng. Res. Center. (PB 213 100)

Schnabel, P.B. et al. (1972) *SHAKE, A Computer Program for Eathquake Resonse Analysis of Horizontally Layered Sites,* EERC-73-12. Berkeley: Univ. of Calif. Earthquake Eng. Res. Center, Dec. (PB 220 207)

Seed, H.B. and Idriss, I.M.(1969) "Influence of Soil Conditions and Ground Motions during Earthquakes," *Proc. ASCE Soil Mech. Div.* 95:SM1, Jan, pp 99-137.

Shannon & Wilson (SW) & Agbabian-Jacobsen Assoc. (AJA) (1972) *Soil Behavior under Earthquake Loading Conditions: State-of-the-Art Evaluation of Soil Characteristics for Seismic Response Analyses.* Seattle, WA: SW & El Segundo, CA: AA (TID 26444)

Shannon & Wilson (SW) & Agbabian Assoc. (AA) (1975a) *Procedures for Evaluation of Vibratory Ground Motions of Soil Deposits at Nuclear Power Plant Sites.* Seattle, WA: SW & El Segundo, CA: AA, Jun. (NUREG-75/072).*

----. (1975b) *In Situ Impulse Test: An Experimental and Analytical Evaluation of Data Interpretation Procedures.* Seattle, WA: SW & El Segundo, CA: AA, Sep. (NUREG-0028).**

----. (1976) *Geotechnical and Strong Motion Earthquake Data from U.S. Accelerograph Stations, Volume I--Ferndale, Cholame, and El Centro, California.* Washington, DC: U.S. Nuclear Regulatory Commission, Office of Nuclear Regulatory Research, Sep. (NUREG-0029).**

----. (1977a) *Geotechnical and Strong Motion Earthquake Data from U.S. Accelerograph Stations: Gavilan College, Gilroy, California; Utah State University, Logan Utah; Montana State University, Bozeman, Montana: County-City Building, Tacoma, Washington; Federal Building, Helena, Montana; Carroll College, Helena, Montana,* Vol. 3. Seattle, WA: SW & El Segundo, CA: AA, NUREG/CR-0985, September 1980.**

----. (1977b) *Geotechnical and Strong Motion Earthquake Data from U.S. Accelerograph Stations, Verification of Subsurface Conditions at Selected "Rock" Accelerograph Stations in California,* Vol. 2. Seattle, WA: SW & El Segundo, CA: AA, NUREG/CR-0055, September 1980.**

----. (1977c) *Site-Dependent Effects at Strong-Motion Accelerograph Stations,* Seattle, WA: SW & El Segundo, CA: AA, NUREG/CR-1639, September 1980.**

----. (1978a) *Effects of Local Site Conditions on Earthquake Ground Motion Paramters,* Seattle, WA: SW & El Segundo, CA: AA, Mar. (draft)

----. (1978b) *Geotechnical and Strong Motion Earthquake Data from U.S. Accelerograph Stations, Verification of Subsurface Conditions at Selected "Rock" Accelerograph Stations in California,* Vol. 1. Seattle, WA: SW & El Segundo, CA: AA, May. (NUREG/CR-0055).**

----. (1978c) *Data from Selected Accelerograph Stations at Wilshire Boulevard, Century City, and Ventura Boulevard, Los Angeles, California,* NUREG/CR-0074. Seattle, WA: SW & El Segundo, CA: AA, Jun. (PB 283 029).**

----. (1978d) *Geotechnical and Strong Motion Earthquake Data from U.S. Accelerograph Stations: Pasadena (CIT Millikan Library), Santa Barbara County Court House, Taft (Lincoln School Tunnel) and Hollister (Melendy Ranch Barn), California,* NUREG-0029, V.2. Seattle, WA: SW & El Segundo, CA: AA, Jun.**

Southern Sierra Power Co. (SSPC) (1926) Plans, sections, and details for Operating Building, El Centro Terminal Station Expansion, Dwg. Nos. 574-31 through 574-42a. Riverside CA:SSPC, Jun.

Troncoso, J.H.; Brown, F.R.; and Miller, R.P. (1977) "In Situ Impulse Measurements of Shear Modulus of Soils as a Function of Strain," *Proc. 6th World Conf. on Earthquake Eng. New Delhi, India, Jan 1977,* Vol. 6, pp 6-165 - 6-168.

U.S. Geol. Survery (USGS) (1957) USGS topographic map, El Centro, California quadrangle. Reston, VA: USGS.

----. (1974-1977) *Seismic Engineering Program Report,* Geological Survey Circulars 713, 717-A to 717-D, 736-A to 736-D, and 762-A to 762-C, Menlo Park, CA: USGS, Oct. to Dec.

----. (1976a) *Strong Motion Accelerograph List - 1975,* Open File Report No. 76-79, Menlo Park, CA: USGS, Mar.

----. (1976b) *Strong Motion Earthquake Accelerograms, Digitization and Analysis, 1971 Records,* Open File Report No. 76-609, Menlo Park, CA: USGS, Jul.

----. (rec'd. 1977) *El Centro, Southern Sierra Power Company Terminal Substation,* internal memorandum. Menlo Park, CA: USGS.

Werner, S.D. (1976) *Seismic Soil/Structure Interaction Analysis Guidelines,* SAN/1011-111. El Segundo, CA: Agbabian Assoc., Apr.

Werner, S.D. and Van Dillen, D. (1977) "Use of Analytical and Statistical Techniques to Assess *In-Situ* Soil Test Procedures," in *Proc. 6th World Conf. on Eartquake Eng. New Delhi, India, Jan 1977,* Vol. 6, pp 141-146.

Westinghouse Electric & Mfg. Co. (WE&M) (1926). Outline drawing for 6000 KVA synchronous condenser unit for Operating Terminal Building, El Centro Terminal Station Building. East Pittsburgh, PA: WE&M; Apr 14.

Wilson, E.L. (1970). *SAP--A General Structural Analysis Program*, SEL-R-70-20. Berkeley, CA: Univ. of Calif., Sep.

*Available for purchase from the National Technical Information Service, Springfield, VA 22161.

**Available for purchase from the NRC/GPO Sales Program, U.S. Nuclear Regulatory Commission, Washington, DC 20555, and the National Technical Information Service, Springfield, VA 22161.

APPENDIX A

DETAILS OF EL CENTRO SUBSTATION BUILDING

1. UNITS ON MAIN FLOOR
2. ROOF TRUSSES
3. PRESENT INSTRUMENTATION ROOM AND PIERS

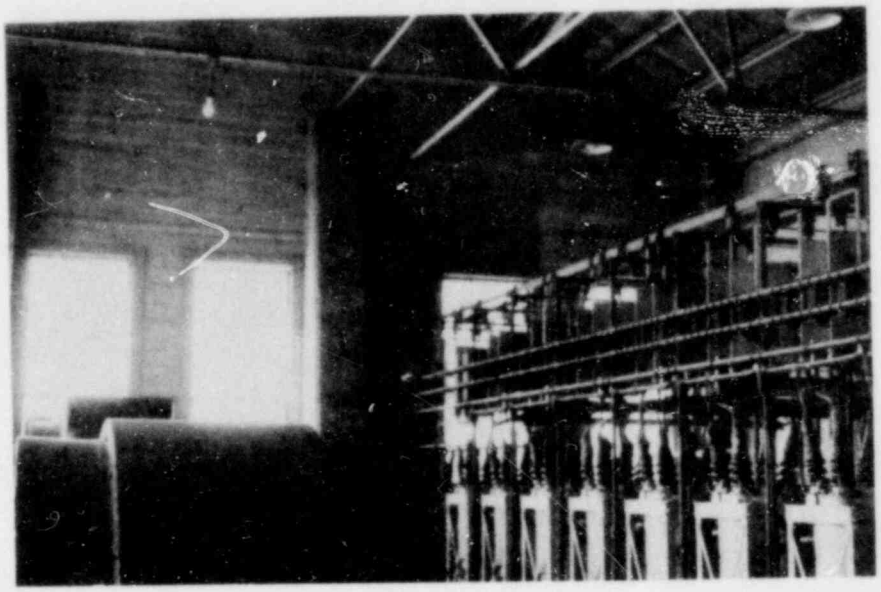

FIGURE A-1. GENERAL VIEW OF SYNCHRONOUS CONDENSER UNITS AND SWITCH UNITS ON MAIN FLOOR

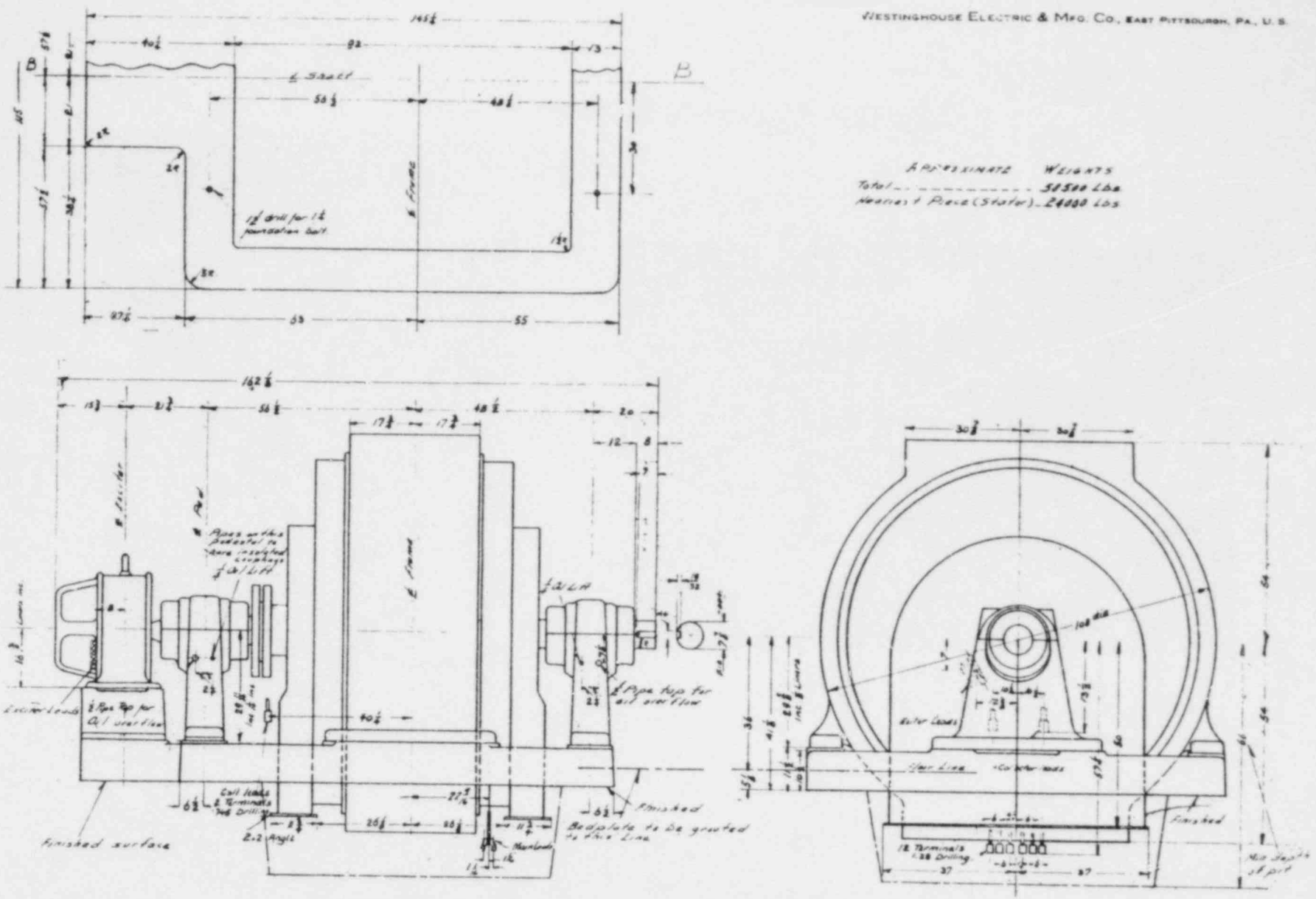

FIGURE A-2. DETAILS OF 6000 KVA SYNCHRONOUS CONDENSER (WE&M, 1926)

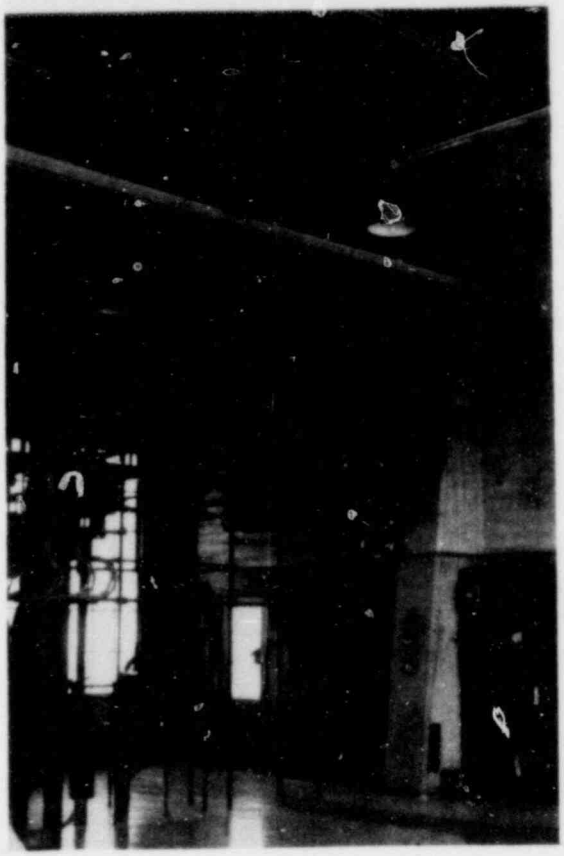

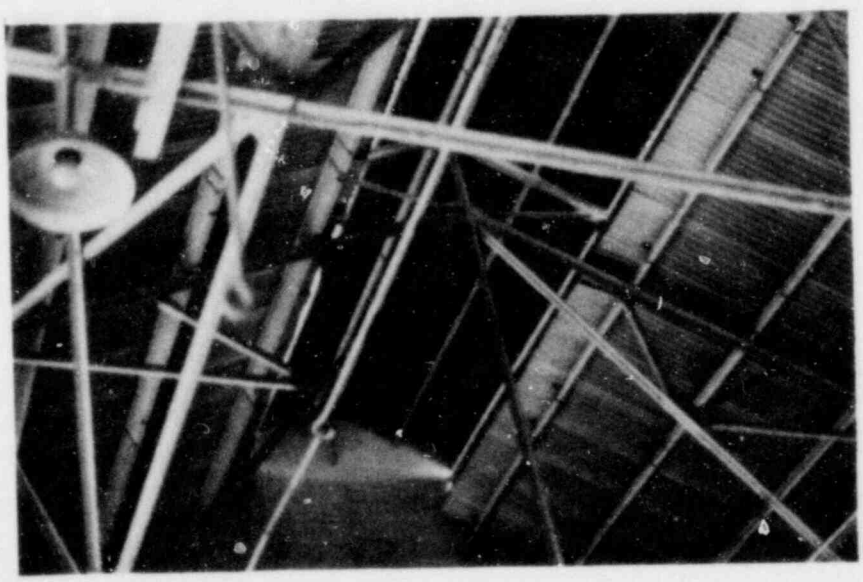

FIGURE A-3. ROOF TRUSSES

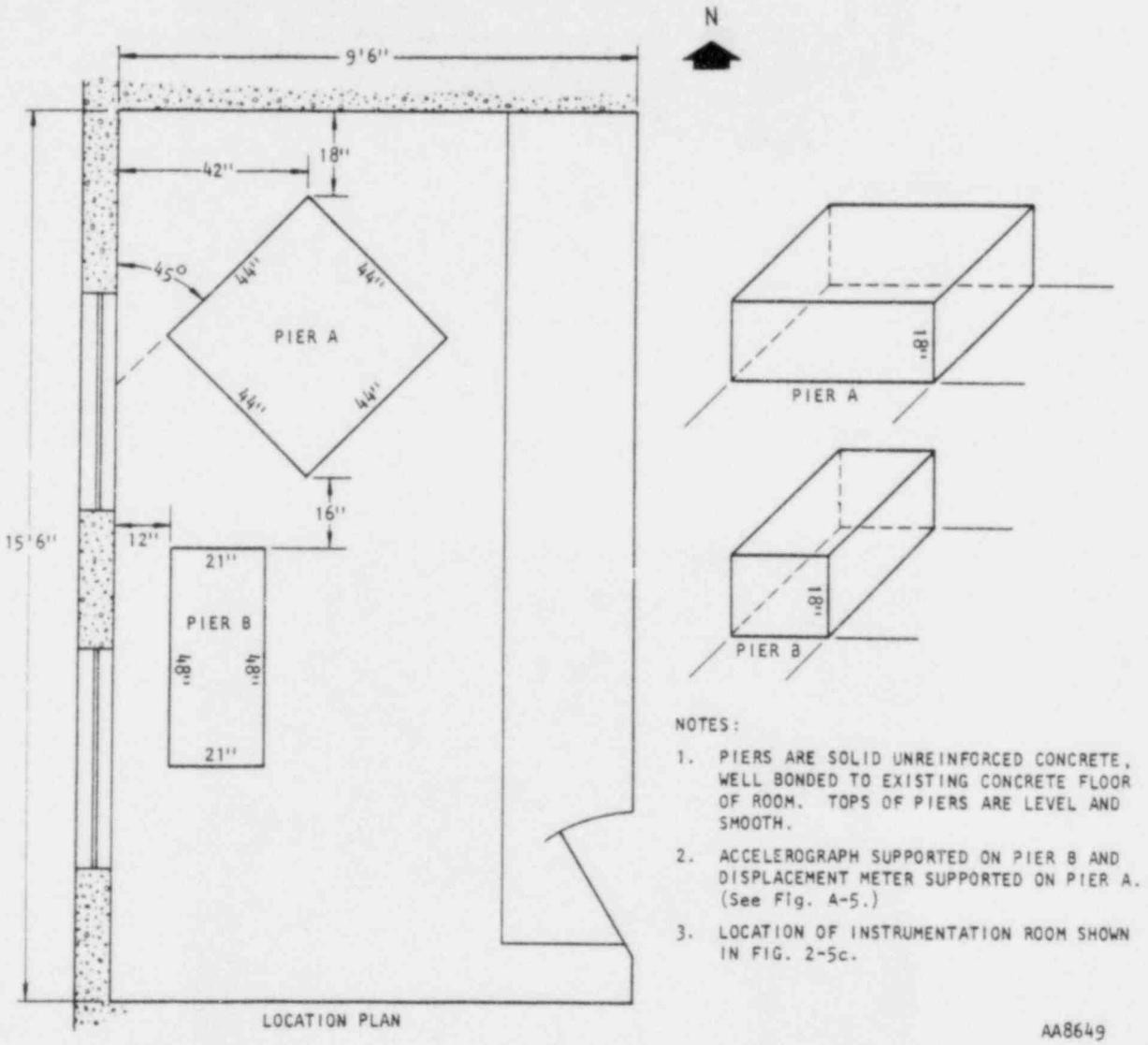

FIGURE A-4. PRESENT INSTRUMENTATION ROOM (USGS, 1977)

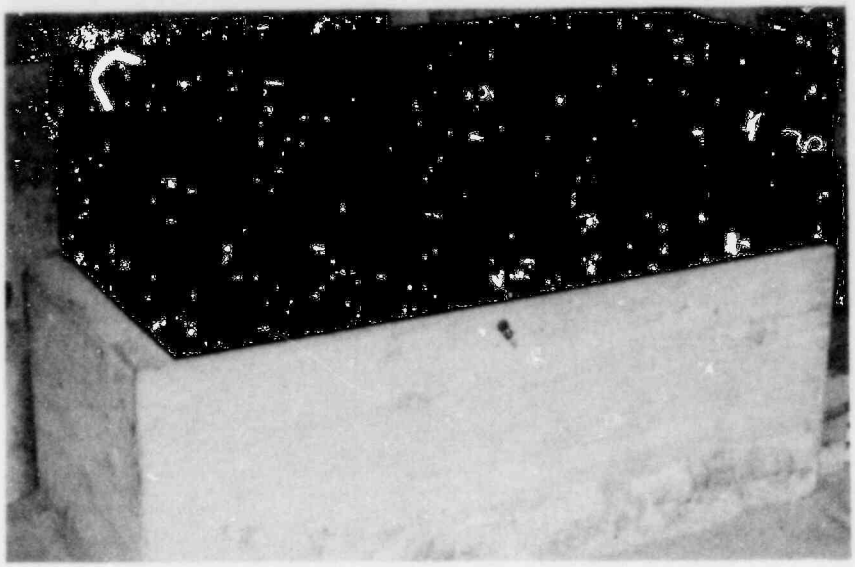

(a) Accelerograph

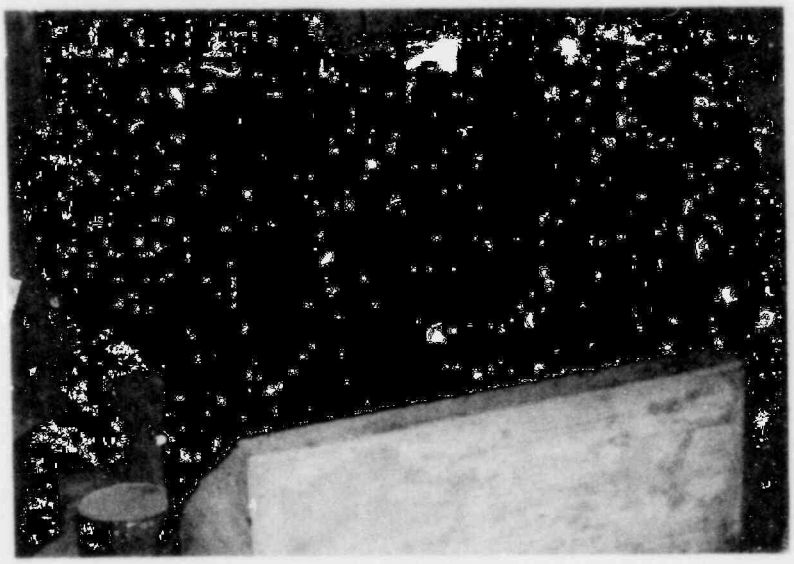

(b) Displacement meter

NOTE: INSTRUMENTS ARE MOUNTED ON 18-IN. HIGH UNREINFORCED CONCRETE PIERS BONDED TO EXISTING CONCRETE FLOOR OF ROOM

FIGURE A-5. STRONG MOTION INSTRUMENT LOCATIONS (USGS, 1977)

APPENDIX B

U.S. GEOLOGICAL SURVEY (USGS)
EL CENTRO
SOUTHERN SIERRA POWER COMPANY
TERMINAL SUBSTATION

INTERNAL MEMORANDUM
MENLO PARK, CALIFORNIA
FORWARDED TO AGBABIAN ASSOCIATES IN APRIL 1977

EL CENTRO

SOUTHERN SIERRA POWER COMPANY TERMINAL STATION

1. General Location of Building.

The instrument is located in the basement of the Terminal Station of the Southern Sierra Power Company which is located just west of Third Street on the north side of Commercial Street.

2. Description of Building.

The building is two stories high of very heavy concrete construction and is very heavily reinforced. It was originally built to house a gas engine, which at that time was the largest gas engine on the Pacific Coast. In the accompanying sketch the dotted lines represent the foundation of the old engine, and this foundation is shown in detail in the sketch in the upper right hand corner. The portion in the center of the block shown cross-hatched, was removed when the old engine was broken up and junked.

In addition to this massive piece of concrete inside the building which, as the sketch shows, extends into the ground about 20 feet below the basement floor, the walls of the building are of heavy construction, being 12 inches thick, and flaring out to a greater thickness underground, and being further strengthened by the heavy buttresses at sides and corners. There is one interior cross wall 10 inches thick as shown in the sketch and the rest of the building is without interior columns. The seismograph room is underneath the stairway, and the walls around the room are of concrete. The building is 60 x 80 feet in size.

3. Plan of room is shown in the accompanying diagram.

4. Geology.

The alluvium beneath El Centro is quite certainly hundreds of feet deep and its thickness may actually be several thousands of feet. The surface material is soft silt. The alluvial strata consist mainly of silt and other soft lake beds with some beds of gravel and sand. It is material deposited by the Colorado River on its alluvial fan or delta. Data regarding depth to the water is not at hand, but it is probably some tens of feet.

The alluvium at El Centro is part of a huge bed of loosedetritus laid down in a trough form by subsidence of slices several miles wide between branches of the San Andreas fault.

5. Pictures.

CSP 23. Shows the Terminal Station of the Southern Sierra Power Co.
CSP 24. Shows the Terminal Station of the Southern Sierra Power Co.

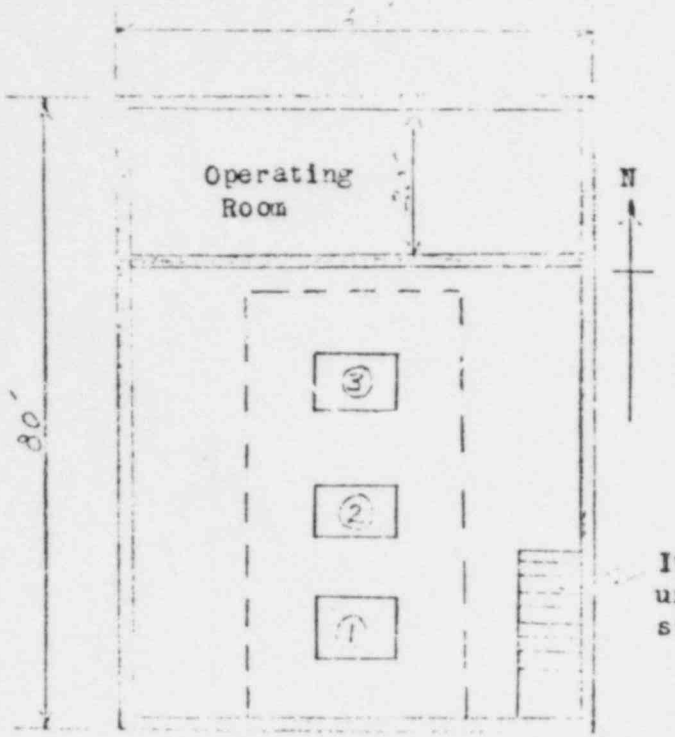

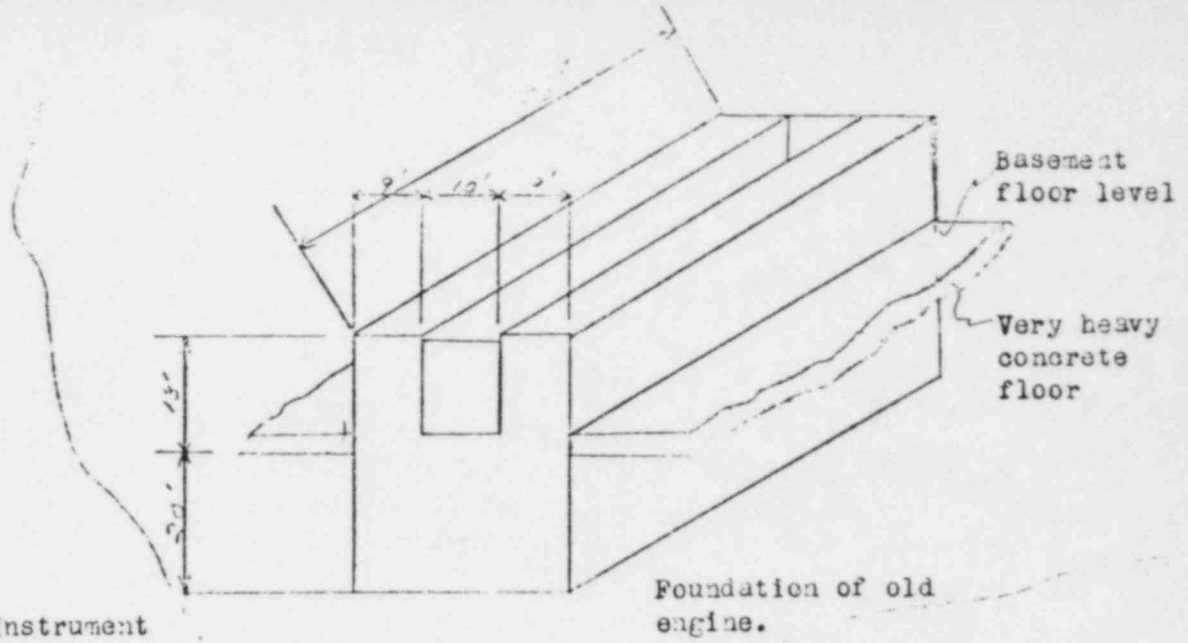

① 5000 KVA Synchronous Condenser

② " " " "

③ " " " " not in use

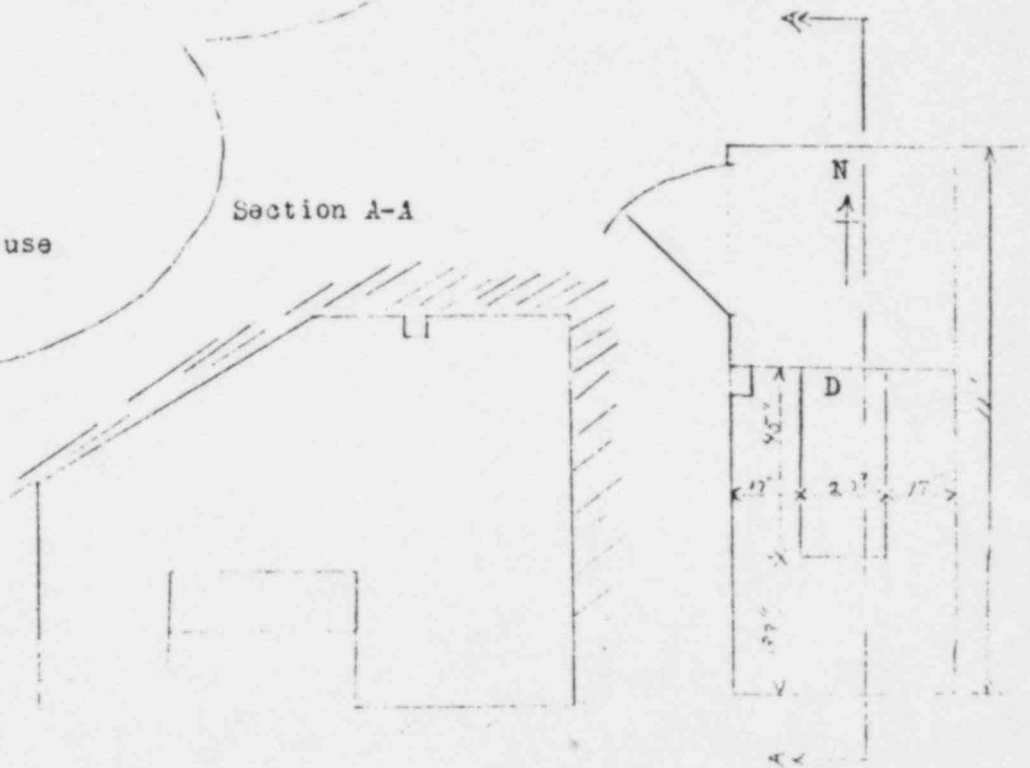

EL CENTRO

[SW/AA Note: According to IVID, 1977, Unit 3 was never installed]

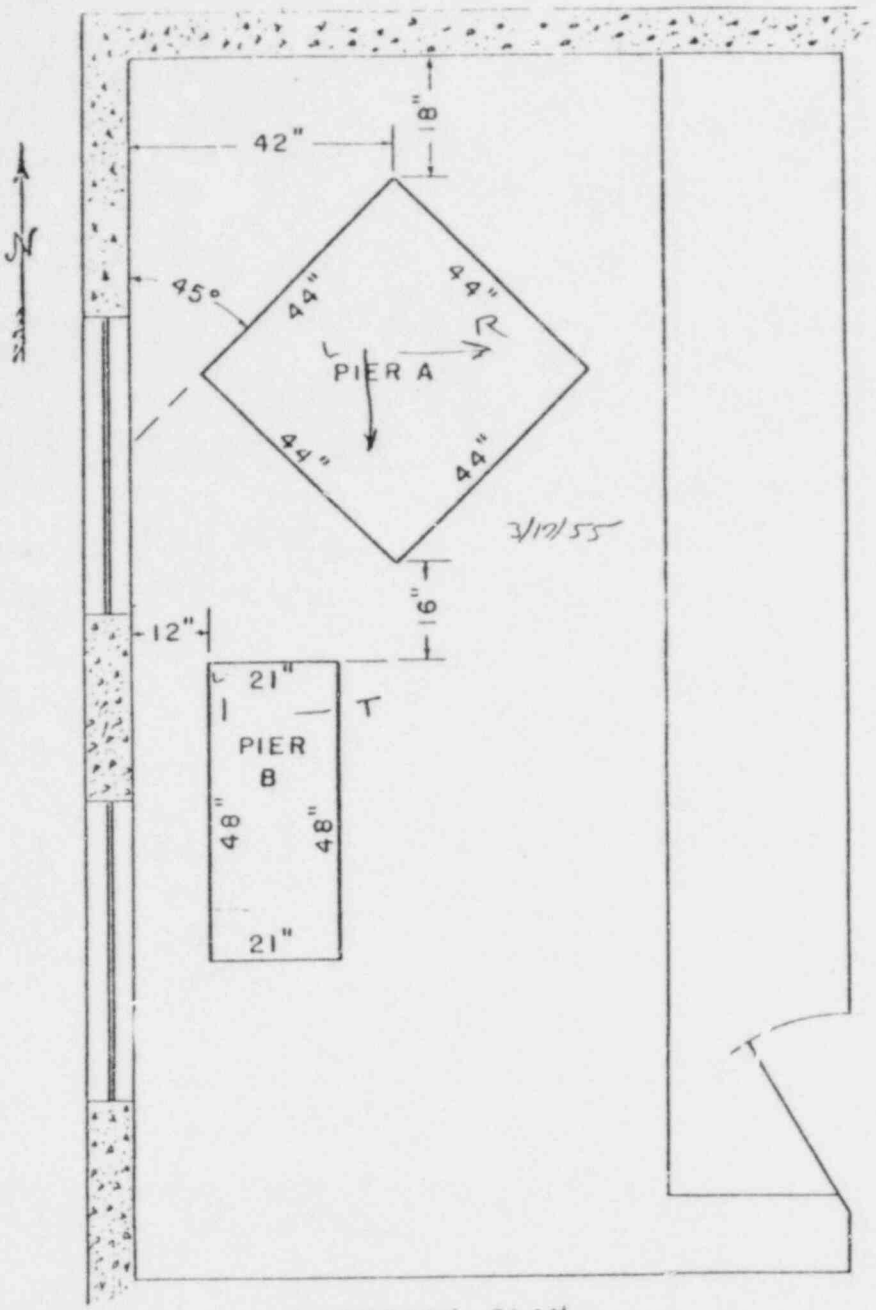

LOCATION PLAN

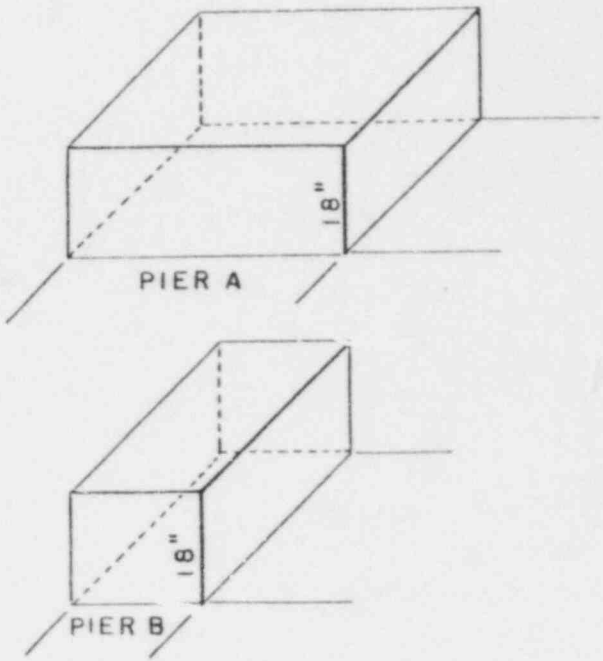

NOTE --- PIERS TO BE SOLID UNREINFORCED CONCRETE, WELL BONDED TO EXISTING CONCRETE FLOOR OF ROOM. TOPS OF PIERS TO BE LEVEL AND SMOOTH.

PROPOSED SEISMOGRAPH STATION
IMPERIAL VALLEY IRRIGATION DISTRICT'S EL CENTRO ELECTRIC SUB-STATION

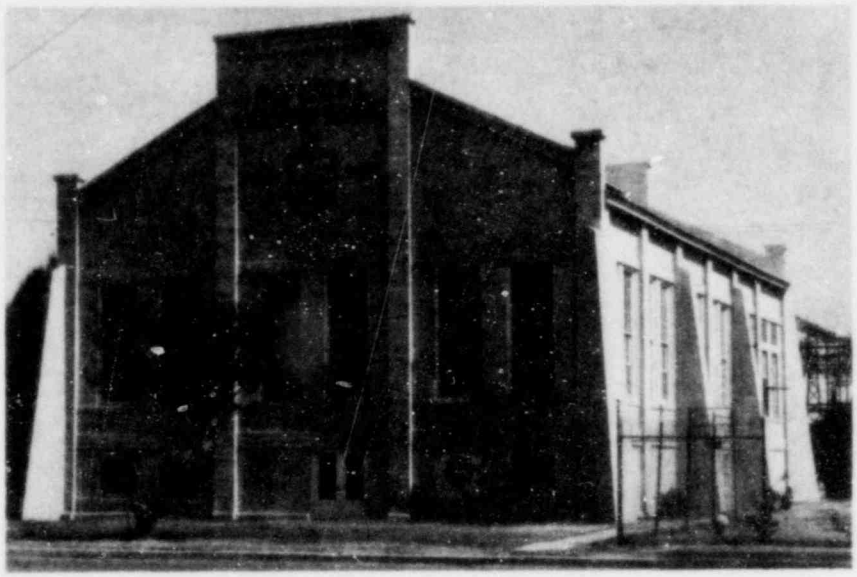

(a) Picture No. CSP 23

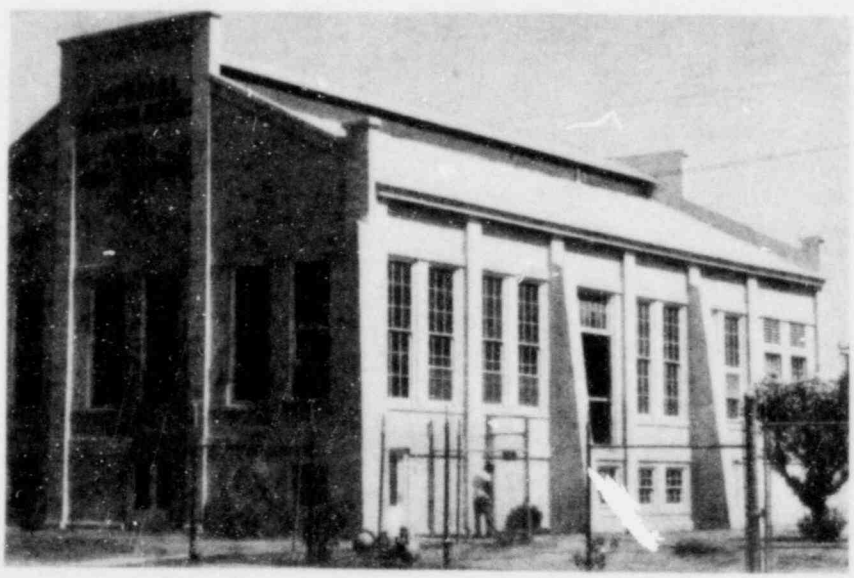

(b) Picture No. CSP 24

PHOTOGRAPHS OF TERMINAL SUBSTATION (OPERATING) BUILDING

APPENDIX C

MICROREFLECTION SURVEY AT EL CENTRO TERMINAL SUBSTATION BUILDING

C.1 INTRODUCTION

This appendix presents the results of a microreflection survey performed by SW/AA at the Terminal Substation Building in El Centro, California. The purpose of this study was to verify the thickness of the concrete foundation block that underlies the Terminal Substation Building. Results of the study, conducted using nondestructive testing techniques at several locations along the block, have been used by SW/AA to complete their soil/structure interaction analyses of the substation.

This survey was performed with the cooperation of the Imperial Irrigation District, current owners of the Terminal Substation. The survey was conducted on 7 February 1978, which was after implementation of the SHAKE/FLUSH analysis of the substation response and was prior to the TRI/SAC analyses.

C.2 SURVEY METHOD

The testing technique employed during this survey measured the time required for a compressional wave to travel from the floor surface of the structure, down to the bottom of the foundation block and back again. This time interval is called the two-way travel time. The two-way travel time was used along with the compressional wave velocity of concrete to compute the thickness of the foundation block. Values of compressional wave velocity were determined from measurements made at several locations on the concrete floor of the structure. The velocity was determined by measuring the time required for the compressional wave to travel along the floor between two sensors spaced at a distance of 2 ft.

The microreflection survey was made using a Textronix 214 Dual-Trace Storage Oscilloscope and piezoelectric velocity transducers. The source of energy for the compressional wave was a hammer blow on the concrete floor.

The following steps were used to determine the two-way travel time of the compressional wave. First, a transducer was fastened to the floor and its electrical leads were connected to the oscilloscope. Next, the oscilloscope was turned on and placed in the storage mode. Then, a single hammer blow was applied to the floor in the vicinity of the transducer. This impact excited the transducer which, in turn, served to activate the oscilloscope. The output of the transducer was then recorded and stored as a wave form trace on the screen of the oscilloscope. This trace was then moved vertically on the screen of the oscilloscope and another blow was applied to the floor. This procedure was continued until a set of six to eight traces were recorded on the oscilloscope screen. These traces were inspected to determine repeated energy arrivals that corresponded to the reflected energy of the hammer blow. The arrival time of the reflected wave was recorded as the two-way travel time.

A similar procedure was used to measure the compressional wave velocities of the concrete. Here, two transducers were fastened to the floor, separated by a gap of 2 ft. The floor was then struck by the hammer and the output from both transducers was simultaneously recorded on the oscilloscope. The time phase shift between the energy arrivals on the two traces was then noted. The 2-ft separation of the transducers divided by this phase shift defind the compressional wave velocity of the concrete.

C.3 TEST RESULTS

Survey measurements were made at three locations in the basement (tunnel) of the structure and at one location on the main floor. All of these locations are shown in Figure C-1. At each location, compressional wave velocities and two-way travel times were measured. These values and the computed thickness of the foundation are summarized in Table C-1.

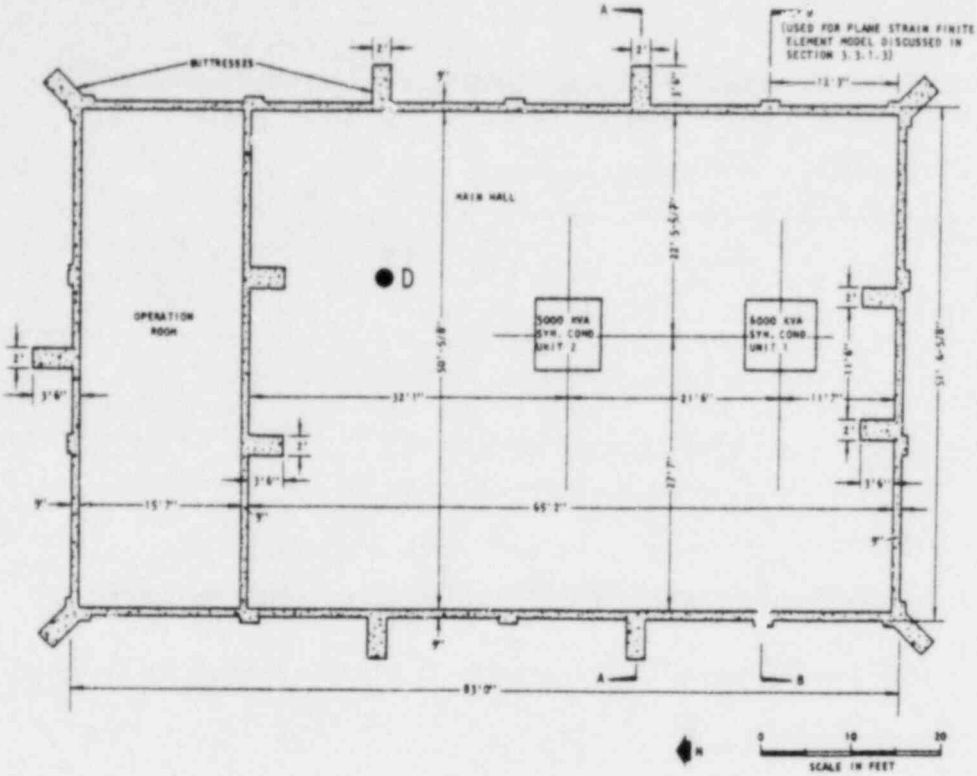

(a) Main floor plan

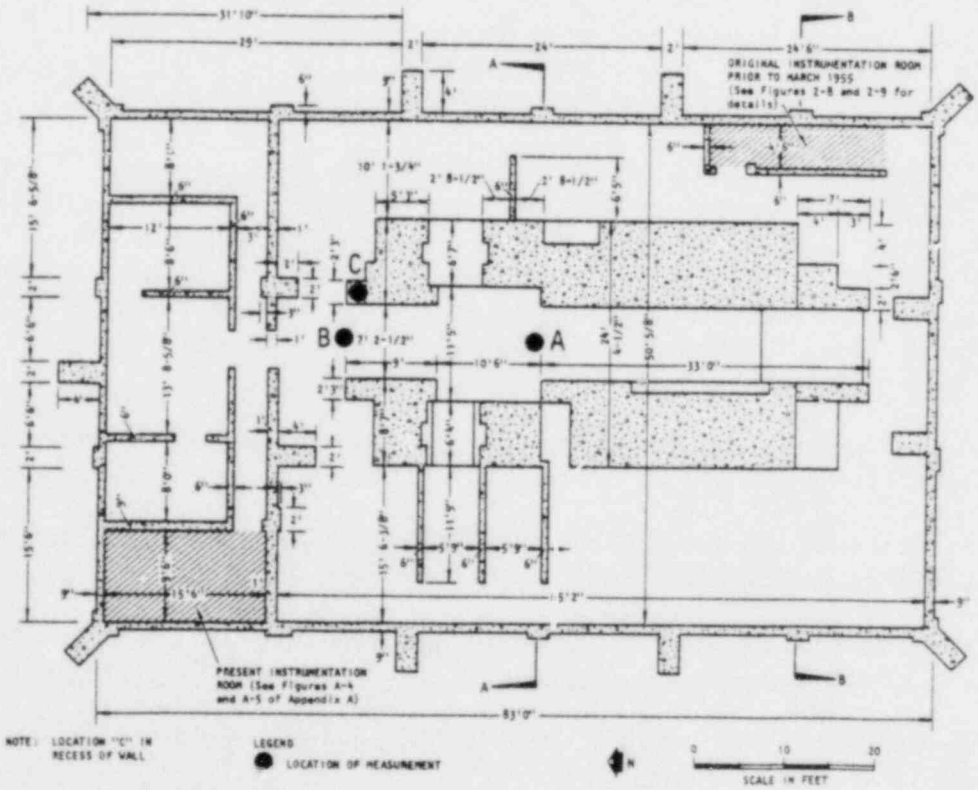

(b) Basement plan

FIGURE C-1. TRANSDUCER LOCATIONS FOR MICROREFLECTION SURVEY

TABLE C-1. MICROREFLECTION SURVEY MEASUREMENTS AT TERMINAL SUBSTATION BUILDING, EL CENTRO, CALIFORNIA

Location[1]	Measured[2] V_p, fps	Velocity[2] Variation, fps	Measured Two-Way Travel Times[3], msec	Computed Concrete Thicknesses, ft	
				Individual[4] Components	Average[5] Components
A	5,700	± 800	7.0	20	
B	5,700	± 800	7.0	20	22.8
C	6,700	±1,000	6.0	20	
D	6,700	±1,000	8.5	28.3	29.8
Floor to Floor	8,300[6]	±1,600[6]	2.0[6]	8.3[7]	7.0
Range	5700-8300				
Average	7,000				

NOTES

1. Measurement locations are indicated in plan on Figure C-1.
2. Compressional wave velocities (V_p) were determined from arrival times of horizontally traveling waves detected at sensors spaced 2 ft apart on the floor.
3. Time for the compressional wave to travel from the energy source, down to the base of the foundation, and back up again to the floor surface.
4. Foundation thickness computed from individually measured velocities (Note 2) and individually measured travel times (Note 3).
5. Foundation thickness computed from average velocity of 7,000 fps for the foundation and average travel times.
6. Velocity determined indirectly from difference in travel times between the basement and main floor levels.
7. Actual vertical floor-to-floor distance from building measurements.

The measured concrete velocities indicated in Table C-1 range from 5,700 to 8,300 fps. The velocities of 5,700 and 6,700 fps were obtained from direct measurements at Locations A to D. The floor-to-floor velocity of 8,300 fps was determined indirectly by considering the differentials in elevation (8.3 ft) and travel time (1.0 msec one way) between the tunnel and the main floor. Immediately to the right of the compressional wave velocities in Table C-1 are values for the range of uncertainty in measuring the wave velocities.

Also presented in Table C-1 are the two-way travel times of the compressional waves. Measurements made at Locations A, B, and C in the tunnel indicate that 6 to 7 msec were required for the compressional wave to travel from the floor surface, down to the base of the foundation, and back again. Measurements made on the main floor (Location D) indicate a two-way travel time of 8.5 msec. The floor-to-floor travel time of 2.0 msec was determined indirectly as the difference between the main floor time (8.5 msec) and an average tunnel time (6.5 msec).

Thicknesses of the concrete foundation, which are also given in Table C-1, were computed from the measured two-way travel times and compressional wave velocities. Two sets of data were used in the computations. First, thicknesses were computed using the individually measured compressional wave velocities and two-way travel times. Next, the thicknesses were computed using an average compressional wave velocity of 7,000 fps and an average two-way travel time of 6.5 msec in the tunnel. As indicated in Table C-1, there is relatively good agreement between both methods with computed thicknesses beneath the tunnel varying from 20 to 23 ft. Since the tunnel is about 6 in. higher than the basement floor (SSPC, 1926), the foundation block would extend about 19 to 22 ft below basement floor slab level.

C.4 DISCUSSION AND CONCLUSIONS

The compressional wave velocities measured at the substation are somewhat lower than values typical of fresh, sound concrete, which may range from 10,000 to 12,000 fps. One explanation of this difference is due to the

age of the structure. That is, as concrete ages, its compressional wave velocity decreases. Another factor that may be related to the relatively low velocity measurements is the quality of the concrete in the foundation. That is, a lean mix concrete would have a velocity lower than that of a fresh, high-cement-content mix. Our observation of the condition of the concrete in the foundation would indicate either significant deterioration has occurred or that a lean concrete mix was used in construction and possible pockets of sand or a poorly cemented mixture exist in the foundation. This condition was indicated by tapping the floor with a hammer at several locations and noting a "hollow" sound in the concrete. Also, at the time of the survey, the Imperial Irrigation District was drilling holes in the concrete for mounting brackets. The concrete exposed in these jack-hammered holes was "punky" and could be easily gouged with a screwdriver.

Considering the above, a relatively low compressional wave velocity would be expected for the concrete at the terminal substation. The measured velocity of 5,700 fps at surface Points A and B may be possibly too low and not representative of the overall foundation. Similarly, the indirectly determined velocity of 8,300 fps may be too high. Consequently, an average value of about 7,000 fps is judged to be most appropriate for representing the compression wave velocity in the foundation.

A foundation thickness of 23 ft at the tunnel was calculated using an average velocity of 7,000 fps and an average two-way travel time of 6.5 msec. This computed thickness is in good agreement with existing USGS information (App. B), which indicates that the foundation block extends 20 ft below the basement slab (about 21 ft below the tunnel). Therefore, it is concluded that the foundation block extends about 20 ft below the basement level.

C.5 SUMMARY

In summary, the measurements described above indicated that an average compressional wave velocity of 7,000 fps would be representative of concrete in the foundation. Furthermore, our measurements substantiate existing information that shows the concrete foundation block to extend about 20 ft below the basement slab level.

APPENDIX D

AVAILABILITY OF STRONG MOTION RECORDS FOR ASSESSING SOIL/STRUCTURE INTERACTION EFFECTS AT EL CENTRO TERMINAL SUBSTATION BUILDING

D.1 INTRODUCTION

The analytical results presented in this report, while providing valuable insights in potential soil/structure interaction effects at the Terminal Substation accelerograph site, can nevertheless not possibly represent all of the physical parameters that might affect the earthquake motions at this site because of certain assumptions inherent in the analysis techniques, cost considerations, etc. Therefore, suitable measured records, if available, could provide valuable additional insights into the importance of soil/structure interaction at this site. The appendix discusses the availability of such records, as assessed from a careful review of USGS strong motion data and from communication with USGS personnel.

D.2 EL CENTRO DATA REVIEW

Since 1971, several new accelerograph stations have been installed in the El Centro, California, area (USGS, 1976a). Such stations could be of value in defining potential soil/structure interaction effects at the Terminal Substation Building if (1) the stations are located sufficiently near the Terminal Substation site so that subsurface soil conditions are reasonably similar; (2) during the same earthquake, records were measured at these stations and at the accelerograph located at the Terminal Substation Building; (3) the records measured at these other stations are themselves representative of free-field motions; and (4) the records had been processed by USGS and were readily available for public use.

To check if such conditions could be met, USGS Seismic Engineering Program Reports and Open File Reports were carefully reviewed to determine if ground motion measurements had recently (since 1971) been obtained simultaneously

in El Centro at several accelerograph sites including the Terminal Substation Building (USGS, 1976b, 1974-1977). From this, two earthquake events were identified where such measurements were obtained--one on 6 December 1974 and the other on 23 January 1975.

Table D-1 summarizes the characteristics of these records. The table shows that these records were primarily of small amplitude (peak acceleration <0.1 g) and were measured at two other stations--Imperial Valley College and Meadows Union School--in addition to the Terminal Substation Building. As shown in Figure D-1, these stations are each located from 4 to 8 km from the Terminal Substation Building and about 20 km from the epicenters of the two earthquake events.

Despite the rather large station-station distances noted above, A.G. Brady of USGS was contacted to determine the availability of the records listed in Table D-1. From this, it was learned that:

a. The USGS data-processing program includes only measured records from record sets having peak accelerations greater than 0.1 g. (Therefore, of the various records listed in Table D-1, only the Imperial Valley College records were processed by USGS).

b. The January 1975 record at Imperial Valley College is missing. (This leaves only the December 1974 Imperial Valley College record which was processed by USGS and is available for public use).

c. 70-mm film copies of the uncorrected accelerograms listed in Table D-1 are available for public use. However, such copies would have to be digitized, baseline correlated, and instrument corrected involving special procedures and apparatus of the type described by Hudson (1976). (Only a few institutions are presently set up to process the data in this way.)

TABLE D-1. RECORDS MEASURED IN EL CENTRO DURING EARTHQUAKES OF DECEMBER 1974 AND JANUARY 1975

Event	Station Location	Station Coordinates	Epicentral Distance, km (mi)	Component	Maximum Horizontal Acceleration, g
Earthquake of 6 December 1974 Calexico, California: Epicenter at 32.71N, 115.40W Magnitude 4.8	El Centro, California Meadows Union School 2059 Bowker (1-story building)	32.80N 115.47W	12 (7)	S52W Down S38E	0.07 0.01 0.07
	El Centro, California Terminal Substation Building 302 Commercial (2-story building)	32.79N 115.55W	17 (10)	N52E Down N38W	-- 0.01 0.05
	Imperial, California Imperial Valley College Administration Building (1-story building)	32.83N 115.50W	16 (10)	S52W Down N38E	0.11 0.03 0.16
Earthquake of 23 January 1975 Brawley, California: Epicenter at 32.71N, 115.40W Magnitude 4.8	El Centro, California Meadows Union School 2059 Bowker (1-story building)	32.80N 115.47W	18 (11)	S52W Down S38E	0.09 0.02 0.08
	El Centro, California Terminal Substation Building* 302 Commercial (2-story building)	32.79N 115.55W	20 (12)	S52W Down S38E	-- 0.03 0.06
				Up South West	0.02 0.05 0.07
	Imperial, California Imperial Valley College Administration Building (1-story building)	32.83N 115.50W	15 (9)	S52W Down S38E	0.11 0.04 0.05

*Two instruments installed in Terminal Substation Building at time of January 1975 earthquake.

AA9652

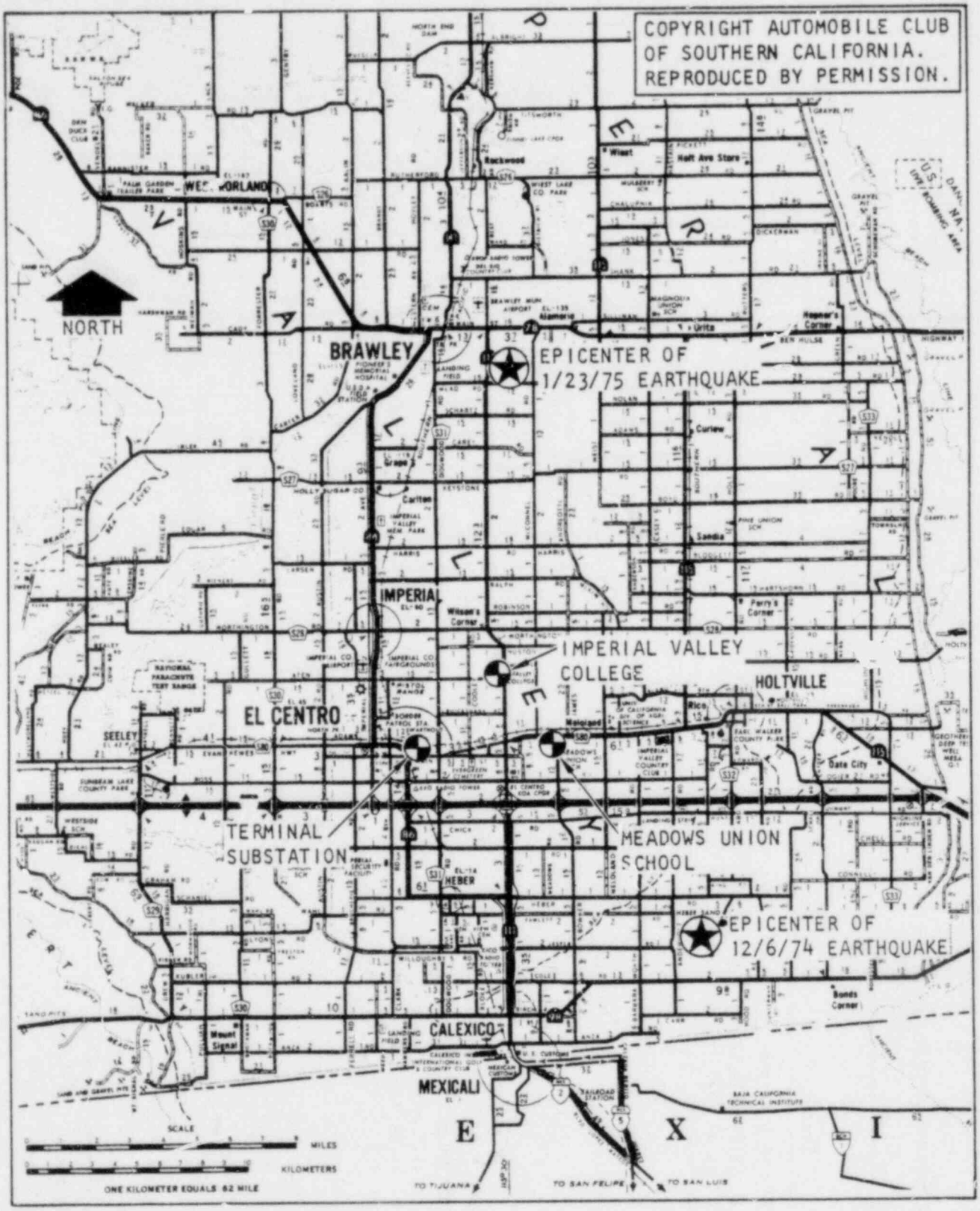

FIGURE D-1. LOCATIONS OF EARTHQUAKE EPICENTERS AND ACCELEROGRAPH STATIONS IN EL CENTRO AREA

d. In addition to the stations listed in Table D-1, there is another station (75 E. Cruickshank) that is less than 2 mi from the Terminal Substation Building. However, the instrument at this station has thus far refused to trigger since installation. (This will apparently be corrected in the near future by USGS.)

D.3 CONCLUSIONS

From this review of the strong motion records measured in El Centro in recent years, it is seen that (1) insufficient processed data are available for public use; and (2) the stations at which measured records were obtained appear to be too far from the Terminal Substation Building to permit definitive assessments of soil/structure interaction effects at that building. For these reasons, no strong motion data could be used to supplement the analytical results obtained from this study.

NRC FORM 335 (7-77)

U.S. NUCLEAR REGULATORY COMMISSION

BIBLIOGRAPHIC DATA SHEET

1. REPORT NUMBER *(Assigned by DDC)*
NUREG/CR-1642

4. TITLE AND SUBTITLE *(Add Volume No., if appropriate)*
Site-Dependent Response at El Centro, California Accelerograph Station Including Soil/Structure Interaction Effects

2. *(Leave blank)*

3. RECIPIENT'S ACCESSION NO.

7. AUTHOR(S)
Shannon and Wilson, Inc., and Agbabian Associates

5. DATE REPORT COMPLETED
MONTH: May | YEAR: 1979

9. PERFORMING ORGANIZATION NAME AND MAILING ADDRESS *(Include Zip Code)*
Shannon & Wilson, Inc.
1105 North 38th Street
Seattle, Washington 98103

Agbabian Associates
250 North Nash Street
El Segundo, California 90245

DATE REPORT ISSUED
MONTH: October | YEAR: 1980

6. *(Leave blank)*

8. *(Leave blank)*

12. SPONSORING ORGANIZATION NAME AND MAILING ADDRESS *(Include Zip Code)*
Site Safety Research Branch
Division of Reactor Safety Research
Office of Nuclear Regulatory Research
U.S. Nuclear Regulatory Commission
Washington, D.C. 20555

10. PROJECT/TASK/WORK UNIT NO.

11. CONTRACT NO.
NRC-04-76-200
FIN No. B3015

13. TYPE OF REPORT

PERIOD COVERED *(Inclusive dates)*

15. SUPPLEMENTARY NOTES

14. *(Leave blank)*

16. ABSTRACT *(200 words or less)*

The El Centro Terminal Substation Building, where many strong motion records have been measured, is underlain by a massive foundation block and rests on deep deposits of soft soil materials. These conditions suggest important soil/structure interaction effects; therefore, the current study has been carried out to analytically investigate the extent to which such effects may cause motions recorded in the basement of this building to differ from the motions of the free field. The investigation was based on two-dimensional models of the building and soil medium and two different analysis techniques--SHAKE/FLUSH and TRI/SAC codes. Both codes showed that, at frequencies above 1.5 Hz, the horizontal and vertical motions of the basement at the accelerograph location fell below the corresponding free-field motions along the ground surface, by factors ranging from 20% to 100%. At lower frequencies, the horizontal motions of the basement and free field were nearly identical, whereas the vertical motions of the basement fell below those of the free field.

17. KEY WORDS AND DOCUMENT ANALYSIS

17a. DESCRIPTORS

17b. IDENTIFIERS/OPEN-ENDED TERMS

18. AVAILABILITY STATEMENT
Unlimited

19. SECURITY CLASS *(This report)*
Unclassified

21. NO. OF PAGES

20. SECURITY CLASS *(This page)*
Unclassified

22. PRICE
$